STAR SHAPED REACTIVE POLYMERIC NANOCARRIERS

by

Hatice Betül Demirer

B.S., Chemistry, Boğaziçi University, 2010

Submitted to the Institute for Graduate Studies in
Science and Engineeering in partial fulfillment of
the requirements for the degree of
Master of Science

Graduate Program in Chemistry

Boğaziçi University

2012

STAR SHAPED REACTIVE POLYMERIC NANOCARRIERS

APPROVED BY:

Assoc. Prof. Amitav Sanyal (Thesis Supervisor)	……...
Assoc. Prof. Rana Sanyal	……
Assoc. Prof. Sinan Şen	……

DATE OF APPROVAL:16.08.2012

Dedicated to my parents Gül and Halil

ACKNOWLEDGEMENTS

Firstly I would wish to express my sincere gratitude to my thesis supervisor Assoc. Prof. Amitav Sanyal for his encouraging attitude, support and scientific guidance which enabled me to do this work. I have gained a great deal of knowledge about chemistry and learned how to cope with problems which accompany research, from him. I really do appreciate his endless attention and encouragement.

I would like to express my thanks to Assoc. Prof. Rana Sanyal for her valuable discussions and recommendations regarding my research. I would wish to extend my thanks to Assoc. Prof. Sinan Şen for his careful and constructive review of the final manuscript of the thesis.

I am so much thankful to Özgül Gök for her very kind interest and generous help during my research. I also thank to my labmates Merve C., Nazlı, Merve T. Sedef, Özlem, Tuğçe, Luca, Pelin, Yasemin, Melike, Nergiz, Merve K., Aslı, Burcu, Rabia, Mehmet, Sadık, Duygu, Fatma and Özge for sharing the joy of making research. Specially I would wish to thank my friend Nurdan for her intimate friendship and support. I would also like to thank all present and former group members and all the members of the faculty in my department.

Finally my deepest thanks go to my family and my fiance Mehmet Zeki for their endless love, patience and support.

This research has been supported by The Scientific and Technological Research Council of Turkey (TÜBİTAK) (BİDEB – 2228).

ABSTRACT

STAR SHAPED REACTIVE POLYMERIC NANOCARRIERS

Thermoresponsive drug delivery has gained much attention in recent years, due to solutions it offers to problems related to conventional drug delivery. Among polymeric architectures used in drug delivery, star shaped ones have some superior properties which make them a better choice as a drug delivery system when compared to their linear analogues. So, a star shaped reactive polymeric nanocarrier which releases its content in response to change in temperature can be an attractive candidate for drug delivery purposes. In this study, 4-arm and 6-arm star shaped reactive polymers which contain pendant furan groups at their side chains are synthesized by atom transfer radical polymerization (ATRP). These furan groups are then functionalized by ethylmaleimide and a fluorescent dye BODIPY-maleimide as a model compound via Diels-Alder reaction. The thermoreversible nature of Diels-Alder reaction makes it a suitable choice for functionalization, since the release of the molecules is possible by retro Diels-Alder reaction of the endo product at physiological temperature.

ÖZET

YILDIZ ŞEKİLLİ REAKTİF POLİMERİK NANOTAŞIYICILAR

Isılduyarlı ilaç taşıyıcı sistemler, konvensiyonel ilaç taşıyıcı sistemlerle ilgili problemlere sundukları çözümlerden dolayı son yıllarda oldukça ilgi çekmektedir. İlaç taşıyıcı sistemler olarak kullanılan polimerik yapılar arasından yıldız şekilli olanlar lineer analoglarına göre birtakım üstün özelliklere sahip oldukları için daha iyi bir tercih olarak öne çıkmaktadır. Dolayısıyla, içeriğindeki molekülleri sıcaklık değişimine bağlı olarak salabilen yıldız şekilli reaktif bir polimerik nanotaşıyıcı, ilaç taşınması amacıyla kullanılmak üzere ilgi çekici bir aday olabilir. Bu çalışmada, furan grupları içeren 4 kollu ve 6 kollu yıldız şekilli reaktif polimerler atom transfer radikal polimerleşmesi yöntemi ile sentezlendi. Elde edilen polimerlerin furan grupları etilmaleimid ve fluorasan bir boya olan BODIPY-maleimid model madde olarak kullanılarak Diels-Alder tepkimesi ile fonksiyonelleştirildi. Diels-Alder tepkimesinin ısılduyarlı niteliği onu fonksiyonelliştirmede kullanılmak üzere iyi bir tercih yapmaktadır çünkü moleküllerin salınımı endo ürünün retro Diels-Alder tepkimesi ile fizyolojik sıcaklıkta mümkündür.

TABLE OF CONTENTS

ABSTRACT v
ÖZET vi
LIST OF FIGURES ix
LIST OF TABLES xii
LIST OF ACRONYMS/ABBREVIATIONS xiii
LIST OF SYMBOLS xiii
1. INTRODUCTION 1
1.1. Cancer and Chemotherapy 1
1.1.1. Camptothecin 2
1.2. Polymer Therapeutics 4
1.2.1. Enhanced Permeability and Retention Effect 6
1.2.2. Clinical Trials With Polymer- Drug Conjugates 7
1.2.3. Polymeric Architectures For Drug Delivery 9
1.3. Star Polymers 11
1.4. Atom Transfer Radical Polymerization 15
1.5. Diels-Alder Reaction 16
1.5.1. Diels-Alder Reaction in Polymer Chemistry 17
2. AIM OF THE STUDY 21
3. RESULTS AND DISCUSSION 22
3.1. Synthesis of the Initiators 22
3.2. Polymerizations by ATRP 26
3.3. Functionalization of Polymers 29
3.3.1. Attachment of N-Ethylmaleimide 29
3.3.2. Attachment of BODIPY-maleimide 31
3.3.3. Release studies 34
3.3.4. Synthesis of linker for drug attachment 36
4. EXPERIMENTAL 39
4.1. Materials and Methods 39
4.2. Synthesis 40

4.2.1. Synthesis of Initiators 40
4.2.1.1. Synthesis of 4-arm initiator..... 40
4.2.1.2. Synthesis of first generation dendrimer. 40
4.2.1.3. Deprotecion of first generation dendrimer..... 41
4.2.1.4. Synthesis of 8-arm initiator..... 41
4.2.2. Synthesis of Polymers..... 43
4.2.2.1. Synthesis of P1..... 43
4.2.2.2. Synthesis of P2..... 43
4.2.2.3. Synthesis of P3..... 44
4.2.2.4. Synthesis of P4..... 44
4.2.2.5. Synthesis of P5..... 45
4.2.2.6. Synthesis of P6..... 45
4.2.2.7. Synthesis of P7..... 46
4.2.2.8. Synthesis of P8..... 46
4.2.3. Functionalization of Polymers 47
4.2.3.1. Attachment of N-Ethylmaleimide..... 47
4.2.3.2. Attachment of BODIPY-maleimide. 47
4.2.3.4. Release studies. 48
4.2.3.5. Synthesis of linker for drug attachment. 49
5. CONCLUSION..... 51
APPENDIX..... 52
REFERENCES 73

LIST OF FIGURES

Figure 1.1.	Schematic illustration of normal cell division vs. cancer cell division. .	1
Figure 1.2.	Camptothecin in the lactone form and open carboxylate form.	2
Figure 1.3.	Binding of CPT to topo I and DNA.	3
Figure 1.4.	Structures of topotecan and irinotecan.	3
Figure 1.5.	Various drug delivery systems employed in polymer therapeutics.	4
Figure 1.6.	Schematic illustration of EPR effect.	6
Figure 1.7.	Polymer-drug conjugates.	8
Figure 1.8.	PEG-based conjugate of prothecan.	9
Figure 1.9.	Polymeric architectures which can be used for drug delivery.	10
Figure 1.10.	Passage of a polymer through a pore during renal filtration.	10
Figure 1.11.	Passage of a polymer through a pore.	11
Figure 1.12.	Star polymers.	11
Figure 1.13.	Methods for star polymer synthesis.	12
Figure 1.14.	Thiol reactive multiarm star polymers.	13
Figure 1.15.	Amphiphilic star shaped polymers.	14
Figure 1.16.	PEG star polymers with GRGDS.	15
Figure 1.17.	Mechanism of ATRP.	16
Figure 1.18.	Diels-Alder reaction.	16
Figure 1.19.	Thermoreversible segment block dendrimers.	17
Figure 1.20.	Polymeric immuno-nanoparticles.	18
Figure 1.21.	Release of the drug from dendrimers.	19
Figure 1.22.	Lipoic acid conjugated dendrimers.	20
Figure 2.1.	General scheme of project.	21

Figure 3.1. Synthesis of the 4-armed initiator. 22

Figure 3.2. ^{1}H NMR spectrum of the 4-armed initiator. 23

Figure 3.3. Synthesis of the first generation dendrimer. 23

Figure 3.4. ^{1}H NMR spectrum of the first generation dendrimer 2. 23

Figure 3.5. Deprotection of first generation dendrimer. 24

Figure 3.6. ^{1}H NMR spectrum of the deprotected first generation dendrimer 3. 24

Figure 3.7. Synthesis of the 8-armed initiator. 25

Figure 3.8. Structure of the 6-armed initiator. 25

Figure 3.9. Synthesis of polymers with 4-armed initiator. 26

Figure 3.10. ^{1}H NMR spectrum of the 4-armed star polymer (P1). 27

Figure 3.11. GPC traces of P2 and P4. 27

Figure 3.12. Attachment of N-Ethylmaleimide. 29

Figure 3.13. ^{1}H NMR spectrum of N-Ethylmaleimide conjugated polymer (exo). 30

Figure 3.14. ^{1}H NMR spectrum of N-Ethylmaleimide conjugated polymer (endo/exo mixture). 30

Figure 3.15. Structure of BODIPY-maleimide. 31

Figure 3.16. ^{1}H NMR spectrum of BODIPY-maleimide conjugated polymer (exo)... 32

Figure 3.17. ^{1}H NMR spectrum of BODIPY-maleimide conjugated polymer (endo/ exo mixture). 32

Figure 3.18. UV spectrum of BODIPY-maleimide conjugated polymer. 33

Figure 3.19. UV spectrum of physically entrapped BODIPY-maleimide. 34

Figure 3.20. UV spectrum for release studies of the dye from polymer (endo/exo mixture). 35

Figure 3.21. UV spectrum for release studies of the dye from polymer (exo). 35

Figure 3.22. Proposed mechanism for drug conjugation to polymers. 36

Figure 3.23. Synthesis of linker for drug attachment. 37

Figure 3.24. ^{1}H NMR spectrum of linker before retro Diels-Alder. 37

Figure 3.25. ^{1}H NMR spectrum of linker after retro Diels-Alder. 38

Figure 4.1. Synthesis of the 4-arm initiator. 40

Figure 4.2. Synthesis of the first generation dendrimer. 41

Figure 4.3. Deprotection of first generation dendrimer. 41

Figure 4.4. Synthesis of the 8-arm initiator. 42

Figure 4.5. Synthesis of polymers with 4-armed initiator. 43

Figure 4.6. First step of synthesis of linker. 49

Figure 4.7. Second step of synthesis of linker. 50

.

LIST OF TABLES

Table 1.1. Polymer-drug conjugates at the market. 7

Table 3.1. Synthesis and characterization of star polymers. 28

LIST OF ACRONYMS/ABBREVIATIONS

ATRP	Atom transfer radical polymerization
Bis-MPA	2,2-bis(hdroxymethyl)propionic acid
BODIPY	Boron-dipyrromethene
$CDCl_3$	Deuterated chloroform
CH_2Cl_2	Dichloromethane
DA	Diels-Alder
DEGMA	Di(ethylene glycol) monomethyl ether methacrylate
DMAP	4-Dimethylaminopyridine
EPR	Enhanced Permeability and Retention
FT-IR	Fourier Transform Infrared
FUMA	Furfuryl methacrylate
GPC	Gel Permeation Chromotography
MeOH	Methanol
MHz	Mega hertz
NMR	Nuclear Magnetic Resonance
P	Polymer
PEGMA	Poly(ethylene glycol) monomethyl ether methacrylate
rDA	Retro Diels-Alder
TEA	Triethylamine
THF	Tetrahydrofuran
TLC	Thin Layer Chromatography
UV	Ultraviolet

LIST OF SYMBOLS

J	Coupling constant
υ	Frequency

1. INTRODUCTION

1.1. Cancer and Chemotherapy

Cancer is a leading cause of death and is accounted for 7.6 million deaths which corresponds to around 13% of all deaths worldwide in 2008 [1]. It is a general term used for a group of diseases which involve unregulated cell growth. Normal cells grow and divide in a controlled way and when they become damaged by mutations they kill themselves by apoptosis. But in the case of cancerous cells, when mutations which affect the normal cell division process occur, the cell starts to proliferate in an uncontrollable manner leading to the formation of a malignant tumor (Figure 1.1). Cancerous cells have the capability of invading nearby tissue and spreading throughout the body by the lymphatic system [2].

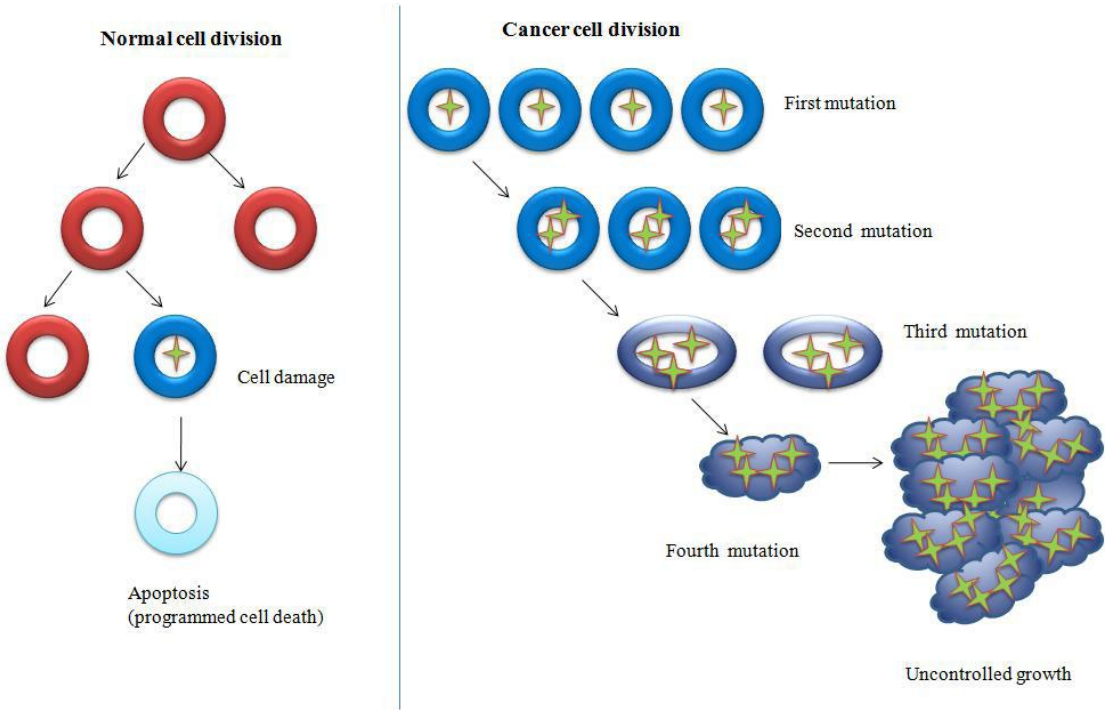

Figure 1.1. Schematic illustration of normal cell division vs. cancer cell division [2].

Chemotherapy is the treatment of cancer using chemicals. Since cancerous cells divide rapidly, chemotherapeutic drugs work by inhibiting the cell division process. But

unfortunately chemotherapeutic drugs cannot distinguish normal cells from cancerous cells. So the chemotherapy results in the inhibition of cell division process of not only cancer cells, but also other cells which divide rapidly under normal circumstances. These rapidly dividing cells include bone marrow, hair follicles, lining of the digestive tract. The side effects of chemotherapy resulting from the toxicity of chemotherapeutic drugs to normal cells, limit the dose which can be given to the patient. In other words, chemotherapy is a delicate balance between toxicity and effectiveness. Currently, researchers are seeking ways of reducing toxicity and increasing effectivenes of chemotherapy [3].

1.1.1. Camptothecin

20-(*S*)-camptothecin (CPT) is a chemotherapy agent which was isolated from the bark of *Camptotheca acuminata* by Wall and Wani in 1966 [4]. It is a cytotoxic quinoline alkoloid with appreciable anticancer activity (Figure 1.2).

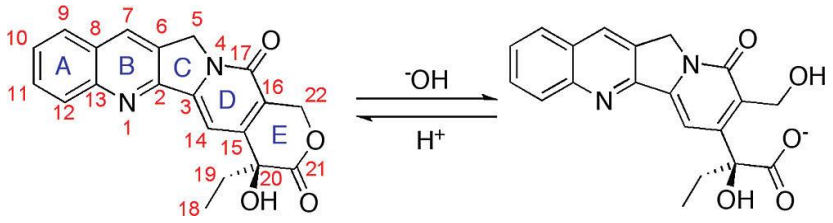

Figure 1.2. Camptothecin in the lactone form and open carboxylate form [5].

The mechanism of action of CPT was discovered in the late 1980s. It was found that CPT inhibits the DNA enzyme topoisomerase I by binding to its appropriate sites through H bonding (Figure 1.3). This situation prevents DNA religation and causes apoptosis. The open carboxylate form of CPT is inactive, so the molecule must be in the closed lactone form to maintain its activity and inhibit topoisomerase I. Fortunately, the closed lactone form is favored in acidic conditions which is present in cancer cell microenvironment [6].

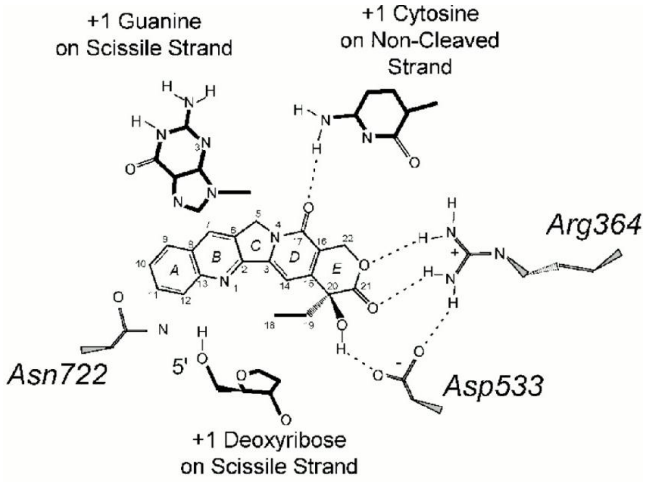

Figure 1.3. Binding of CPT to topo I and DNA [7].

In order to improve properties such as water solubility and stability, many derivatives of CPT have been synthesized. Although there are many analogues in clinical trials, currently there are only two CPT analogues, irinotecan and topotecan, which are approved for clinical use (Figure 1.4). Irinotecan is used in the treatment of metastatic colorectal cancer. Topotecan is used for ovarian, cervical and small-cell lung cancer [5].

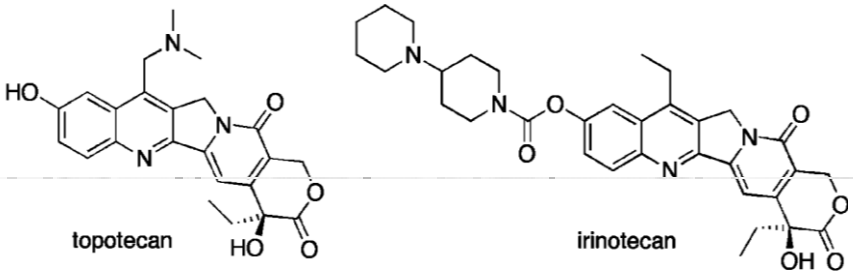

Figure 1.4. Structures of topotecan and irinotecan [5].

1.2. Polymer Therapeutics

The attempts of the researchers to improve efficacy and reduce toxicity of cancer therapy together with the advances in polymer chemistry lead to an innovative and interdisciplinary approach named as "Polymer Therapeutics". This is a comprehensive concept which is used to describe polymeric drugs, polymer-drug conjugates, polymer-protein conjugates and polymeric micelles (Figure 1.5) [8].

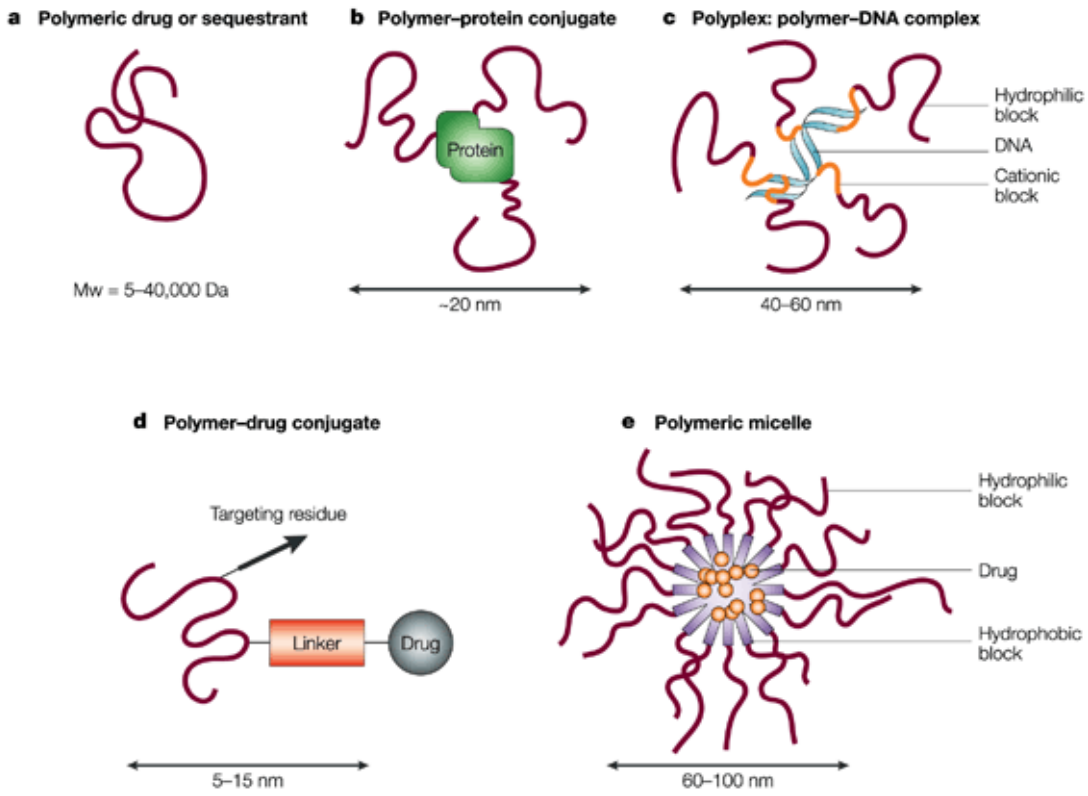

Figure 1.5. Various drug delivery systems employed in polymer therapeutics [8].

The idea of conjugating drugs to polymers was introduced by Ringsdorf in 1975, and has attracted the attention of researchers ever since. According to Ringsdorf's model the polymer should be biocompatible and biodegradable and the drugs should be attached to the backbone via a cleavable linker. Additionally the polymer should have solubilizing groups and targeting moeities [9]. Research on polymer-drug conjugates has increased rapidly especially in the last decades, and still remains as a hot topic.

The increasing interest in polymer-drug conjugates arises from the solutions it offers to problems related to conventional chemotherapy. These problems include short half-life due to rapid elimination, low solubility and toxicity to healthy cells [10]. First of all, common chemotherapeutic drugs have a low molecular weight, so they have a short half-life in the blood stream and they are rapidly eliminated. Conjugating drugs to large molecular weight polymers reduces their elimination and prolonges their half-life, resulting in a better pharmacokinetic profile. This situation increases the efficacy of chemotherapy. Chemotherapeutic drugs generally have a hydrophobic nature and require toxic solubilizers in drug formulation. To solubilize chemotherapeutic drugs, conjugating them to a water soluble polymer is a common approach. Polymers chosen for the preparation of drug–polymer conjugates should ideally be water-soluble, nontoxic and nonimmunogenic. Poly(ethylene glycol) (PEG), Poly(Hydroxypropyl methacrylate) (HPMA) and Poly(glycolic acid) (PGA) are widely used polymers for drug conjugation.

Toxicity is another major problem related to chemotherapy. Since chemotherapeutic drugs cannot distinguish normal cells from cancerous cells, all rapid dividing cells get affected and this situation causes serious side effects to the patient receiving chemotherapy. Furthermore, the toxicity of the drug to healthy tissue limits the dose which can be administered to the patient. The use of polymer-drug conjugates helps to reduce the toxicity problem. Conjugating chemotherapeutic drugs to polymers localize the drug concentration at one place and decreases the distribution of the drug to healthy tissues. The polymer-drug conjugate accumulates in the tumor tissue due to a phenomenon called “enhanced permeability and retention effect” (EPR effect) which will be discussed in the following section. After accumulation in tumor tissue, the drug is released from the polymer just at the right place for maximum effectiveness and minimum toxicity for healthy tissue.

Another benefit of using polymer-drug conjugates is the possibility of attaching a targeting group, such as an antibody specific for the receptors which are overexpressed on the cancerous cells. This will enhance the accumulation of the polymeric construct in cancer tissue.

1.2.1. Enhanced Permeability and Retention Effect

The idea of using macromolecules which do not contain targeting groups as drug delivery vehicles, is based on pioneering work of Maeda and co-workers [11]. They had synthesized a polymer–protein conjugate with styrene maleic anhydride (SMA) and neocarzinostatin (NCS) with a molecular weight of 16000 g mol^{-1}. Their aim was to hydrophobize the anti-tumor protein NCS and make a dispersion, but during pharmacokinetic studies, they realized that SMANCS had a liver tumor : blood ratio > 2500. Maeda named this concept of passive accumulation of macromolecules as 'enhanced permeability and retention effect' (EPR effect).

The rationale behind this idea lies on the differences in anatomical and physiological properties of healthy and tumor tissue (Figure 1.6). In healthy tissue the endothelium cells on the walls of blood vessels are in an ordered and continuous structure. But in the case of tumour tissue, they are disorded, discontinuous and permeable to macromolecules. The reason of this defective structure is the rapid vascularization to provide oxygen and nutrients to fast growing cancer cells. Furthermore, there is a lack of lymphatic drainage at tumor tissue which leads to accumulation of macromolecules.

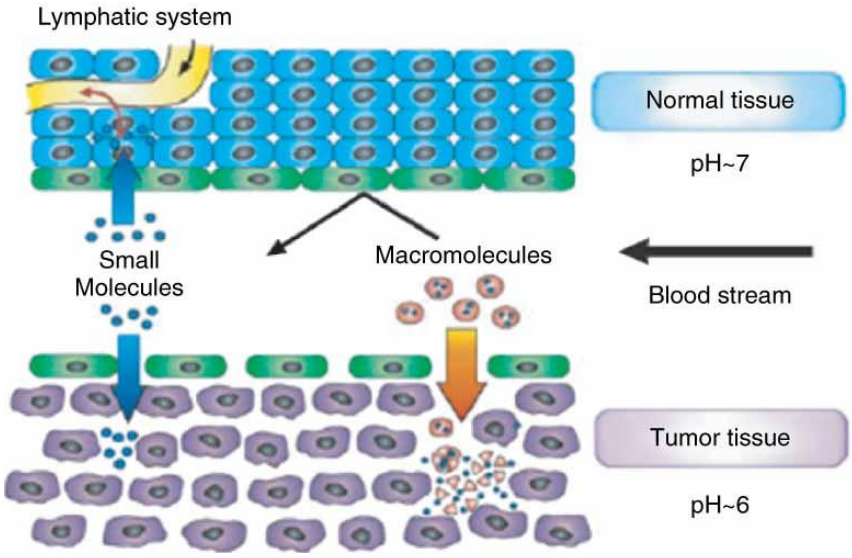

Figure 1.6. Schematic illustration of EPR effect [12].

Small moleules are able to diffuse through the endothelium cells on the walls of the blood vessels and enter both the healthy and tumor tissue. On the other hand,

macromolecules cannot pass through the blood vessels to enter healthy tissue, but they can only enter to tumour tissue due to the physiological differences stated above. Furthermore, after the macromolecules enter tumor tissue, they accumulate there because of the lack of lymphatic drainage.

1.2.2. Clinical Trials With Polymer- Drug Conjugates

Many polymer-drug conjugates have entered clinical trials and some of them have even reached the market since research in the field of polymer therapeutics has started (Table 1.1) [13]. Still there is a large number of ongoing studies with novel polymeric architectures.

Table 1.1. Polymer-drug conjugates at the market [14].

Compound	Polymer	M mass (g/mol)	Linker	Drug (loading)	Cleavage Conditions
XYOTAX	Poly-L-glutamic acid	40000	Ester	Paclitaxel (37 wt%)	PGA degraded by cathepsin B and ester linker by esterases or acid hydrolysis
PK1	HPMA copolymer	30000	Amide	Doxorubicin (8.5 wt%)	Thiol protease cathepsin B
PK2	HPMA copolymer	25000	Amide	Doxorubicin (7.5 wt%) and galactosamine (1.5-2.5 mol%)	Thiol protease cathepsin B
AP5280	HPMA copolymer	25000	Malonate	Pt (7 wt%)	Hydrolysis
AP5346	HPMA copolymer	25000	Malonate-DACH	Pt (7 wt%)	Hydrolysis
CT2106	Poly-L-glutamic acid	40000	Ester	Camptothecin (33-35 wt%)	PGA degraded by cathepsin B and ester linker by esterases or acid hydrolysis
PROTHECAN	PEG	40000	Ester	Camptothecin (1.7 wt%)	Esterases or acid hydrolysis

A doxorubicin-HPMA polymer conjugate named as PK1 is the first polymer-drug conjugate which entered clinical trials. PK1 has a molecular weight of approximately 30kDa and is conjugated to doxorubicin through a peptidyl linker, Gly-Phe-Leu-Gly. According to phase I trials, the maximum tolerated dose (doxorubicin equivalent) has a five-fold increase relative to the standard dose of the free drug. Also pharmacokinetic

studies confirmed prolonged plasma half-life of the polymer –drug conjugate. PK2 is a polymer–drug conjugate similar to PK1, but contains galactosamine as a targeting ligang. Galactosamine targets hepatocyte asialoglycoprotein receptor with the aim of treating liver cancer [15]. Other polymer-drug conjugates with HPMA polymer are AP5280 and AP5286 which contain a diamine- or a diaminocyclohexaneplatinum(II) group respectively. The drugs are linked to a 25kDa HPMA polymer via the peptidyl linker Gly-Phe-Leu-Gly which is sensitive to the protease cathepsin B. Studies revealed a high antitumor efficacy and increased maximum tolerated dose relative to standard dose of the free drug [16].

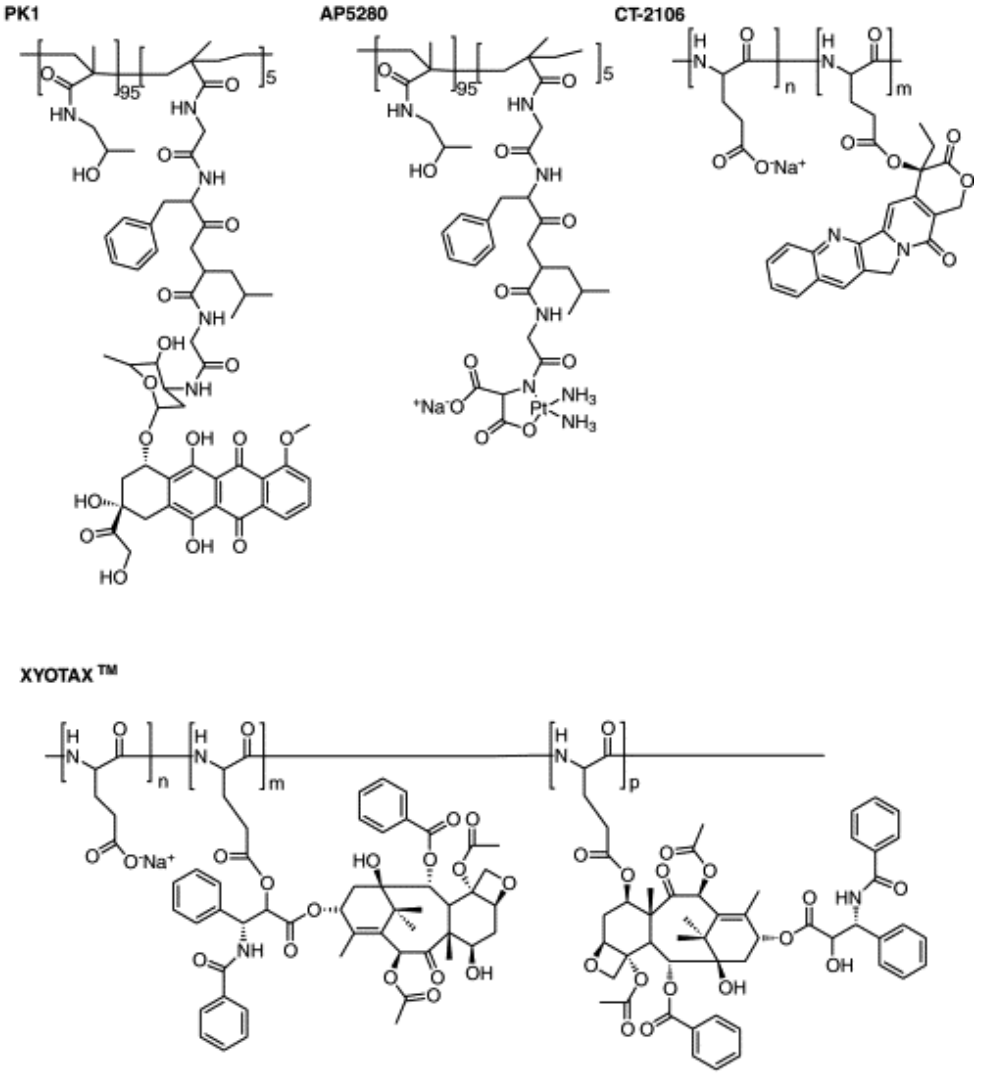

Figure 1.7. Polymer-Drug conjugates [14]

CT-2103 (Opaxio, formerly known as Xyotax) consists of polyglutamate as the polymer and paclitaxel as the chemotherapeutic drug. Paclitaxel is linked to polyglutamate

through an ester bond with a high percent of loading. Polyglutamate, is biodegradable and has a molecular weight of 40kDa. The release of the drug can be either by acidic hydrolysis or esterases [17].

Prothecan is a polymer-drug conjugate consisting of 40kDa PEG as the polymer and camptothecin as the drug (Figure 1.8). Since PEG has only two reactive sites at the ends for drug conjugation, the polymer-drug conjugate has a very low loading capacity. It has a drug content of 1.7 wt% [18].

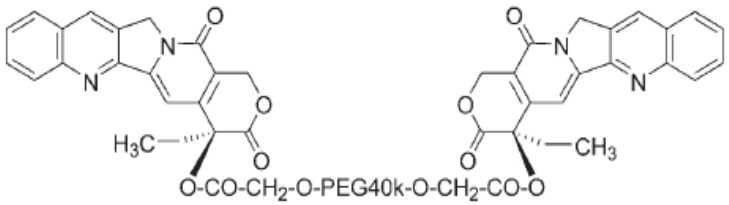

Figure 1.8. PEG-based conjugate of prothecan [12].

1.2.3. Polymeric Architectures For Drug Delivery

Recent progress in polymer and macromolecular chemistry has provided opportunities towards the synthesis of constructs for drug delivery purposes with innovative architectures and advanced functionalities. Researchers tailor the constructs with the appropriate molecular weight, flexibility and molecular conformation suitable for the intended application. Commonly used polymeric architectures include graft polymers, star polymers, multivalent polymers, dendrimers and dendronized polymers (Figure 1.9).

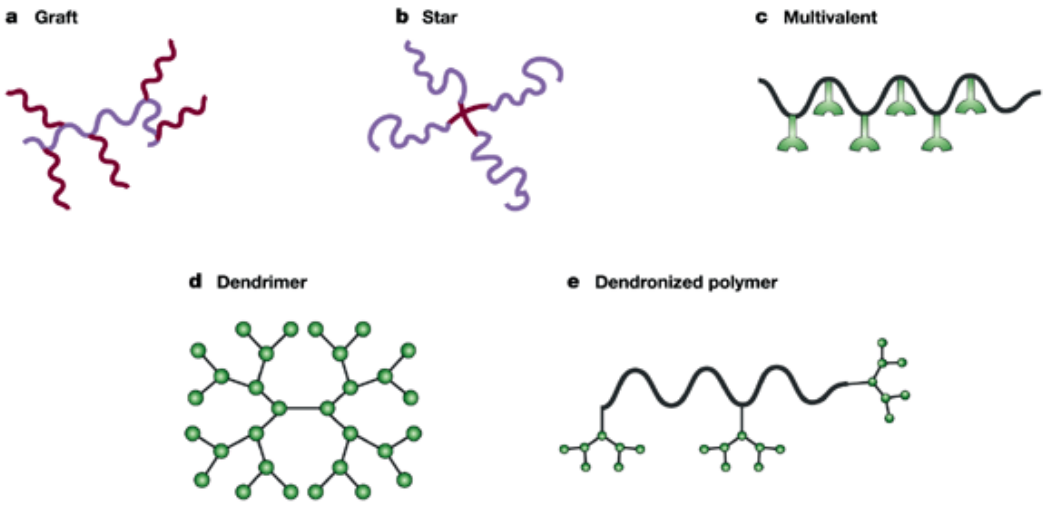

Figure 1.9. Polymeric architectures which can be used for drug delivery [8].

Among the diverse choice of architectures the branched ones, especially star polymers and dendrimers, have superior residence time in the bloodstream when compared to their linear analogues. Rigid and spherical polymers have decreased renal filtration and longer blood circulation time, whereas flexible and elongated polymers are filtered rapidly. Furthermore increasing the number of polymer arms increases blood circulation time due to decreased pore penetration during renal filtration (Figure 1.10) [19].

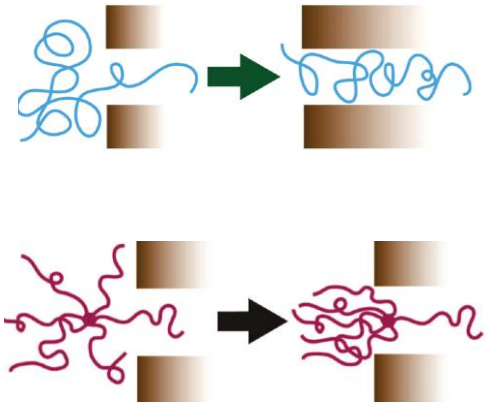

Figure 1.10. Passage of a polymer through a pore during renal filtration [19].

The graph below shows the effect of molecular architecture on plasma half-life (Figure 1.11). Polymers with globular and branched structures have a higher plasma half life as indicated in the red regions. On the other hand, the linear polymers represented in the blue regions are cleared rapidly from the body.

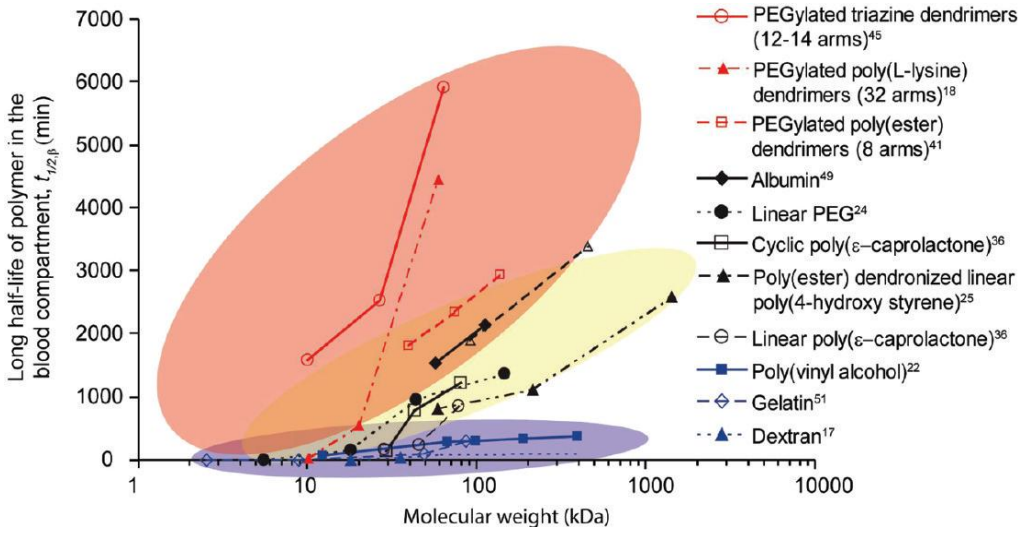

Figure 1.11: Passage of a polymer through a pore [19].

1.3. Star Polymers

Star polymers are globular molecules which are composed of a multiple number of linear polymers chains that are connected to each other at the core (Figure 1.12). The compact and globular structure of star polymers provide them some special properties. Star polymers have a multiple number of arms, thus giving them a large oppurtunity for functionalization purposes.



Figure 1.12. Star Polymers [20].

Star polymers can be synthesized by three different approaches, namely “core-first”, “arm-first” and “coupling-onto” methods (Figure 1.13). In the “core-first” method, a multifunctional initiator (the core) initiates the polymerization resulting in a star polymer with a well defined shape and pre-determined number of arms. In the “arm-first” method, either linear living polymer chains are used as a macroinitiator and a divinyl compound is added to form a crosslinked core; or a small initiator molecule is added to a macromonomer. This method results in relatively ill defined structures. In the "coupling-onto" method a core molecule is reacted with a linear polymer chain which has a suitable end group for the coupling reaction. This method suffers from low reaction efficiency due to steric hinderance around the core.

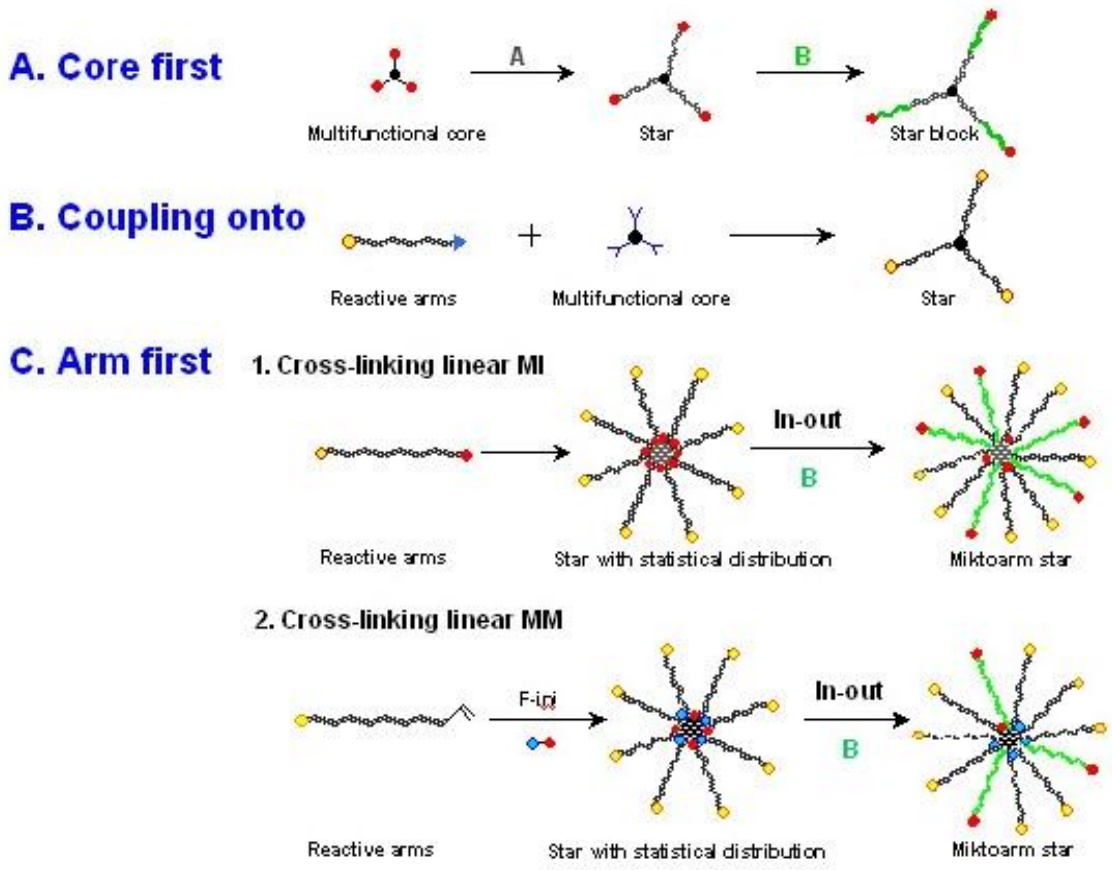

Figure 1.13. Methods for Star Polymer Synthesis [20].

Our research group synthesized thiol-reactive multiarm star polymers via "core-first" method Figure (1.14) [21]. Firstly, different generations of dendritic initiators which have a masked maleimide moeity at their core were synthesized. These dendritic initiators were polymerized by ATRP and then mask at the core was removed resulting in star polymers with a maleimide core which is thiol reactive. The functionalization was done by bioconjugation of a thiol containing tripeptide, glutathione, to the core of these star polymers.

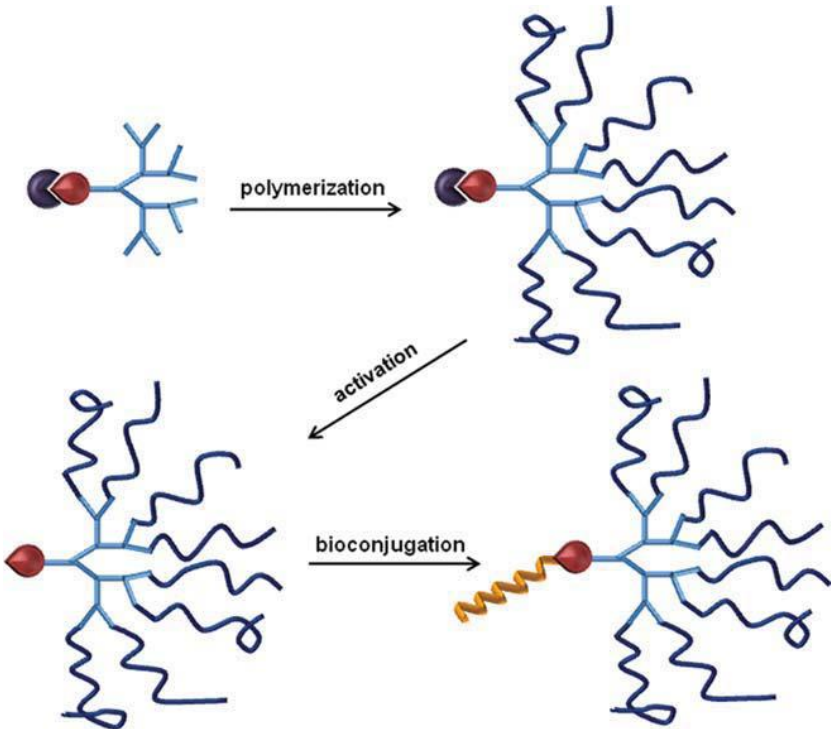

Figure 1.14. Thiol reactive multiarm star polymers [21].

Schubert group synthesized amphiphilic star-shaped polymers with dense hydrophilic shells by a combination of ring opening polymerization and ATRP (Figure 1.15) [22]. They used the "core-first" method leading to the formation of well-defined 4-, 6-, 8-, and 12-arm star PCL*p*PEGMAs. The presence of PEG at the shell makes the whole system a promising candidate for drug delivery applications

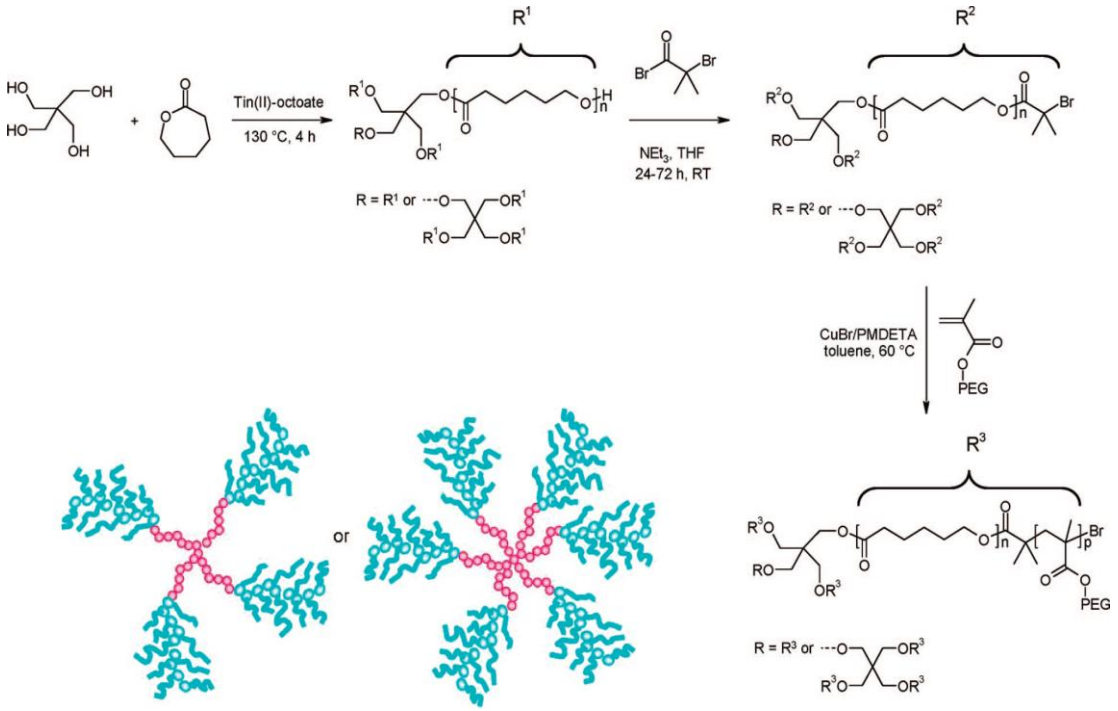

Figure 1.15. Amphiphilic star shaped polymers [22].

Matyjaszewski group synthesized PEG star polymers which contain GRGDS (Gly-Arg-Gly-Asp-Ser) peptide sequences on the periphery by ATRP of poly(ethylene glycol) methyl ether methacrylate (PEGMA), GRGDS modified poly(ethylene glycol) acrylate, fluorescein *o*-methacrylate (FMA), and ethylene glycol dimethacrylate (EGDMA) as the crosslinker via "arm-first" method (Figure 1.16) [23]. The light scattering and atomic force microscopy indicated that the star polymers were approximately 20 nm in diameter. These star polymers were cultured with MC3T3-E1.4 cells and were biocompatible. Uptake of PEG star polymers by MC3T3-E1.4 cells were observed by confocal microscopy and flow cytometry. The results suggest that these functional star polymers have a potential use as a drug delivery system.

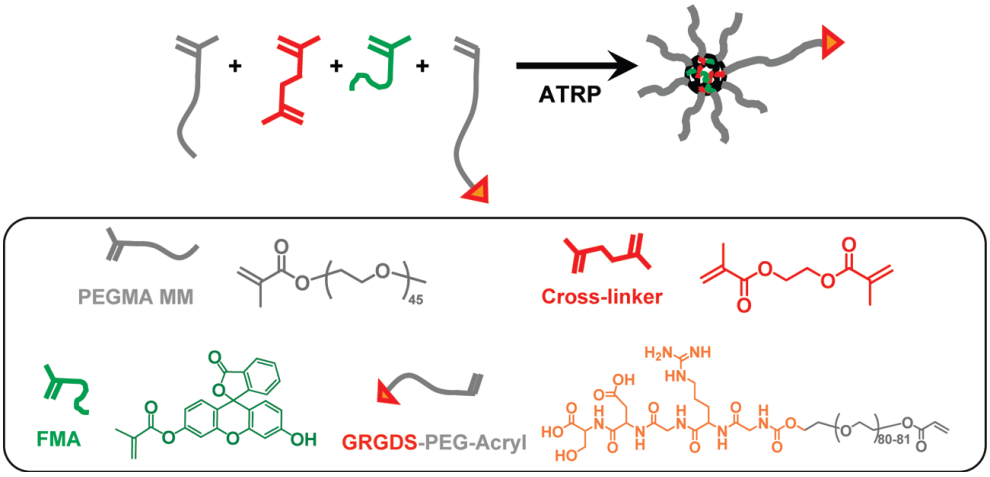

Figure 1.16. PEG star polymers with GRGDS [23].

1.4. Atom Transfer Radical Polymerization

Atom transfer radical polymerization (ATRP) is a kind of controlled/living radical polymerization (CRP) technique. It was discovered by Mitsuo Sawamoto and Krzysztof Matyjaszewski in 1995. ATRP has captured attention of scientist due to its advantages and became one of the most popular CRP methods. ATRP allows scientists to easily control the composition and architecture of polmers to create highly specific materials to be used in many appliations from coatings and adhesives to environmental, biotechnological and medical areas.

The components of ATRP are the monomer, initiator with a transferable halogen atom, and a catalyst which is composed of a transition metal species and ligand. The atom transfer step is the reason for the controlled chain growth. The catalyst provides an equilibrium between the active (propagating) and inactive (dormant) form of the polymer. This equilibrium mechanism reduces the concentration of propagating polymer chains and therefore minimizes termination steps (Figure 1.17) [24].

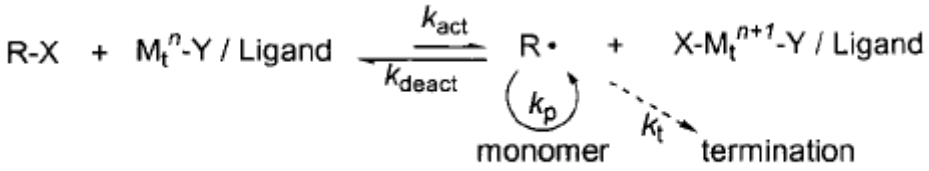

Figure 1.17. Mechanism of ATRP [24].

1.5. Diels-Alder Reaction

Diels-Alder (DA) reaction is the [4+2] cycloaddition of a conjugated diene and a dienophile that involves the 4 π-electrons of the diene and 2 π-electrons of the dienophile (Figure 1.18) [25]. It is an electrocyclic reaction in which new σ-bonds are formed that are energetically more stable than the π-bonds. Diels-Alder reaction is a reaction that is widely used in synthetic organic chemistry due to its high yields without formation of offensive side products.

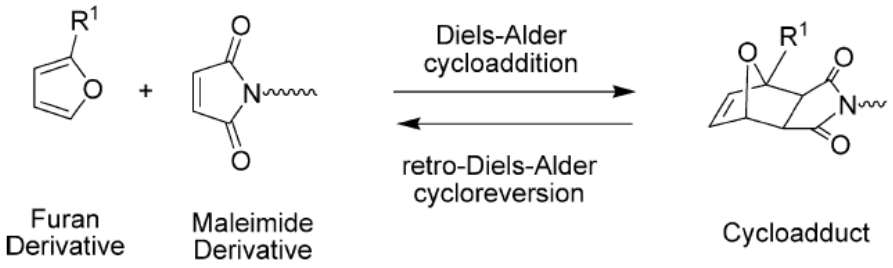

Figure 1.18. Diels-Alder Reaction [26].

Diels-Alder reaction forms two stereoisomers named as the *endo* and *exo* products. The endo product is the kinetically controlled product with a lower activation energy due to the orbital overlap in transition state. It is favored at low temperatures. On the other hand, the exo product is the thermodynamicallly controlled product due to the formation of a more stable final conformation with less steric hinderance. It is favored at high temperatures.

Besides the stated advantages above, it is possible to shift the reaction towards the reactants by only increasing the heat. The reverse reaction is named as retro Diels-Alder

reaction (rDA). This property of Diels-Alder reaction makes it useful in contruction of thermoreversible systems especiaaly in polymer chemistry.

1.5.1. Diels-Alder Reaction in Polymer Chemistry

Our group synthesized unsymmetrical segment block dendrimers composed of polyester and polyaryl ether dendrons via Diels-Alder reaction (Figure 1.19) [27]. Three generations of polyaryl ether dendrons with a furan group at the core were reacted with polyester dendrons of same generation which contain a maleimide group at their core. The Diels-Alder reaction gave good yields and no offensive side products such as metal impurities. The thermoreversibility of these macromolecular systems were investigated by exposing them to high temperatures in the presence of a scavenger group. Anthracene was used as a scavenger diene to prevent reassembly of the dendrons because it binds irreversibly to maleimide.

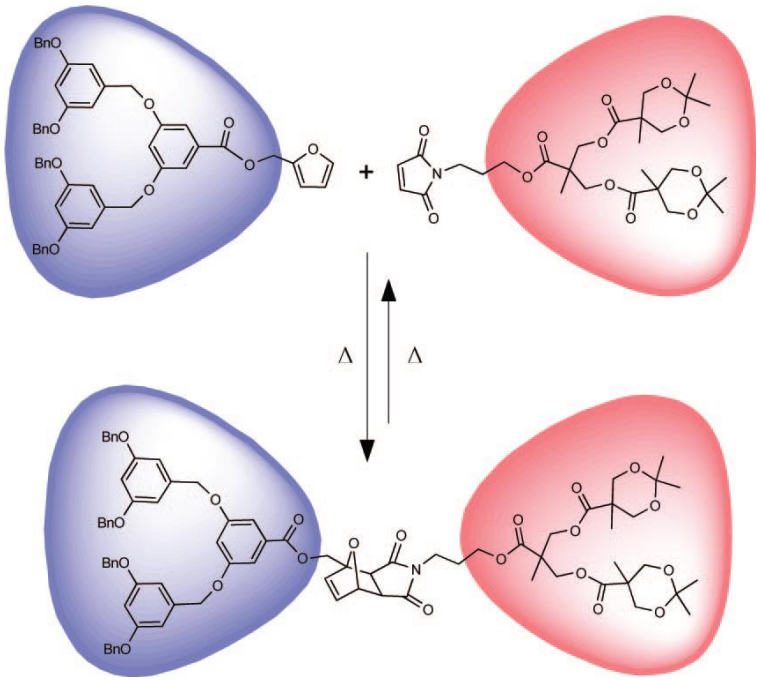

Figure 1.19. Thermoreversible segment block dendrimers [27].

Shoichet group synthesized nanoparticles which have furan groups on the peripheral PEG chains Figure (1.20) [27]. These furan groups can easily react with an antibody which contains a maleimide group through Diels-Alder reaction. Here Diels-Alder reaction is especially useful for conjugation of sensitive antibodies due to its highly selective and efficient nature under mild conditions. An antibody used to treat breast cancer (anti-HER2) is used in this study. A biodegradable and biocompatible copolymer poly(TMCC-co-LA)-g-PEG-furan is designed to undergo self assembly to form the nanoparticle and then conjugation with the antibody is done.

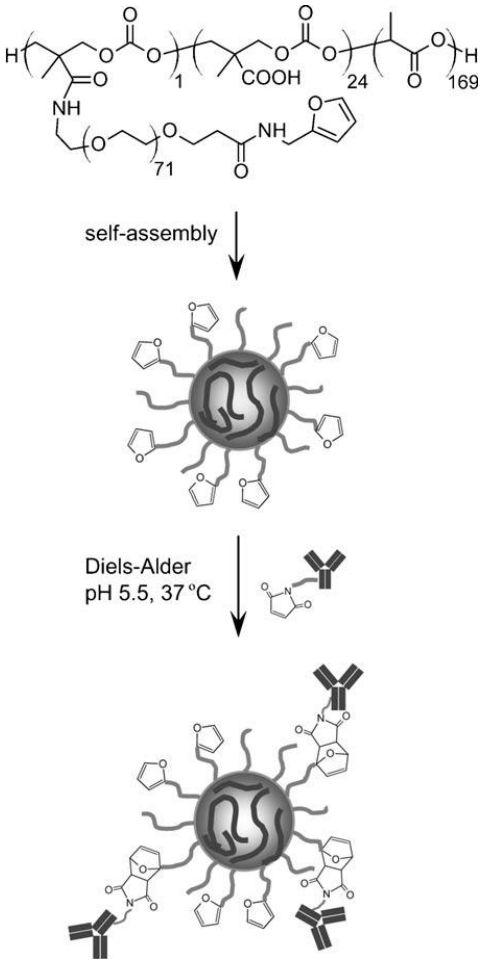

Figure 1.20. Polymeric immuno-nanoparticles [28].

Kakkar group investigated the reversible nature of Diels-Alder reaction for drug delivery purposes [29]. They synthesized different generations of dendrimers starting from the core by consecutive CuAAC and Diels-Alder click reactions. The periphery of the dendrimers contain furan groups. These furans were conjugated to an antioxidant molecule, lipoic acid (LA) derivative containing a maleimide unit (Figure 1.22). Lipoic acid was used as a model compound to demonstrate the release by retro Diels-Alder reaction at temperatures in the physiological and pathological range (37 – 42 ^{o}C). In the figure below, it can be clearly seen that at 37 ^{o}C nearly 40% and at 42 ^{o}C nearly 50% of the lipoic acid is released from the dendrimer (Figure 1.21).

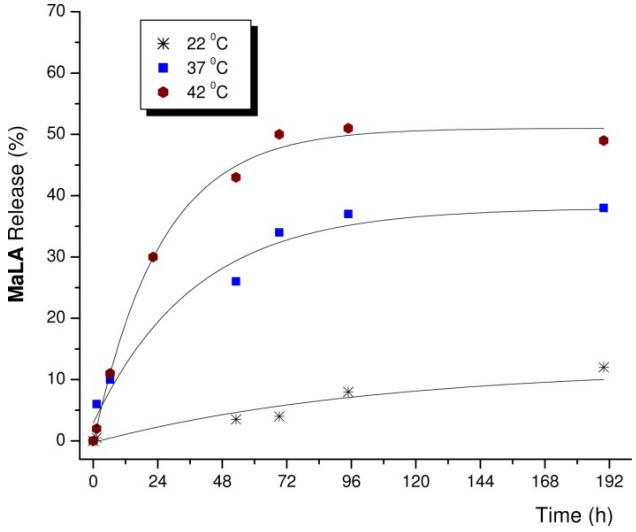

Figure 1.21. Release of the drug from dendrimers [29].

Further studies demonstrated that the released lipoic acid retained its activity and rescued microglia cells from oxidative stress. This thermosensitive dendrimer based platform is a good candidate for drug delivery applications.

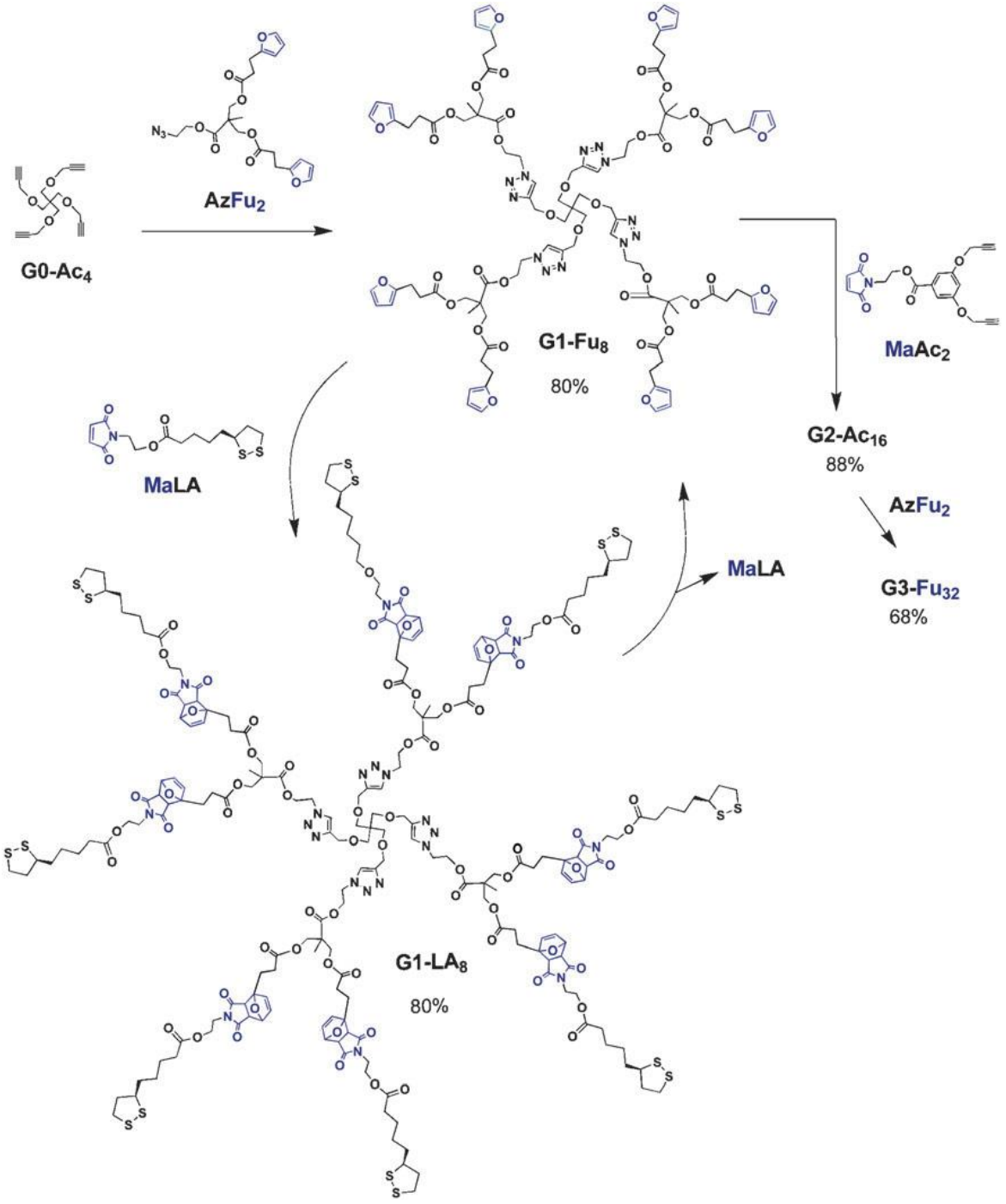

Figure 1.22. Lipoic acid conjugated dendrimers [29]

2. AIM OF THE STUDY

Star shaped reactive polymers have been synthesized from pentaerithritol based 4-arm and 6-arm dendritic initiators by atom transfer radical polymerization (ATRP) via "core first" approach. Copolymers of furfuryl methacrylate are synthesized either with diethylene glycol methyl ether methacrylate or polyethylene glycol methyl ether methacrylate to give water solubility to the polymer. The resulting polymers have pendant furan groups on side chains which are available to undergo Diels-Alder reaction with molecules bearing a maleimide group. Functionalization of polymers are done with different maleimide containing molecules such as ethyl maleimide and a fluorescent dye BODIPY-maleimide. The endo product of the Diels-Alder reaction undergoes retro Diels-Alder reaction at physiological temperature which makes this polymeric system a candidate for drug delivery purposes.

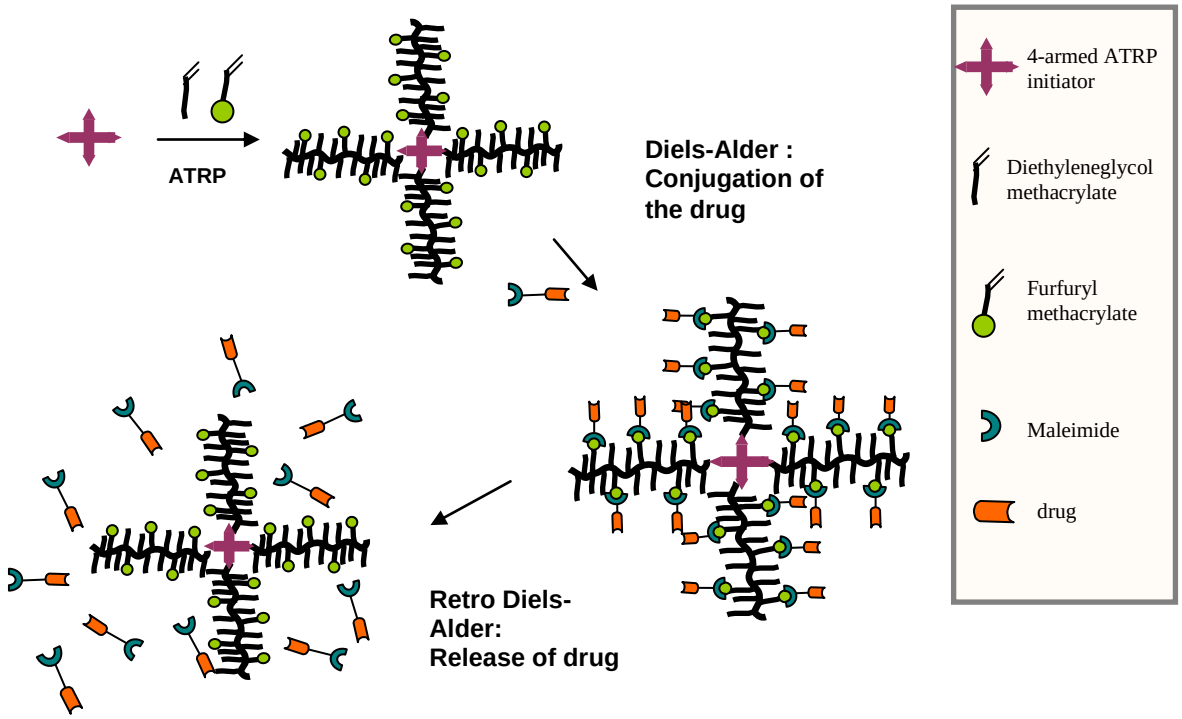

Figure 2.1. General scheme of project

3. RESULTS AND DISCUSSION

3.1. Synthesis of the Initiators

In order to synthesize the desired polymers, firstly the initiators were synthesized. Pentaerithritol is used as the core molecule to make the 4-armed initiator (1). The hydroxyl groups of pentaerithritol were esterified using 2-bromoisobutyryl bromide in the presence of triethylamine and DMAP to give the 4-armed initiator in a moderate yield (Figure 3.1). The product was obtained in high purity as evident from its ^{1}H NMR (Figure 3.2) and FT-IR (Figure A.2).

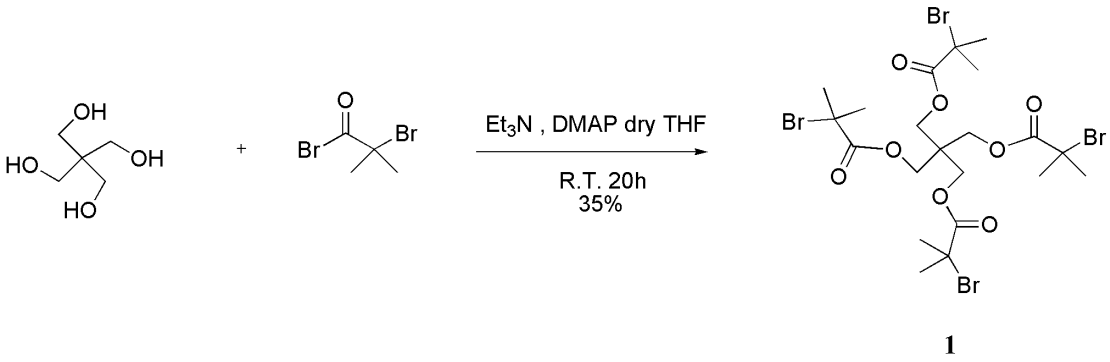

Figure 3.1. Synthesis of the 4-armed initiator.

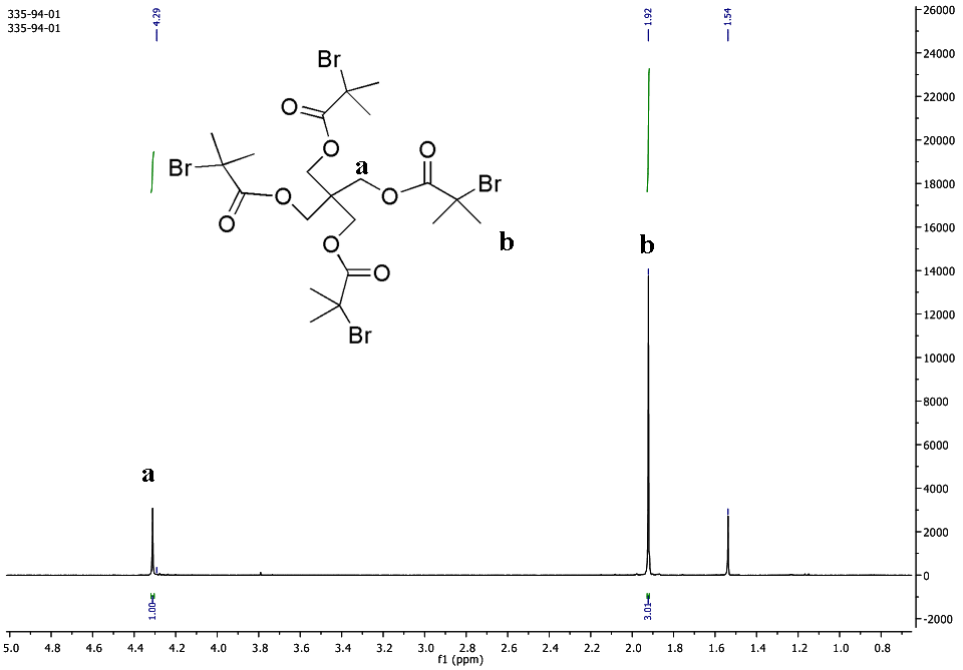

Figure 3.2. ^{1}H NMR spectrum of the 4-armed initiator.

To obtain the 8-armed initiator, the first generation polyester dendrimer was synthesized starting from pentaerithritol and bisMPA anhydride which is synthesized according to previously reported literature [27]. The esterification reaction was done by using DMAP and pyridine with dry CH_2Cl_2 as the solvent (Figure 3.3). The product was obtained with a high yield and was characterized by ^{1}H NMR (Figure 3.4) and FT-IR (Figure A.4).

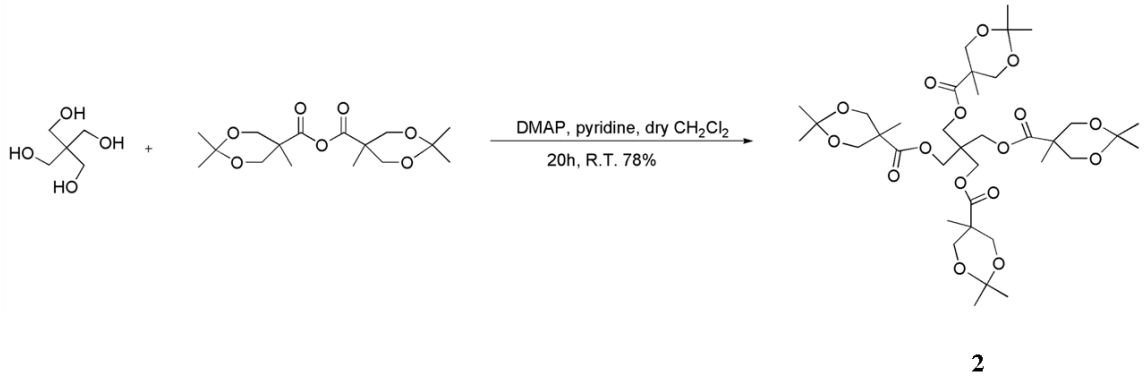

2

Figure 3.3. Synthesis of the first generation dendrimer.

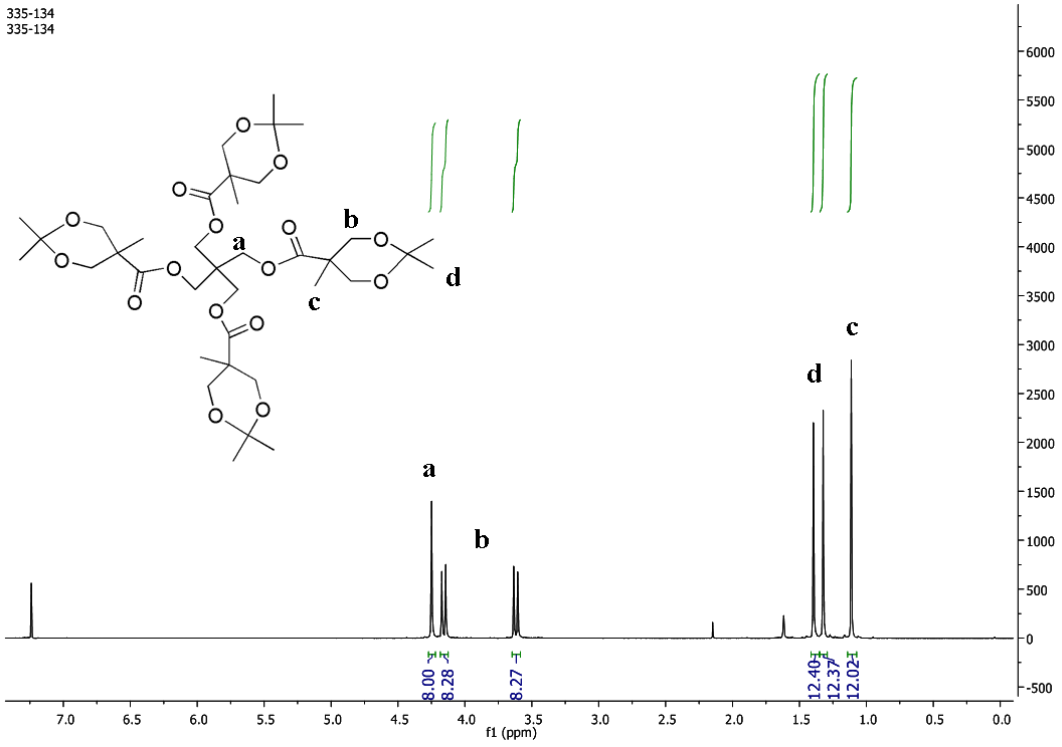

Figure 3.4. ^{1}H NMR spectrum of the first generation dendrimer 2.

Then the acetal protecting groups at the periphery of these polyester dendrimers were deprotected to polyols by acidic resin DOWEX 50W-X2 in MeOH (Figure 3.5). Dissappearance of peaks corresponding to the methyl groups of the acetals at 1.32 ppm and 1.40 ppm and formation of a peak corresponding to alcohol groups at 4.72 ppm in the ^{1}H NMR spectrum (Figure 3.6) indicate the successfull deprotection of the acetal groups. Also the FT-IR spectrum proves the presence of alcohol groups in the final structure (Figure A.4.).

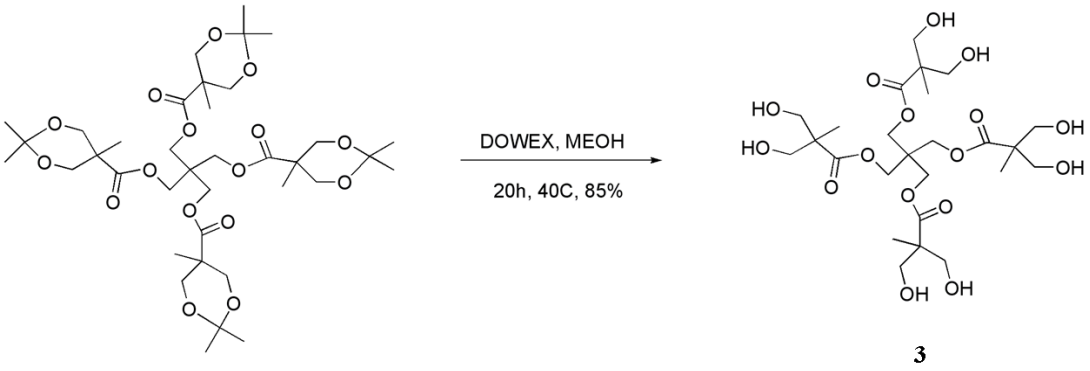

Figure 3.5. Deprotection of first generation dendrimer.

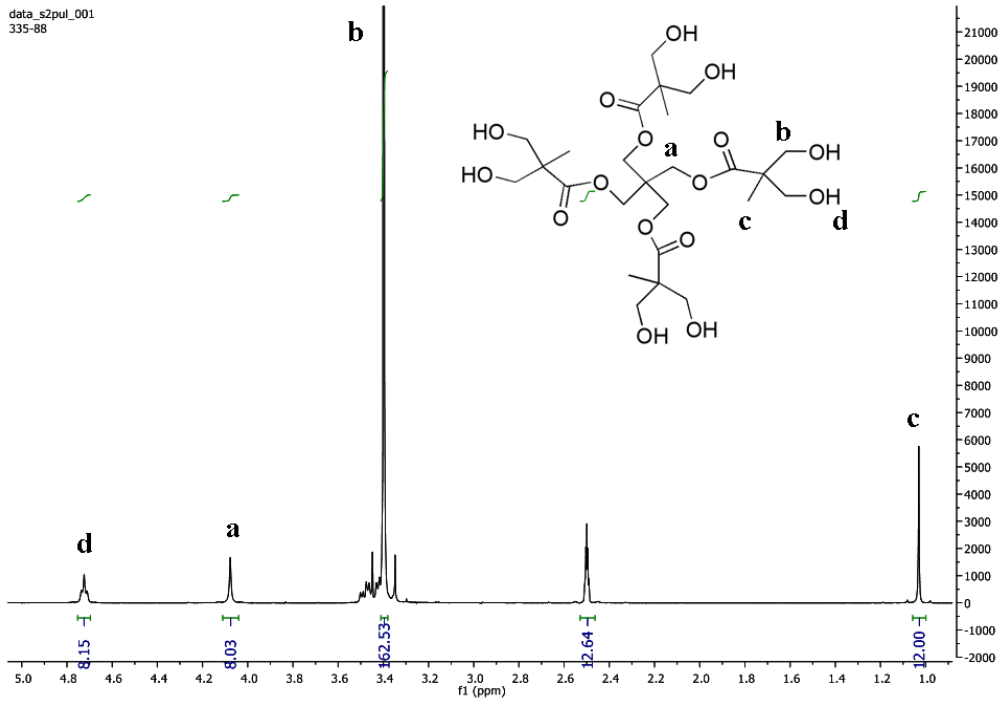

Figure 3.6. ^{1}H NMR spectrum of the deprotected first generation dendrimer 3.

Consequently, the hydroxyl groups at the periphery of dendrimers were esterified by 2-bromoisobutyryl bromide in the presence of triethylamine and DMAP to give the 8-armed initiator (4) (Figure 3.7). But unfortunately, the reaction did not work efficiently, and resulted in incomplete attachment of 2-bromo-isobutyryl bromide to the dendrimer probably due to steric hinderance around the core. Product 4 could not be isolated in pure form. Therefore we decided to use a 6-armed commercially available initiator, instead of the 8-armed initiator (4) that we tried to synthesize. The 6-armed initiator is based on a dipentaerithritol core (Figure 3.8).

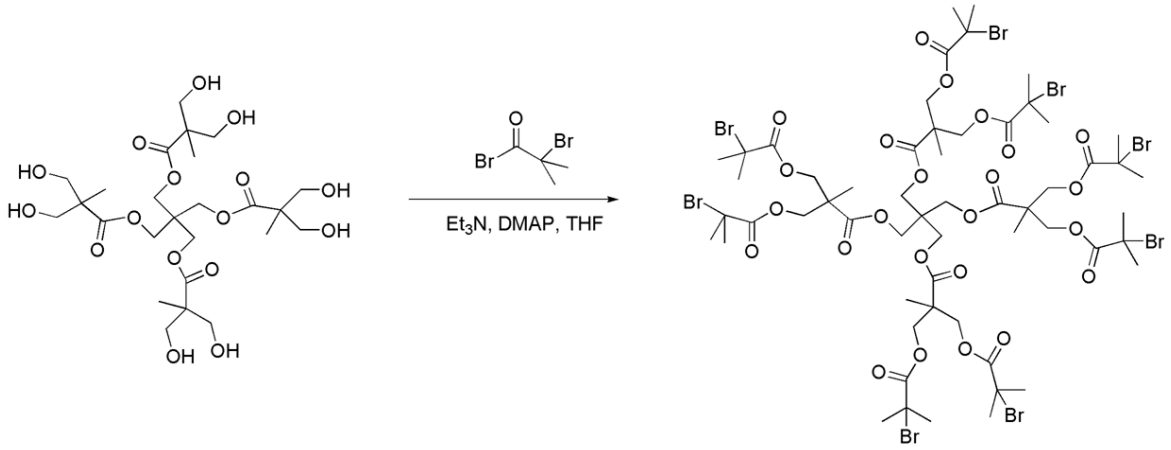

4

Figure 3.7. Synthesis of the 8-armed initiator.

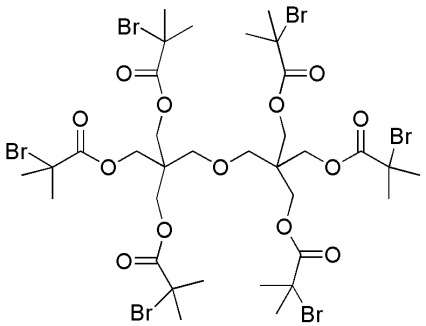

Figure 3.8. Structure of the 6-armed initiator.

3.2. Polymerizations by ATRP

Furfuryl methacrylate (FUMA) is chosen as a functional monomer due to its capability to undergo Diels-Alder reaction. Diels-Alder reaction is a widely used reaction in polymer and macromolecular chemistry, because it has high yields without formation of offensive side products. Furthermore the thermoreversible nature of Diels-Alder reaction enables the release of the attached molecules at elevated temperatures, which is especially useful in the design of smart delivery systems.

Furfuryl methacrylate is copolymerized either with diethylene glycol methyl ether methacrylate or polyethylene glycol methyl ether methacrylate. These monomers are both hydrophilic, when they are polymerized they form water-soluble, nontoxic and nonimmunogenic polymers suitable for biological applications. Polymerizations are done either with the 4-armed or 6-armed initiator (Figure 3.9).

For polymerizations, atom transfer radical polymerization (ATRP) is used as a controlled living polymerization technique. With ATRP it is possible to control the molecular weight and obtain monomodal polymers with low polydispersities. All the synthesized polymers were characterized with ^{1}H NMR and gel permeation chromatography (GPC).

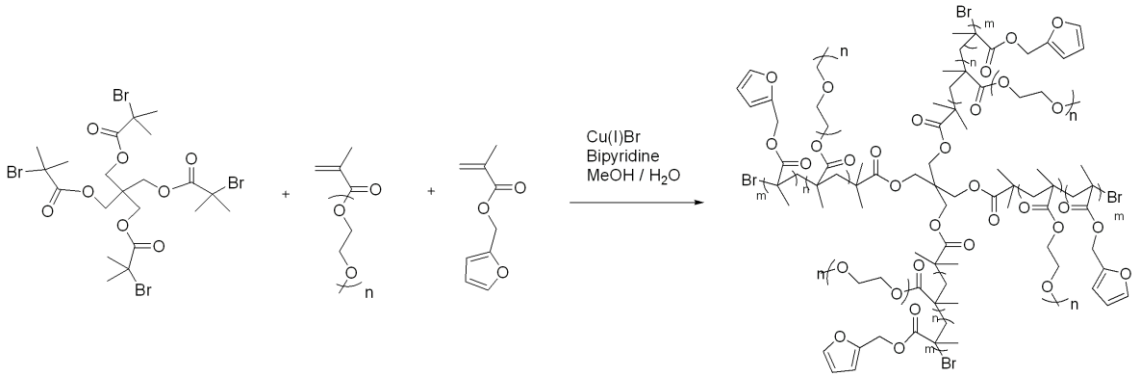

Figure 3.9. Synthesis of polymers with 4-armed initiator.

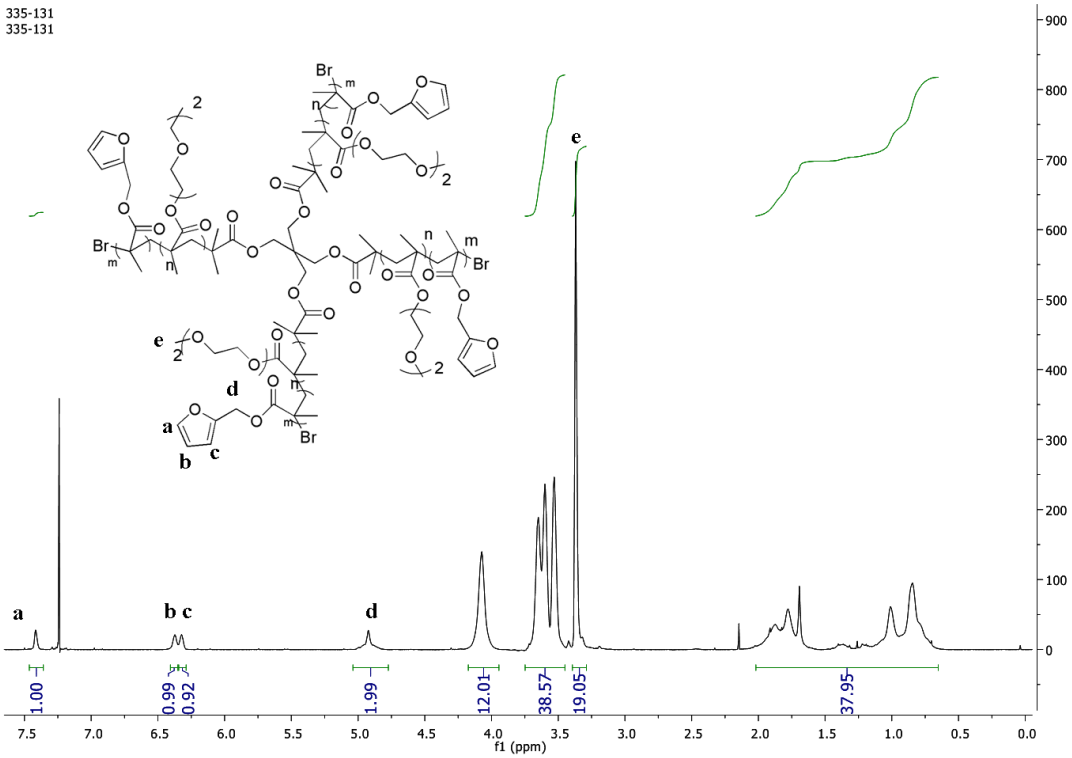

Figure 3.10. ^{1}H NMR spectrum of the 4-armed star polymer (P1).

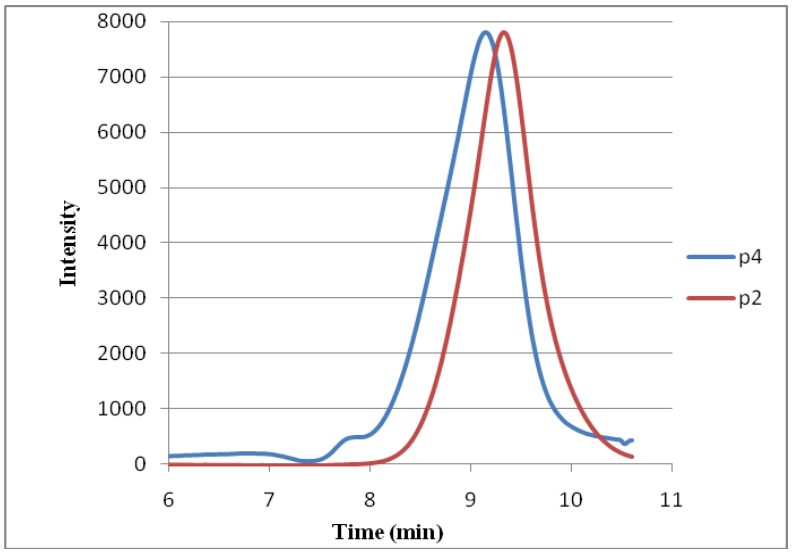

Figure 3.11. GPC traces of P2 and P4.

Table 3.1. Synthesis and characterization of star polymers.

Polymer [a]	Monomer Ratio (Feed)	Monomer Ratio (NMR)	$[M]_0/[I]_0$	[I]	Time (min)	Temp. (^oC)	Conv. (%)	GPC [b]		$M_{n,\,theo}$
								M_n (g/mol)	M_w/M_n	
P1	10% FUMA-90%DEGMA	14% FUMA-86%DEGMA	200	4-arm	20	50	43%	16000	1.3	16653
P2	30% FUMA-70%DEGMA	36% FUMA-64%DEGMA	200	4-arm	20	50	39%	20000	1.4	14794
P3	10% FUMA-90%DEGMA	15% FUMA-85%DEGMA	300	6-arm	20	50	32%	25000	1.2	18900
P4	30% FUMA-70%DEGMA	35% FUMA-65%DEGMA	300	6-arm	20	50	23%	31000	1.4	13605
P5	10% FUMA-90%PEGMA	20% FUMA-80%PEGMA	200	4-arm	30	40	28%	17000	1.2	16033
P6	30% FUMA-70%PEGMA	40% FUMA-60%PEGMA	200	4-arm	30	40	18%	14000	1.2	8873
P7	10% FUMA-90%PEGMA	16% FUMA-84%PEGMA	300	6-arm	30	40	29%	28000	1.3	25385
P8	30% FUMA-70%PEGMA	40% FUMA-60%PEGMA	300	6-arm	30	40	30%	24000	1.2	23332

[a] $[I]_0$:[Cu(I)Br]:[Bipyridine]=1:1:2.5 [b] Calibration with linear polystyrene

3.3. Functionalization of Polymers

3.3.1. Attachment of N-Ethylmaleimide

N-Ethylmaleimide is used as a model compound for Diels-Alder reaction to observe the effect of reaction conditions on the formation of endo and exo products (Figure 3.12). Diels-Alder reaction forms two stereoisomers named as the *endo* and *exo* products. The endo product is the kinetically controlled product with a lower activation energy due to the orbital overlap in transition state. It is favored at low temperatures. On the other hand, the exo product is the thermodynamicallly controlled product due to the formation of a more stable final conformation with less steric hinderance. It is favored at high temperatures.

The retro Diels-Alder reaction takes place at lower temperatures for the endo product whereas it requires elevated temperatures for the exo product. So the domination of the endo product is desired for drug delivery purposes since the drug gets released at low temperatures.

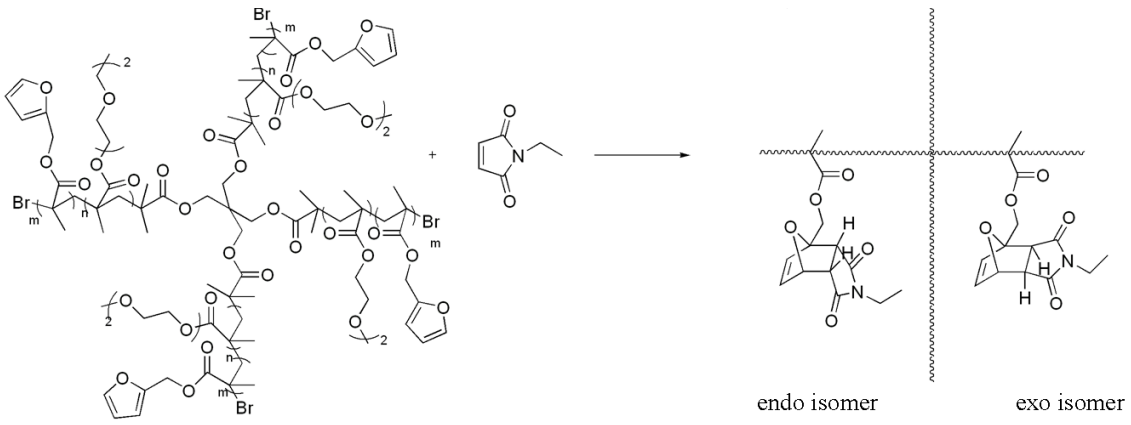

Figure 3.12. Attachment of N-Ethylmaleimide.

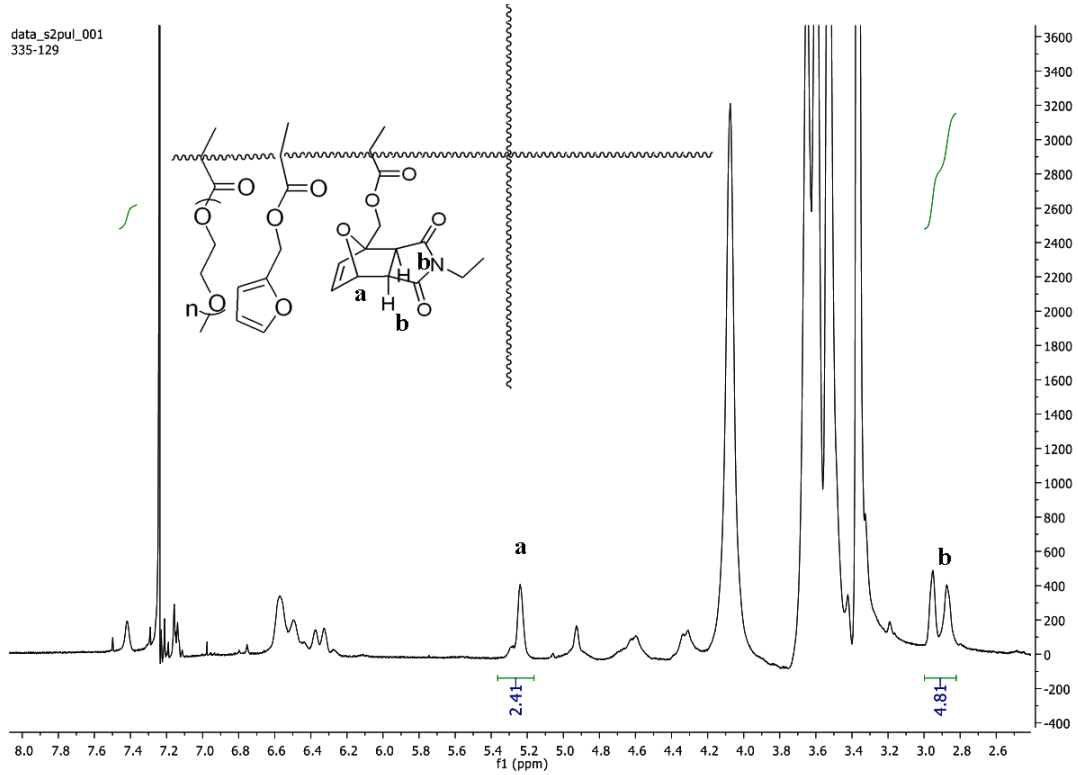

Figure 3.13. ^{1}H NMR spectrum of N-Ethylmaleimide conjugated polymer (exo).

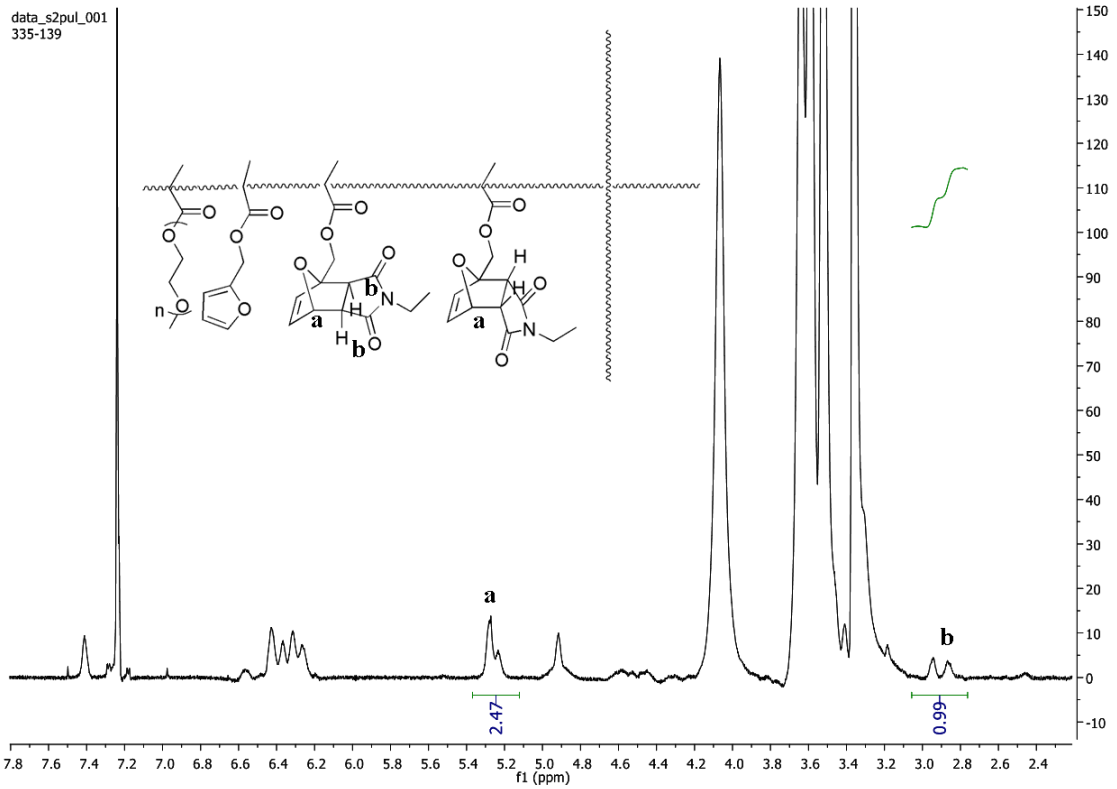

Figure 3.14. ^{1}H NMR spectrum of N-Ethylmaleimide conjugated polymer (endo/exo mixture).

For ^{1}H NMR spectrums of both compounds above, appearance of new characteristic peaks at around 5.2 ppm & 6.5 ppm corresponding to the furan-maleimide cycloadduct proves the formation of the bicyclic core. The CH-CH bridge protons of the exo stereoisomer gives peaks at around 2.9 ppm, but the endo stereoisomer gives at above 3 ppm and overlaps with the peaks of the polymer. Therefore the integration value of the endo steroisomer is calculated by dividing the integration value of the exo stereoisomer into two (because it corresponds to two protons) and subtracting it from the integration value of the bridgehead proton at around 5.2 ppm (this peak is same for endo & exo stereoisomers). At the first ^{1}H NMR spectrum (Figure 3.13) there is only the exo stereoisomer whereas at the second ^{1}H NMR spectrum (Figure 3.14) there is 20% exo and 80% endo stereoisomer.

3.3.2. Attachment of BODIPY-maleimide

BODIPY-maleimide which is a florescent dye is chosen for the functionalization of polymers because the release of it can be monitored by UV spectroscopy (Figure 3.15). The dye is conjugated to the polymer with two different conditions, the first one at low temperarture to give an endo/exo mixture and the second one at high temperature to give the exo product. ^{1}H NMR spectrums of both compounds contain characteristic peaks at around 5.2 ppm and 6.5 ppm corresponding to the furan-maleimide cycloadduct (Figure 3.16 and Figure 3.17). This proves the formation of the bicyclic core. Also the ^{1}H NMR spectrums contain characteristic peaks at around 6 ppm, 2.4 ppm and 2.5 ppm that belong to the dye.

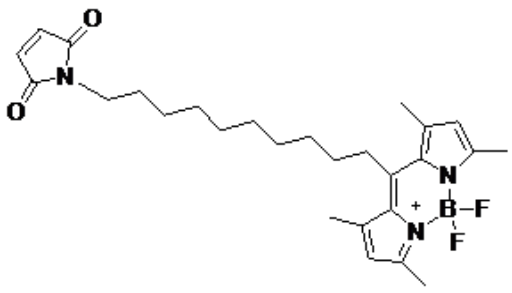

Figure 3.15. Structure of BODIPY-maleimide.

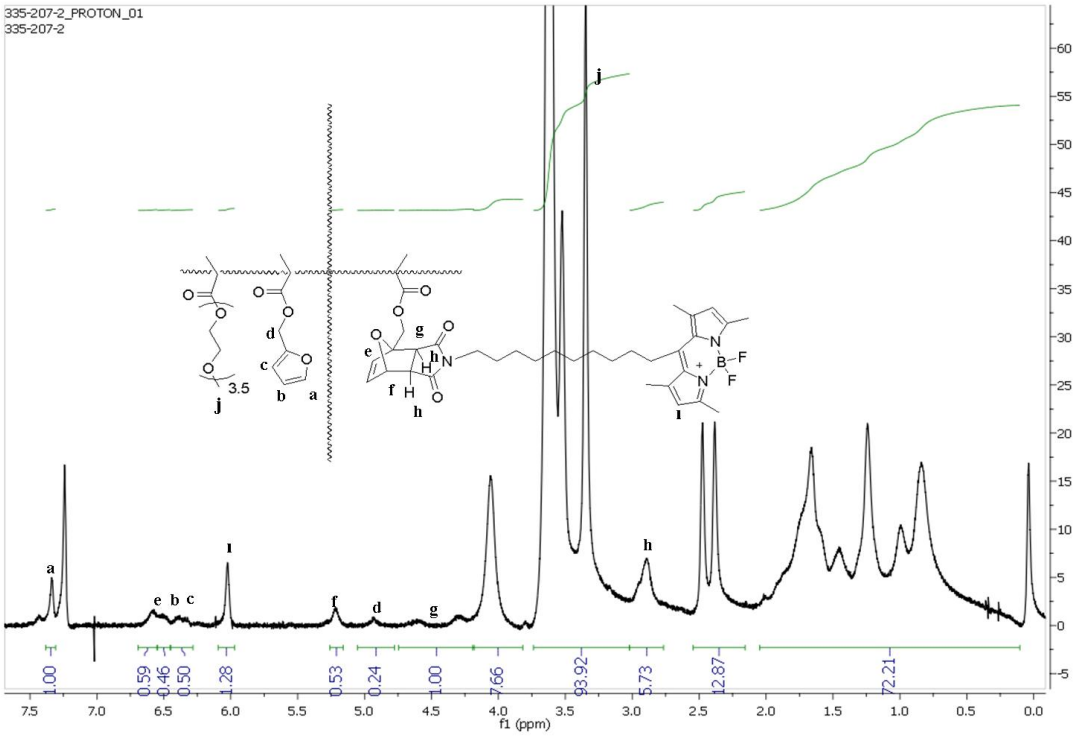

Figure 3.16. ^{1}H NMR spectrum of BODIPY-maleimide conjugated polymer (exo).

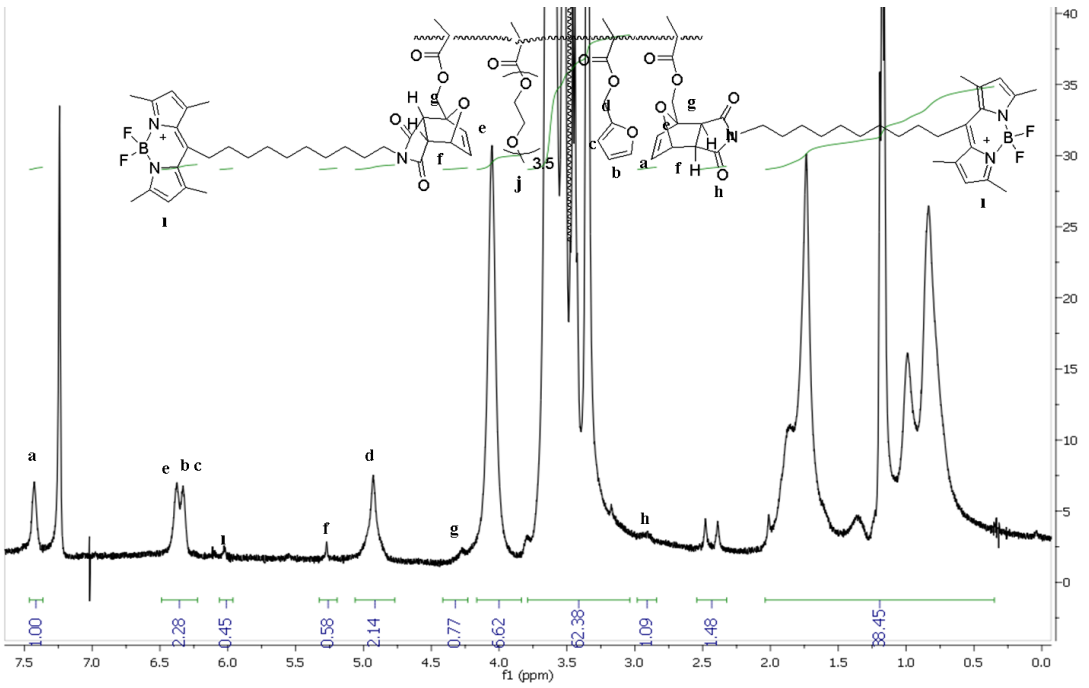

Figure 3.17. ^{1}H NMR spectrum of BODIPY-maleimide conjugated polymer (exo/endo mixture).

Attachment of BODIPY-maleimide to the star polymer P7 by Diels-Alder reaction is also done in water to observe the reaction by UV spectroscopy. The dye itself is insoluble in water, but when it gets attached to the polymer it gets solubilized and gives an absorbance peak at the UV spectrum. As the reaction proceeds the absorbance increases which indicates the successful attachment of the dye to the polymer (Figure 3.18).

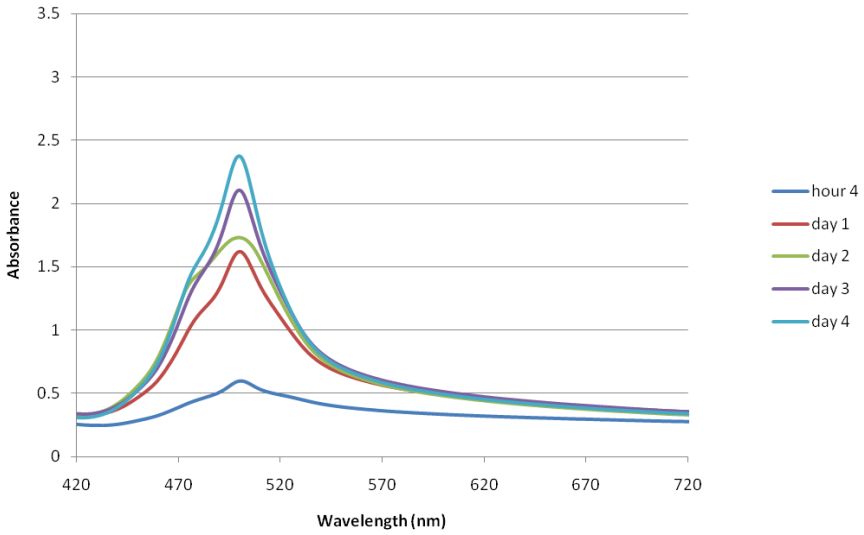

Figure 3.18. UV spectrum of BODIPY-maleimide conjugated polymer.

A control experiment is done by a 6 arm star polymer P(PEGMA) which is obtained by ATRP of only PEGMA and does not contain any furan group. In this case, the dye cannot attach itself to the polymer by Diels-Alder reaction, however there is a slight increase in the absorbance (Figure 3.19). This implies that the insoluble dye molecules get physically entrapped inside the the arms of the polymer and solubilizes to some extent. This kind of behaviour may be interesting for further applications.

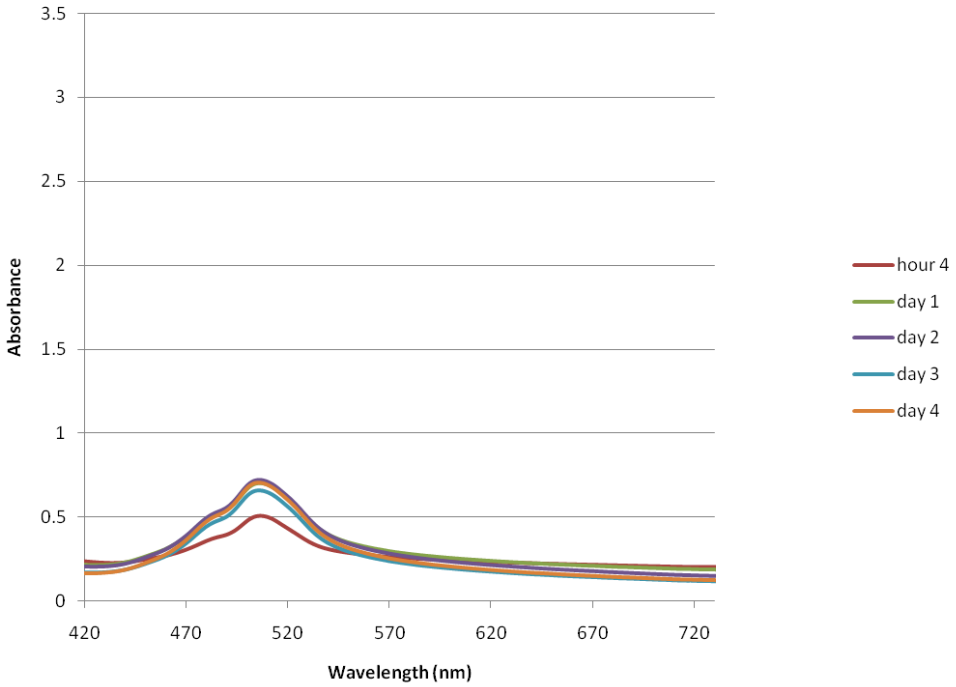

Figure 3.19. UV spectrum of physically entrapped BODIPY-maleimide.

3.3.3. Release studies

Release studies were done with the exo and endo/exo mixture dye conjugated polymers by stirring them at 40 ^{o}C for 4 days. The mechanism of release is by retro Diels-Alder reaction. When the dye is in conjugated to the polymer, it solubilizes in water and gives an absorbance peak in the UV spectrum. But free dye is insoluble in water, and thus gives no absorbance in the UV spectrum. So with the release of the dye molecules from the polymer, the molecules become insoluble and the intensity of absorbance is expected to decrease by time for the endo/exo mixture (Figure 3.20). But in the case of the exo product 40 ^{o}C is not a sufficient temperature for the release of the dye molecules by retro Diels-Alder reaction, so the absorbance did not change much by time (Figure 3.21).

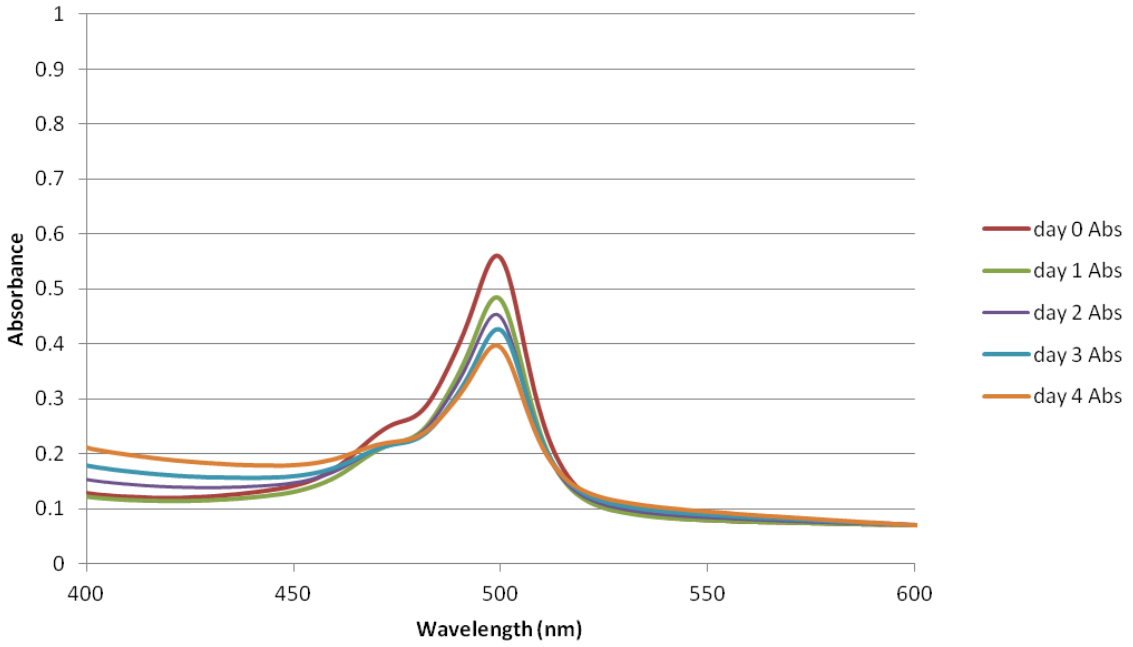

Figure 3.20. UV spectrum for release studies of the dye from polymer (endo/exo mixture).

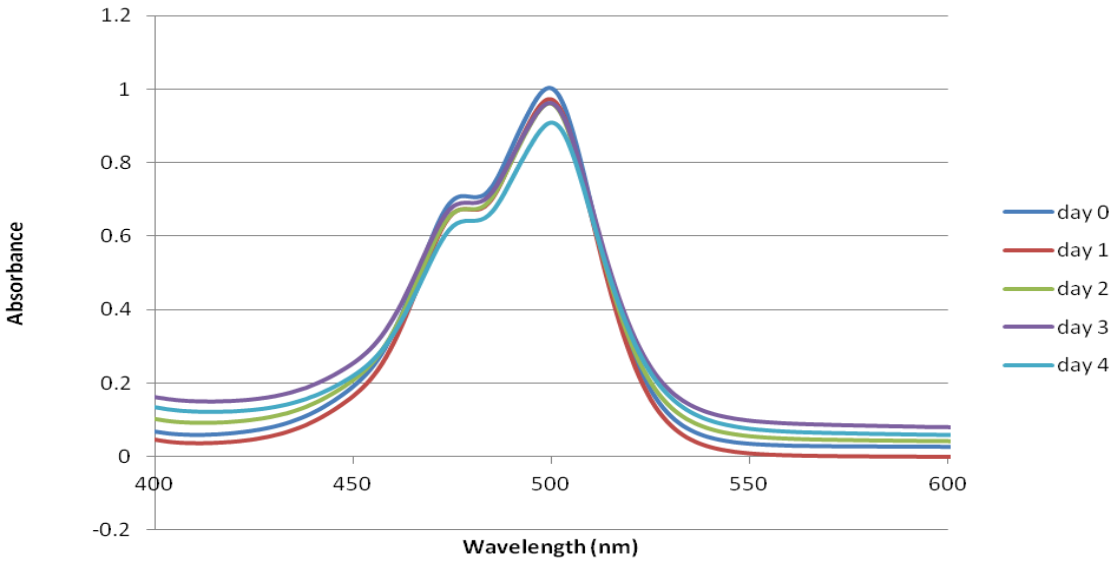

Figure 3.21. UV spectrum for release studies of the dye from polymer (exo).

3.3.4. Synthesis of linker for drug attachment

A linker is synthesized with the aim of using for drug attachment to the polymer. The linker contains a maleimide group which will react with the furans on the polymer and an acid group which will react with the alcohol group of the drug camptothecin by esterification reaction (Figure 3.22).

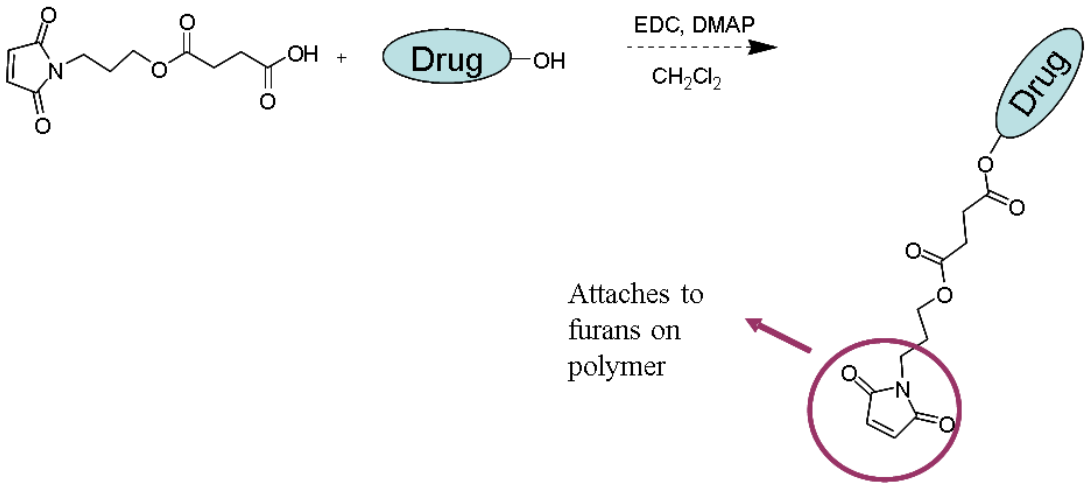

Figure 3.22. Proposed mechanism for drug conjugation to polymers.

In the synthesis of the linker the first step is synthesis of 5, which is synthesized according to a previously reported literature procedure [30] (Figure 3.23). Then the alcohol group of 5 is converted to an acid group by reacting with succinic anhydride. The acid group of the linker is suitable for attachment of an alcohol containing drug molecule by esterification. The furan on the other side of the linker is removed by retro Diels-Alder reaction and the maleimide is activated. The maleimide part on 7 will react with furans on the polymer and enable the conjugation of drug molecules to the polymer. Products 6 and 7 were obtained in high yields in pure form and characterized by ^{1}H NMR (Figure 3.24) (Figure 3.25).

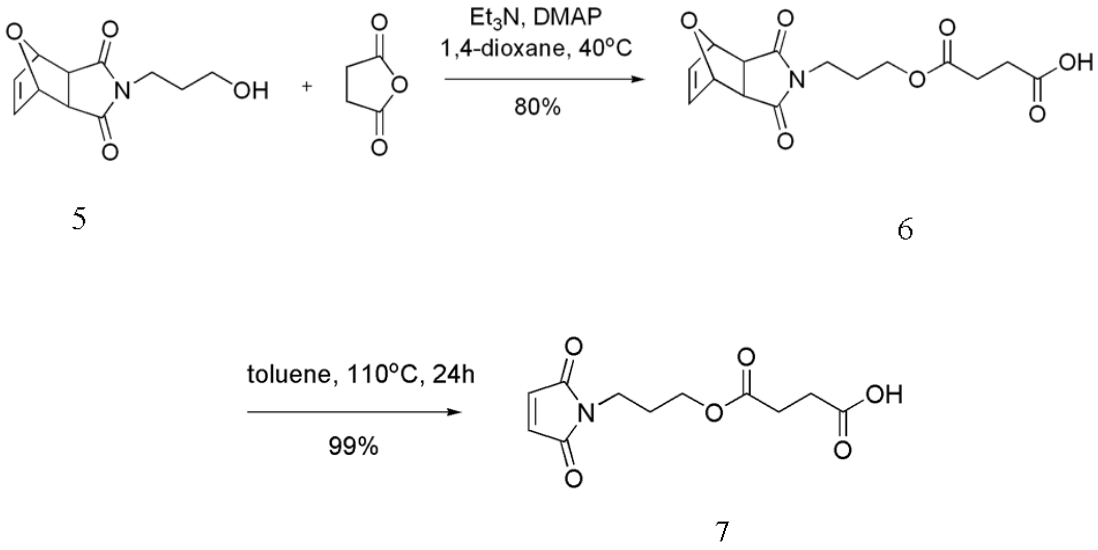

Figure 3.23. Synthesis of linker for drug attachment.

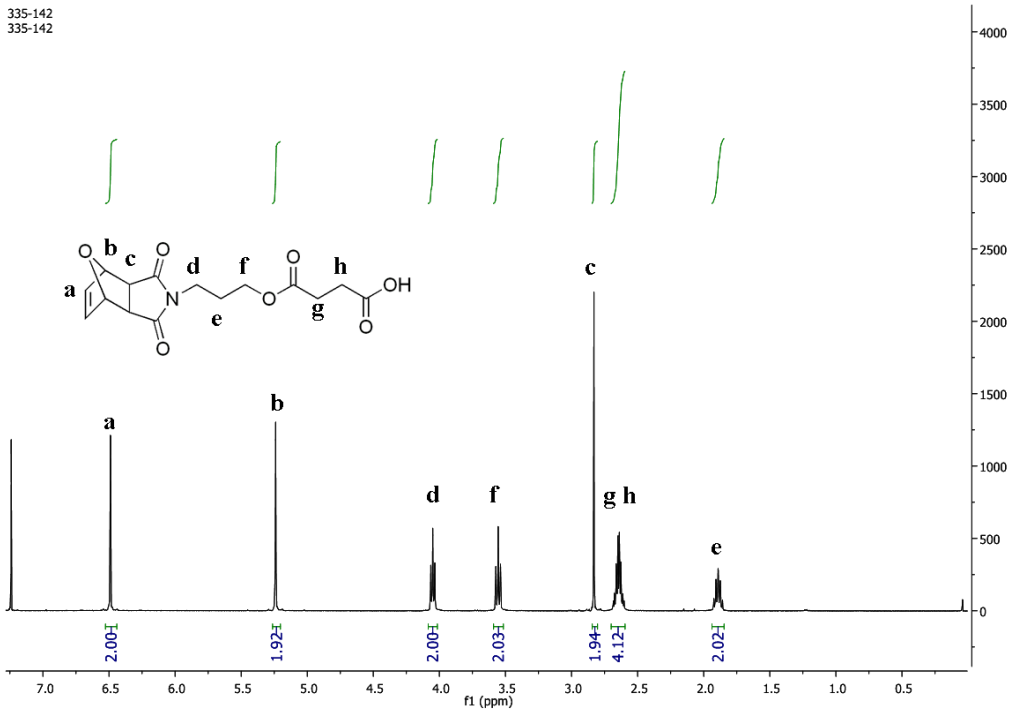

Figure 3.24. ^{1}H NMR spectrum of linker before retro Diels-Alder.

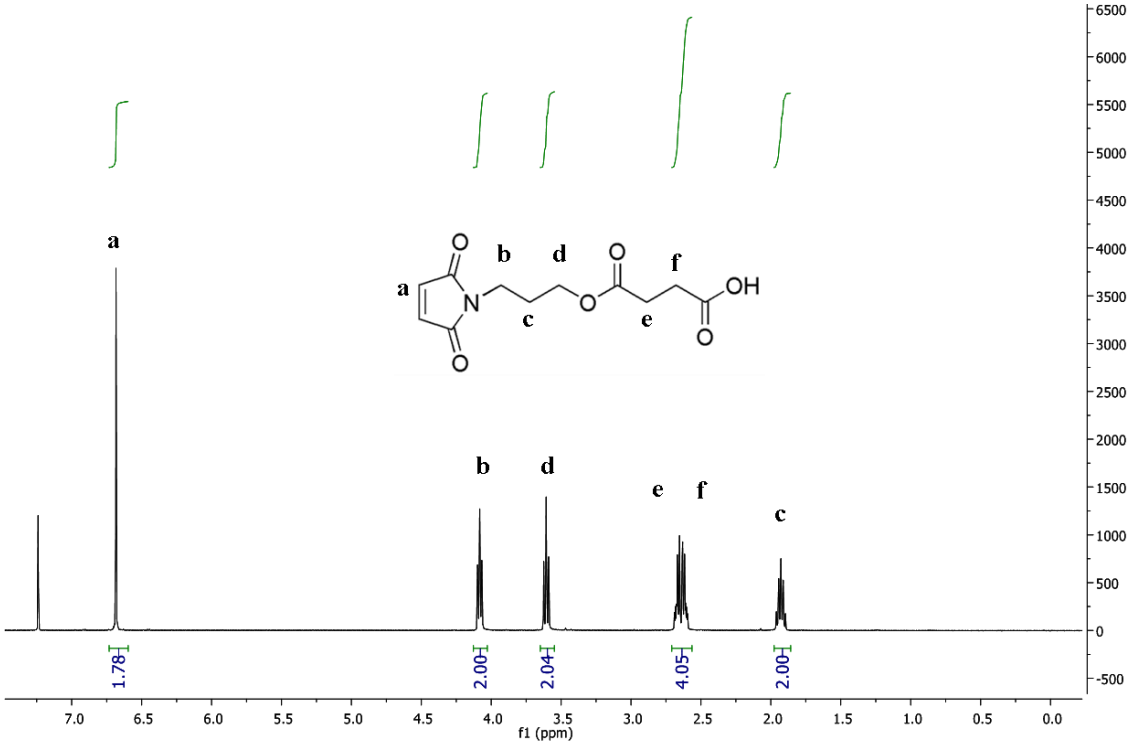

Figure 3.25. ^{1}H NMR spectrum of linker after retro Diels-Alder.

4. EXPERIMENTAL

4.1. Materials and Methods

All chemicals were obtained from commercial sources (Merck, Aldrich and Alfa Aesar) and were used as received unless otherwise stated. Dry solvents (CH_2Cl_2, THF) were obtained from ScimatCo Purification System, other dry solvents were dried over molecular sieves. Poly(ethylene glycol) methyl ether metacrylate (Mw = 300) (PEGMA, 99%, Aldrich), Di(ethylene glycol) methyl ether metacrylate (Mw = 188) (DEGMA, 99%, Aldrich) and Furfuryl methacrylate (Mw = 166) (FUMA, 99%, Aldrich) were passed through basic alumina column to remove inhibitor and then distilled over CaH_2 in vacuum prior to use.

The initiator and polymer characterizations involved ^1H solution NMR spectroscopy (Varian 400 MHz and and Bruker 260 MHz), UV-Vis spectroscopy (Varian Cary 100 Scan) and Fourier transform infrared (FTIR) spectroscopy (Perkin Elmer 1600 Series). The molecular weights were estimated by gel permeation chromatography (GPC) analysis using a Shimadzu PSS-SDV (length/ID 8 x 300 mm, 10 nm particle size) mixed-C column calibrated with polystyrene standards (1-150 kDa) using a refractive index detector. THF was used as elutent at a flow rate of 1 mL/min at 30 ^oC.

4.2. Synthesis

4.2.1. Synthesis of Initiators

4.2.1.1. Synthesis of 4-arm initiator. Pentaerithritol (0.50 g, 3.68 mmol), triethylamine (2.39 mL, 25.73 mmol) and DMAP (0.27 g, 2.20 mmol) were mixed in THF (50 mL) under N_2. The mixture was cooled to 0 °C in an ice bath. On the other side, 2-bromo-isobutyryl bromide (2.72 mL, 22.05 mmol) was diluted in THF (10 mL) and added into the former mixture dropwise (30 min). The obtained white suspension was stirred for 4 h at 0 °C, then warmed up to room temperature and stirred for 20 hours. The salt formed was filtered off and the residue was concentrated in *vacuo*. The product 1 was purified by column chromatography and obtained as a white solid (1.12 g, 42 %). ^{1}H NMR ($CDCl_3$, δ, ppm) 4.29 (s, 8H, CH_2 ester protons), 1.92 (s, 24H, $CBr(CH_3)$).

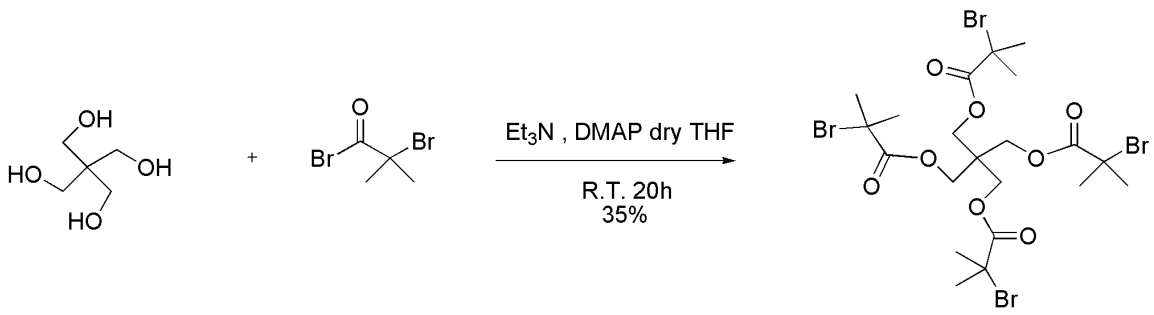

1

Figure 4.1. Synthesis of the 4-arm initiator.

4.2.1.2. Synthesis of first generation dendrimer. Pentaerithritol (0.50 g, 3.68 mmol), bisMPA anhydride (7.29 g, 22.05 mmol) and DMAP (0.72 g, 5.88 mmol) were mixed in dry CH_2Cl_2 (35 mL) under N_2. Then pyridine (3.57 mL, 44.12 mmol) was added to this mixture and stirred for 20 hours at room temperature. The excess anhydride was quenched with water after the reaction was complete and extracted with $NaHSO_4$(1M), Na_2CO_3 (10%) and brine. Then product 2 was recrystallized from cold ether as a pure white solid (2.43 g, 87%) ^{1}H NMR ($CDCl_3$, δ, ppm) 4.25 (s, 8H, CH_2 ester protons), 4.16 (d, 8H, J=12 Hz, OCH_2), 3.62 (d, 8H, J=12 Hz, OCH_2), 1.40 (s, 12H, $OC(CH_3)$), 1.32 (s, 12H, $OC(CH_3)$), 1.11 (s, 12H, $C(CH_3)$).

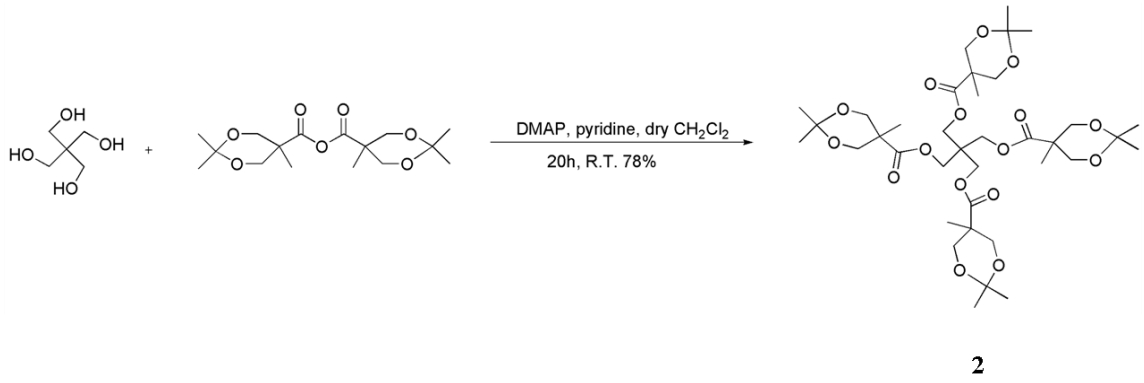

2

Figure 4.2. Synthesis of the first generation dendrimer.

4.2.1.3. Deprotecion of first generation dendrimer. First generation dendrimer 2 (1.0 g, 1.31 mmol) was dissolved in MeOH (20 mL) and to this solution, a small amount of Dowex H^+ resin was added. The resulting mixture was stirred at ambient temperature until the consumption of the starting compound was observed by TLC. The resin was then filtered off and washed with MeOH. The crude product was purified by recrystallization from $CHCl_2$ and obtained as a white solid 3 (0.67 g, 85% yield). ^{1}H NMR (DMSO, δ, ppm) 4.72 (t, 8H, *J*=6 Hz, OH), 4.08 (s, 8H, CH_2 ester protons), 3.40 (s, 16H, CCH_2O), 1.03 (s, 12H, $C(CH_3)$).

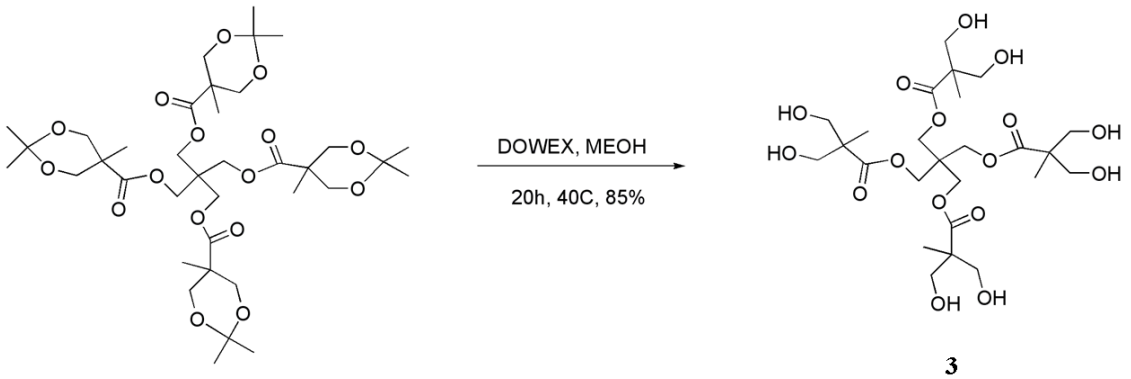

3

Figure 4.3. Deprotection of first generation dendrimer.

4.2.1.4. Synthesis of 8-arm initiator. Deprotected first generation dendrimer 3 (0.50 g, 0.83 mmol), triethylamine (1.08 mL, 11.65 mmol) and DMAP (0.16 g, 1.33 mmol) were mixed in THF (50 mL) under N_2. The mixture was cooled to 0 °C in an ice bath. On the

other side, 2-bromo-isobutyryl bromide (1.65 mL, 13.31 mmol) was diluted in THF (10 mL) and added into the former mixture dropwise (30 min). The obtained white suspension was stirred for 4 h at 0 °C, then warmed up to room temperature and stirred for 20 hours. The ammonium salt formed was filtered off and the residue was concentrated in *vacuo*. According to TLC, the reaction did not work efficiently, and resulted in incomplete attachment of 2-bromo-isobutyryl bromide to the dendrimer probably due to steric hinderance around the core. The product could not be isolated.

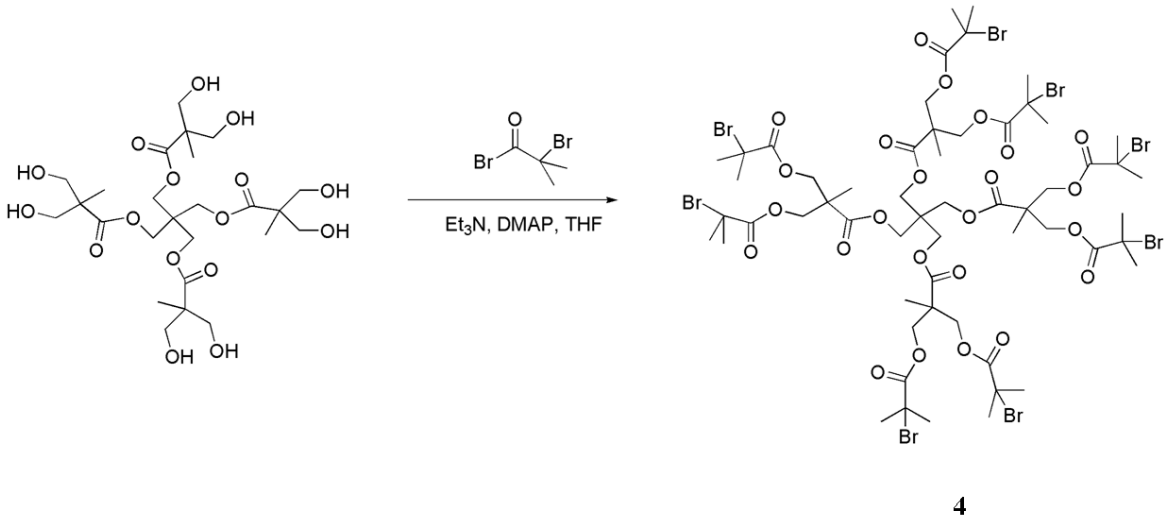

4

Figure 4.4. Synthesis of the 8-arm initiator.

4.2.2. Synthesis of Polymers

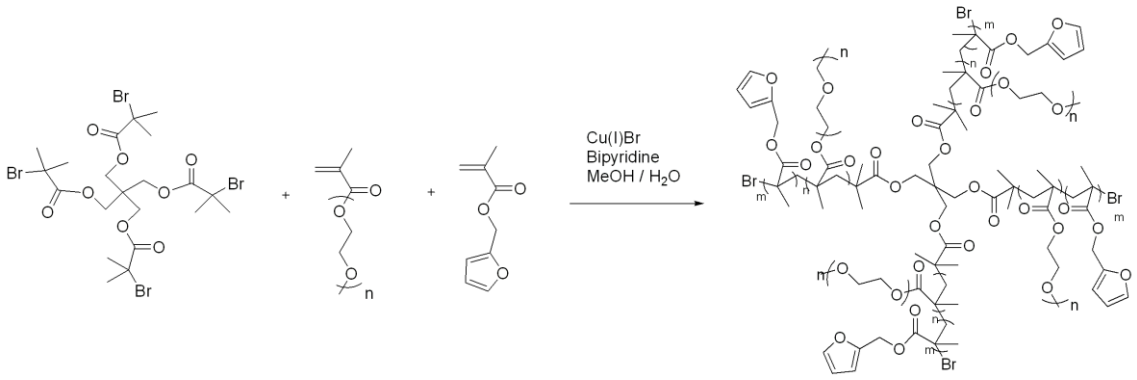

Figure 4.5. Synthesis of polymers with 4-armed initiator.

4.2.2.1. Synthesis of P1. P1 was synthesized by ATRP. 4-arm initiator (40 mg, 0.055 mmol) was dissolved in minimum amount of degassed methanol and introduced into a flask containing Cu(I)Br (31.0 mg, 0.22 mmol), degassed bipyridine (85 mg, 0.55 mmol), degassed DEGMA (1.80 mL, 9.84 mmol) and degassed FUMA (0.16 mL, 1.09 mmol) dissolved in degassed methanol-water mixture (10 mL, $V_{MeOH} : V_{water} = 9:1$) under stirring. The flask was then placed in a thermostated oil bath at 50 °C for 20 min. After polymerization, the reaction mixture was passed through a neutral alumina column to remove the catalyst. Then methanol was removed by rotary evaporator and the mixture was precipitated in diethyl ether twice. P1 was obtained as a clear viscous liquid. $[M]_0/[I]_0$= 200; $[I]_0$:[CuBr]:[Bipyridine]=1:4:10; conversion = 43 %. $M_{n,theo}$= 16653, $M_{n,GPC}$= 16000, M_w/M_n= 1.29, relative to PS. ^{1}H NMR ($CDCl_3$, δ, ppm) 7.42 (br s, 1H, CH_2= CH_2), 6.37 (br s, 1H, CH_2= CH_2), 6.32 (br s, 1H, CH_2= CH_2), 4.92 (s, 2H, CH_2), 4.14-3.96 (m, 10H, CH_2 ester protons), 3.71-3.43 (m, 2H, OCH_2 of DEGMA), 3.37 (s, 3H, OCH_3 of DEGMA), 2.01–0.63 (m, 32H, $CBr(CH_3)_2$, CH_2 and CH_3 along polymer backbone).

4.2.2.2. Synthesis of P2. P2 was synthesized by ATRP. 4-arm initiator (40 mg, 0.055 mmol) was dissolved in minimum amount of degassed methanol and introduced into a flask containing Cu(I)Br (31.0 mg, 0.22 mmol), degassed bipyridine (85 mg, 0.55 mmol), degassed DEGMA (1.40 mL, 7.64 mmol) and degassed FUMA (0.50 mL, 3.28 mmol) dissolved in degassed methanol-water mixture (10 mL, $V_{MeOH} : V_{water} = 9:1$) under stirring.

The flask was then placed in a thermostated oil bath at 50 °C for 20 min. After polymerization, the reaction mixture was passed through a neutral alumina column to remove the catalyst. Then methanol was removed by rotary evaporator and the mixture was precipitated in diethyl ether twice. P2 was obtained as a clear viscous liquid. $[M]_0/[I]_0$= 200; $[I]_0$:[CuBr]:[Bipyridine]=1:4:10; conversion = 39 %. $M_{n,theo}$= 14794, $M_{n,GPC}$= 20000, M_w/M_n= 1.38, relative to PS. ^{1}H NMR ($CDCl_3$, δ, ppm) 7.41 (br s, 1H, CH_2= CH_2), 6.37 (br s, 1H, CH_2= CH_2), 6.32 (br s, 1H, CH_2= CH_2), 4.95 (s, 2H, CH_2), 4.13-3.97 (m, 10H, CH_2 ester protons), 3.66-3.46 (m, 2H, OCH_2 of DEGMA), 3.37 (s, 3H, OCH_3 of DEGMA), 1.92–0.57 (m, 32H, $CBr(CH_3)_2$, CH_2 and CH_3 along polymer backbone).

4.2.2.3. Synthesis of P3. P3 was synthesized by ATRP. 6-arm initiator (40 mg, 0.035 mmol) was dissolved in minimum amount of degassed methanol and introduced into a flask containing Cu(I)Br (30.0 mg, 0.20 mmol), degassed bipyridine (81 mg, 0.52 mmol), degassed DEGMA (1.74 mL, 9.40 mmol) and degassed FUMA (0.16 mL, 1.04 mmol) dissolved in degassed methanol-water mixture (10 mL, V_{MeOH} : V_{water} = 9:1) under stirring. The flask was then placed in a thermostated oil bath at 50 °C for 20 min. After polymerization, the reaction mixture was passed through a neutral alumina column to remove the catalyst. Then methanol was removed by rotary evaporator and the mixture was precipitated in diethyl ether twice. P3 was obtained as a clear viscous liquid. $[M]_0/[I]_0$= 300; $[I]_0$:[CuBr]:[Bipyridine]=1:6:15; conversion = 32 %. $M_{n,theo}$= 18900, $M_{n,GPC}$= 25000, M_w/M_n= 1.22, relative to PS. ^{1}H NMR ($CDCl_3$, δ, ppm) 7.42 (br s, 1H, CH_2= CH_2), 6.37 (br s, 1H, CH_2= CH_2), 6.33 (br s, 1H, CH_2= CH_2), 4.93 (s, 2H, CH_2), 4.19-3.96 (m, 14H, CH_2 ester protons), 3.77-3.43 (m, 6H, OCH_2 of DEGMA and initiator), 3.37 (s, 3H, OCH_3 of DEGMA), 2.09–0.67 (m, 44H, $CBr(CH_3)_2$, CH_2 and CH_3 along polymer backbone).

4.2.2.4. Synthesis of P4. P4 was synthesized by ATRP. 6-arm initiator (40 mg, 0.035 mmol) was dissolved in minimum amount of degassed methanol and introduced into a flask containing Cu(I)Br (30.0 mg, 0.20 mmol), degassed bipyridine (81 mg, 0.52 mmol), degassed DEGMA (1.35 mL, 7.31 mmol) and degassed FUMA (0.48 mL, 3.13 mmol) dissolved in degassed methanol-water mixture (10 mL, V_{MeOH} : V_{water} = 9:1) under stirring. The flask was then placed in a thermostated oil bath at 50 °C for 20 min. After polymerization, the reaction mixture was passed through a neutral alumina column to remove the catalyst. Then methanol was removed by rotary evaporator and the mixture was

precipitated in diethyl ether twice. P4 was obtained as a clear viscous liquid. $[M]_0/[I]_0$= 300; $[I]_0$:[CuBr]:[Bipyridine]=1:6:15; conversion = 23 %. $M_{n,theo}$= 13605, $M_{n,GPC}$= 31000, M_w/M_n= 1.36, relative to PS. ^{1}H NMR ($CDCl_3$, δ, ppm) 7.39 (br s, 1H, CH_2= CH_2), 6.37 (br s, 1H, CH_2= CH_2), 6.32 (br s, 1H, CH_2= CH_2), 4.92 (s, 2H, CH_2), 4.12-3.98 (m, 14H, CH_2 ester protons), 3.71-3.44 (m, 6H, OCH_2 of DEGMA and initiator), 3.37 (s, 3H, OCH_3 of DEGMA), 1.95–0.62 (m, 44H, $C(CH_3)$, $CBr(CH_3)$, CH_2 and CH_3 along polymer backbone).

4.2.2.5. Synthesis of P5. P5 was synthesized by ATRP. 4-arm initiator (40 mg, 0.055 mmol) was dissolved in minimum amount of degassed methanol and introduced into a flask containing Cu(I)Br (31.0 mg, 0.22 mmol), degassed bipyridine (85 mg, 0.55 mmol), degassed PEGMA (2.80 mL, 9.83 mmol) and degassed FUMA (0.17 mL, 1.09 mmol) dissolved in degassed methanol-water mixture (15 mL, V_{MeOH} : V_{water} = 9:1) under stirring. The flask was then placed in a thermostated oil bath at 40 °C for 30 min. After polymerization, the reaction mixture was passed through a neutral alumina column to remove the catalyst. Then methanol was removed by rotary evaporator and the mixture was precipitated in diethyl ether twice. P5 was obtained as a clear viscous liquid. $[M]_0/[I]_0$= 200; $[I]_0$:[CuBr]:[Bipyridine]=1:4:10; conversion = 28 %. $M_{n,theo}$= 16033, $M_{n,GPC}$= 17000, M_w/M_n= 1.17, relative to PS. ^{1}H NMR ($CDCl_3$, δ, ppm) 7.43 (br s, 1H, CH_2= CH_2), 6.38 (br s, 1H, CH_2= CH_2), 6.33 (br s, 1H, CH_2= CH_2), 4.93 (s, 2H, CH_2), 4.12-3.96 (m, 10H, CH_2 ester protons), 3.70-3.46 (m, 2H, OCH_2 of PEGMA), 3.35 (s, 3H, OCH_3 of PEGMA), 1.91–0.65 (m, 32H, $CBr(CH_3)_2$, CH_2 and CH_3 along polymer backbone).

4.2.2.6. Synthesis of P6. P6 was synthesized by ATRP. 4-arm initiator (40 mg, 0.055 mmol) was dissolved in minimum amount of degassed methanol and introduced into a flask containing Cu(I)Br (31.0 mg, 0.22 mmol), degassed bipyridine (85 mg, 0.55 mmol), degassed PEGMA (2.20 mL, 7.64 mmol) and degassed FUMA (0.50 mL, 3.28 mmol) dissolved in degassed methanol-water mixture (13.5 mL, V_{MeOH} : V_{water} = 9:1) under stirring. The flask was then placed in a thermostated oil bath at 40 °C for 30 min. After polymerization, the reaction mixture was passed through a neutral alumina column to remove the catalyst. Then methanol was removed by rotary evaporator and the mixture was precipitated in diethyl ether twice. P6 was obtained as a clear viscous liquid. $[M]_0/[I]_0$= 200; $[I]_0$:[CuBr]:[Bipyridine]=1:4:10; conversion = 18 %. $M_{n,theo}$= 8873, $M_{n,GPC}$ = 13700,

M_w/M_n= 1.25, relative to PS. ^{1}H NMR ($CDCl_3$, δ, ppm) 7.42 (br s, 1H, CH_2= CH_2), 6.37 (br s, 1H, CH_2= CH_2), 6.33 (br s, 1H, CH_2= CH_2), 4.92 (s, 2H, CH_2), 4.16-3.95 (m, 10H, CH_2 ester protons), 3.70-3.46 (m, 2H, OCH_2 of PEGMA), 3.35 (s, 3H, OCH_3 of PEGMA), 1.99–0.61 (m, 32H, $CBr(CH_3)_2$ CH_2 and CH_3 along polymer backbone).

4.2.2.7. Synthesis of P7. P7 was synthesized by ATRP. 6-arm initiator (40 mg, 0.035 mmol) was dissolved in minimum amount of degassed methanol and introduced into a flask containing Cu(I)Br (30.0 mg, 0.20 mmol), degassed bipyridine (81 mg, 0.52 mmol), degassed PEGMA (2.70 mL, 9.40 mmol) and degassed FUMA (0.16 mL, 1.04 mmol) dissolved in degassed methanol-water mixture (14 mL, V_{MeOH} : V_{water} = 9:1) under stirring. The flask was then placed in a thermostated oil bath at 40 °C for 30 min. After polymerization, the reaction mixture was passed through a neutral alumina column to remove the catalyst. Then methanol was removed by rotary evaporator and the mixture was precipitated in diethyl ether twice. P7 was obtained as a clear viscous liquid. $[M]_0/[I]_0$= 300; $[I]_0$:[CuBr]:[Bipyridine]=1:6:15; conversion = 29 %. $M_{n,theo}$= 25385, $M_{n,GPC}$= 28240, M_w/M_n= 1.27, relative to PS. ^{1}H NMR ($CDCl_3$, δ, ppm) 7.43 (br s, 1H, CH_2= CH_2), 6.38 (br s, 1H, CH_2= CH_2), 6.33 (br s, 1H, CH_2= CH_2), 4.93 (s, 2H, CH_2), 4.11-3.97 (m, 14H, CH_2 ester protons), 3.71-3.48 (m, 6H, OCH_2 of PEGMA), 3.35 (s, 3H, OCH_3 of PEGMA), 1.93–0.60 (m, 44H, $CBr(CH_3)_2$, CH_2 and CH_3 along polymer backbone).

4.2.2.8. Synthesis of P8. P8 was synthesized by ATRP. 6-arm initiator (40 mg, 0.035 mmol) was dissolved in minimum amount of degassed methanol and introduced into a flask containing Cu(I)Br (30.0 mg, 0.20 mmol), degassed bipyridine (81 mg, 0.52 mmol), degassed PEGMA (2.00 mL, 7.32 mmol) and degassed FUMA (0.48 mL, 3.13 mmol) dissolved in degassed methanol-water mixture (12.5 mL, V_{MeOH} : V_{water} = 9:1) under stirring. The flask was then placed in a thermostated oil bath at 40 °C for 30 min. After polymerization, the reaction mixture was passed through a neutral alumina column to remove the catalyst. Then methanol was removed by rotary evaporator and the mixture was precipitated in diethyl ether twice. P8 was obtained as a clear viscous liquid. $[M]_0/[I]_0$= 300; $[I]_0$:[CuBr]:[Bipyridine]=1:6:15; conversion = 32 %. $M_{n,theo}$= 23332, $M_{n,GPC}$= 25000, M_w/M_n= 1.22, relative to PS. ^{1}H NMR ($CDCl_3$, δ, ppm) 7.42 (br s, 1H, CH_2= CH_2), 6.37 (br s, 1H, CH_2= CH_2), 6.32 (br s, 1H, CH_2= CH_2), 4.92 (s, 2H, CH_2), 4.10-3.94 (m, 14H,

CH_2 ester protons), 3.67-3.45 (m, 6H, OCH_2 of PEGMA), 3.35 (s, 3H, OCH_3 of PEGMA), 1.97–0.64 (m, 44H, $CBr(CH_3)_2$, CH_2 and CH_3 along polymer backbone).

4.2.3. Functionalization of Polymers

4.2.3.1. Attachment of N-Ethylmaleimide. P1 (54 mg, 3.37 x 10^{-3} mmol) and N-Ethylmaleimide (11.8 mg, 0.094 mmol) was dissolved in 1mL of degassed benzene. The mixture was stirred at 85 °C for 24 hours and was precipitated into cold diethyl ether. ^{1}H NMR analysis indicated that the Diels-Alder reaction resulted in 100% exo stereoisomer. ^{1}H NMR ($CDCl_3$, δ, ppm) 7.42 (br s, 1H, CH_2= CH_2), 6.53 (s, 2H, CH=CH bridge protons), 6.38 (br s, 1H, CH_2= CH_2), 6.33 (br s, 1H, CH_2= CH_2), 5.24 (s, 1H, -CHO bridge-head protons), 4.93 (s, 2H, CH_2), 4.45 (m, 2H, CH_2) 4.14-3.96 (m, 10H, CH_2 ester protons), 3.71-3.43 (m, 2H, OCH_2 of DEGMA), 3.37 (s, 3H, OCH_3 of DEGMA), 2.91 (m, 2H, exo CH-CH bridge protons), 2.01–0.63 (m, 32H, $CBr(CH_3)_2$, CH_2 and CH_3 along polymer backbone).

P1 (67 mg, 14.8 x 10^{-3} mmol) and N-Ethylmaleimide (14.6 mg, 0.12 mmol) was dissolved in 1mL of degassed methanol. The mixture was stirred at room temperature for 7 days and was precipitated into cold diethyl ether. ^{1}H NMR analysis indicated that the Diels-Alder reaction resulted in 20% exo and 80% endo stereoisomer. ^{1}H NMR ($CDCl_3$, δ, ppm) ^{1}H NMR ($CDCl_3$, δ, ppm) 7.41 (br s, 1H, CH_2= CH_2), 6.53 (s, 2H, CH=CH bridge protons), 6.38 (br s, 1H, CH_2= CH_2), 6.33 (br s, 1H, CH_2= CH_2), 5.24 (s, 2H, -CHO bridge-head protons), 4.92 (s, 2H, CH_2), 4.47 (m, 2H, CH_2) 4.14-3.96 (m, 10H, CH_2 ester protons), 3.71-3.43 (m, 2H, OCH_2 of DEGMA), 2.91 (m, 2H, exo CH-CH bridge protons), 3.37 (s, 3H, OCH_3 of DEGMA), 1.97–0.61 (m, 32H, $CBr(CH_3)_2$, CH_2 and CH_3 along polymer backbone).

4.2.3.2. Attachment of BODIPY-maleimide. BODIPY-maleimide is obtained from Tuğçe Nihal Gevrek who has synthesized it according to a previously reported literature [30].

P7 (12 mg, 4.25 x 10^{-4} mmol) and BODIPY-maleimide (6 mg, 14.44 x 10^{-4} mmol) was dissolved in 0.5 mL of degassed benzene. The mixture was refluxed at 85° C for 24 hours and was precipitated into cold diethyl ether. ^{1}H NMR ($CDCl_3$, δ, ppm) 7.34 (br s, 1H, CH_2= CH_2), 6.54 (s, 4H, CH=CH bridge protons), 6.37 (br s, 1H, CH_2= CH_2), 6.31 (br

s, 1H, CH_2= CH_2), 6.02 (s, 2H, from dye), 5.21 (s, 1H, -CHO bridge-head protons), 4.93 (s, 2H, CH_2), 4.45 (m, 2H, CH_2) 4.14-3.96 (m, 10H, CH_2 ester protons), 3.71-3.43 (m, 6H, OCH_2 of PEGMA and initiator), 3.37 (s, 3H, OCH_3 of PEGMA), 2.91 (m, 2H, exo CH-CH bridge protons), 2.49 (s, 6H from dye), 2.38 (s,6H from dye), 2.01–0.63 (m, 32H, $CBr(CH_3)_2$, CH_2, CH_3 along polymer backbone and CH_2 along alkane chain of dye). (Some peaks form dye overlap with polymer peaks between 3.5-3.0 ppm and 1.8-1.2 ppm)

P7 (12 mg, 4.25 x 10^{-4} mmol) and BODIPY-maleimide (6 mg, 14.44 x 10^{-4} mmol) was dissolved in 0.5 mL of degassed ethyl acetate. The mixture was stirred at room temperature for 7 days and was precipitated into cold diethyl ether. ^{1}H NMR ($CDCl_3$, δ, ppm) 7.43 (br s, 1H, CH_2= CH_2), 6.58 (s, 4H, CH=CH bridge protons), 6.37 (br s, 1H, CH_2= CH_2), 6.33 (br s, 1H, CH_2= CH_2), 6.01 (s, 2H, from dye), 5.26 (s, 1H, -CHO bridge-head protons), 4.93 (s, 2H, CH_2), 4.45 (m, 2H, CH_2) 4.13-3.93 (m, 10H, CH_2 ester protons), 3.69-3.36 (m, 6H, OCH_2 of PEGMA and initiator), 3.35 (s, 3H, OCH_3 of PEGMA), 2.92 (m, 2H, exo CH-CH bridge protons), 2.48 (s, 6H from dye), 2.39 (s,6H from dye), 2.01–0.63 (m, 32H, $CBr(CH_3)_2$, CH_2, CH_3 along polymer backbone and CH_2 along alkane chain of dye). (Some peaks form dye overlap with polymer peaks between 3.5-3.0 ppm and 1.8-1.2 ppm)

Attachment of BODIPY-maleimide in water: 1.5 mg P7 was dissolved in 3 mL of water, then 0.5 mg BODIPY-maleimide was added to this solution. The mixture was stirred at room temperature for 4 days. UV spectrum of the sample was taken each day.

Control experiment for attachment of BODIPY-maleimide in water: 1.5 mg P(PEGMA) was dissolved in 3 mL of water, then 0.5 mg BODIPY-maleimide was added to this solution. The mixture was stirred at room temperature for 4 days. UV spectrum of the sample was taken each day.

4.2.3.4. Release studies. 1.5 mg of dye conjugated polymer (endo/exo mixture) was dissolved in 3 mL of water and stirred at 40 °C for 4 days. UV spectrum of the sample was taken each day. 1.5 mg of dye conjugated polymer (endo/exo mixture) was dissolved in 10 mL of water and stirred at 40 °C for 4 days. UV spectrum of the sample was taken each day.

4.2.3.5. Synthesis of linker for drug attachment. 5 is synthesized according to a previously reported literature procedure [31]. Then 5 (2 g, 9.56 mmol), DMAP (1.76 g, 14.32 mmol) and succinic anhydride (3.84 g, 38.24 mmol) was dissolved in 60 mL of 1,4-dioxane. To the reaction mixture Et_3N (6.63 ml, 47.84 mmol) was added, and the mixture was stirred for 24 hours at 40 °C. The reaction solution was poured into cold water and extracted with CH_2Cl_2. Then the organic phase was washed with 1 M HCl, dried over Na_2SO_4 and concentrated. **6** is recrystallized from ethanol as pure white crystalls. (2.36 g, 80% yield). ^{1}H NMR ($CDCl_3$, δ, ppm) 6.49 (s, 2H, CH=CH bridge protons), 5.24 (s, 2H, -CHO bridge-head protons), 4.05 (t, *J*=8 Hz, 2H, NCH_2 CH_2 CH_2OC=O), 3.56 (t, *J*=6 Hz, 2H, NCH_2 CH_2 CH_2OC=O), 2.83 (s, 2H, CH-CH bridge protons), 2.56-2.68 (m, 4H, C=OCH_2CH_2C=OOH), 1.89 (m, 2H, NCH_2 CH_2 CH_2OC=O).

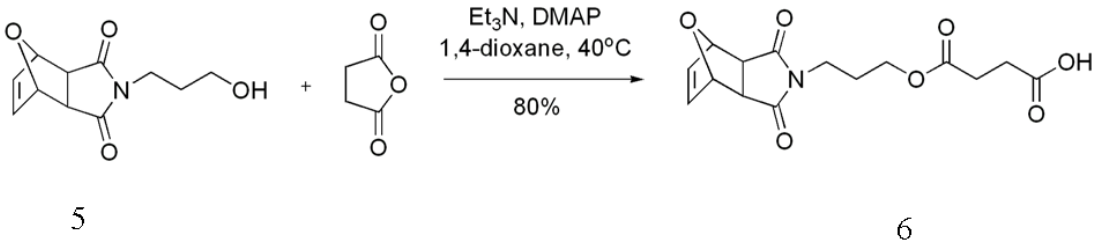

Figure 4.6. First step of synthesis of linker

6 (150 mg, 0.46 mmol) was refluxed in 20 mL of toluene for 24 hours. Then toluene was removed by rotary evaporation and 7 is obtained as pure white crystalls. (116 mg, 99% yield). ^{1}H NMR ($CDCl_3$, δ, ppm) 6.68 (s, 2H, CH_2=CH_2), 4.08 (t, *J*=6 Hz, 2H, NCH_2 CH_2 CH_2OC=O), 3.61 (t, *J*=6 Hz, 2H, NCH_2 CH_2 CH_2OC=O), 2.58-2.69 (m, 4H, C=OCH_2CH_2C=OOH), 1.93 (m, 2H, NCH_2 CH_2 CH_2OC=O).

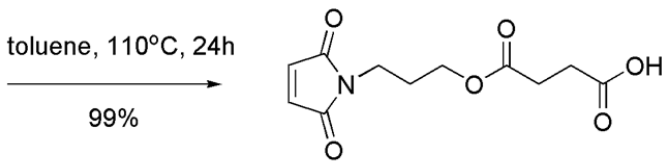

7

Figure 4.7. Second step of synthesis of linker.

5. CONCLUSION

In this study, 4-arm and 6-arm star shaped reactive polymers which contain pendant furan groups at their side chains are synthesized by atom transfer radical polymerization (ATRP). After polymerization, the furan groups on the polymers are functionalized successfully by ethylmaleimide as a model compound via Diels-Alder reaction. Furthermore, a fluorescent dye BODIPY-maleimide is conjugated to these star shaped polymers. Then the release of BODIPY-maleimide by retro Diels-Alder reaction of the endo product is monitored by UV spectroscopy. Conjugation of the drug camptothecin to the star shaped polymers by the synthesized linker will be done as a future work.

APPENDIX

^{1}H NMR and FT-IR spectra of the synthesized products are included.

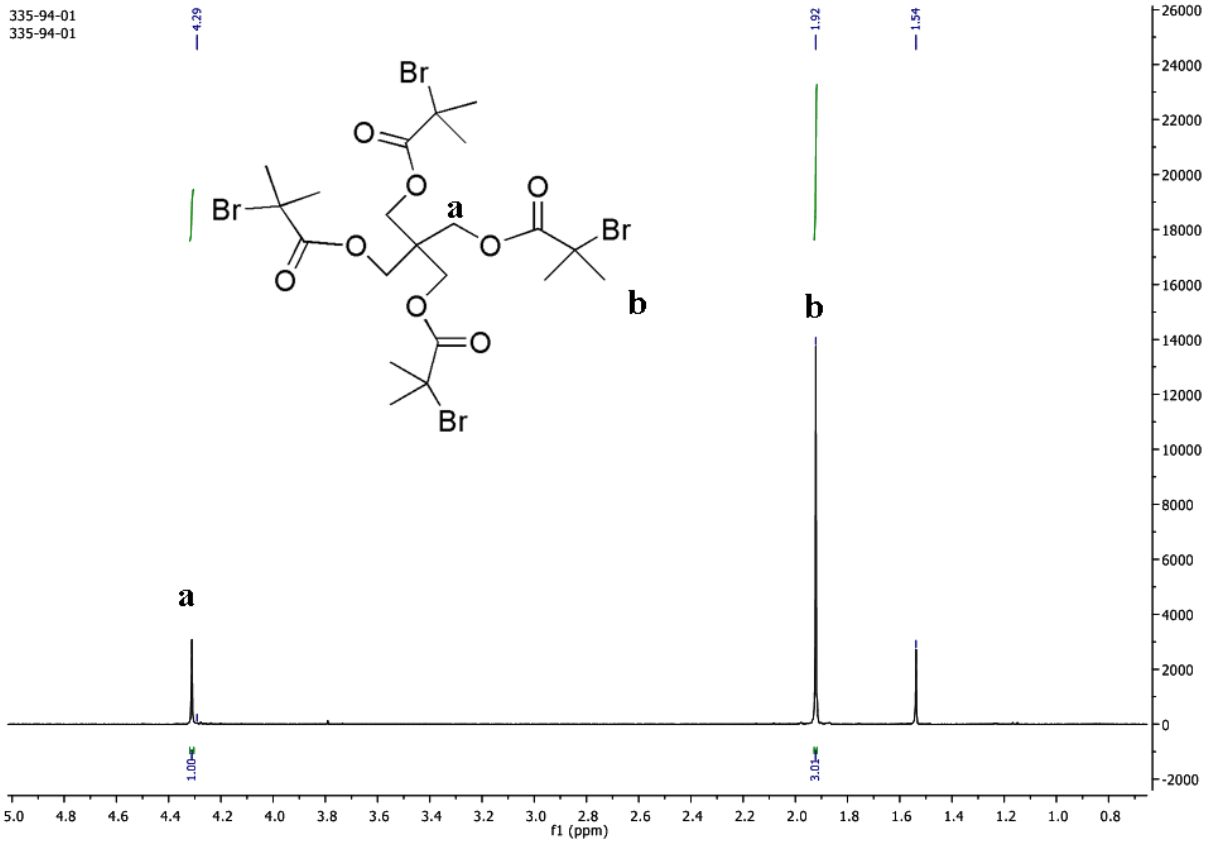

Figure A.1. ^{1}H NMR spectrum of 1.

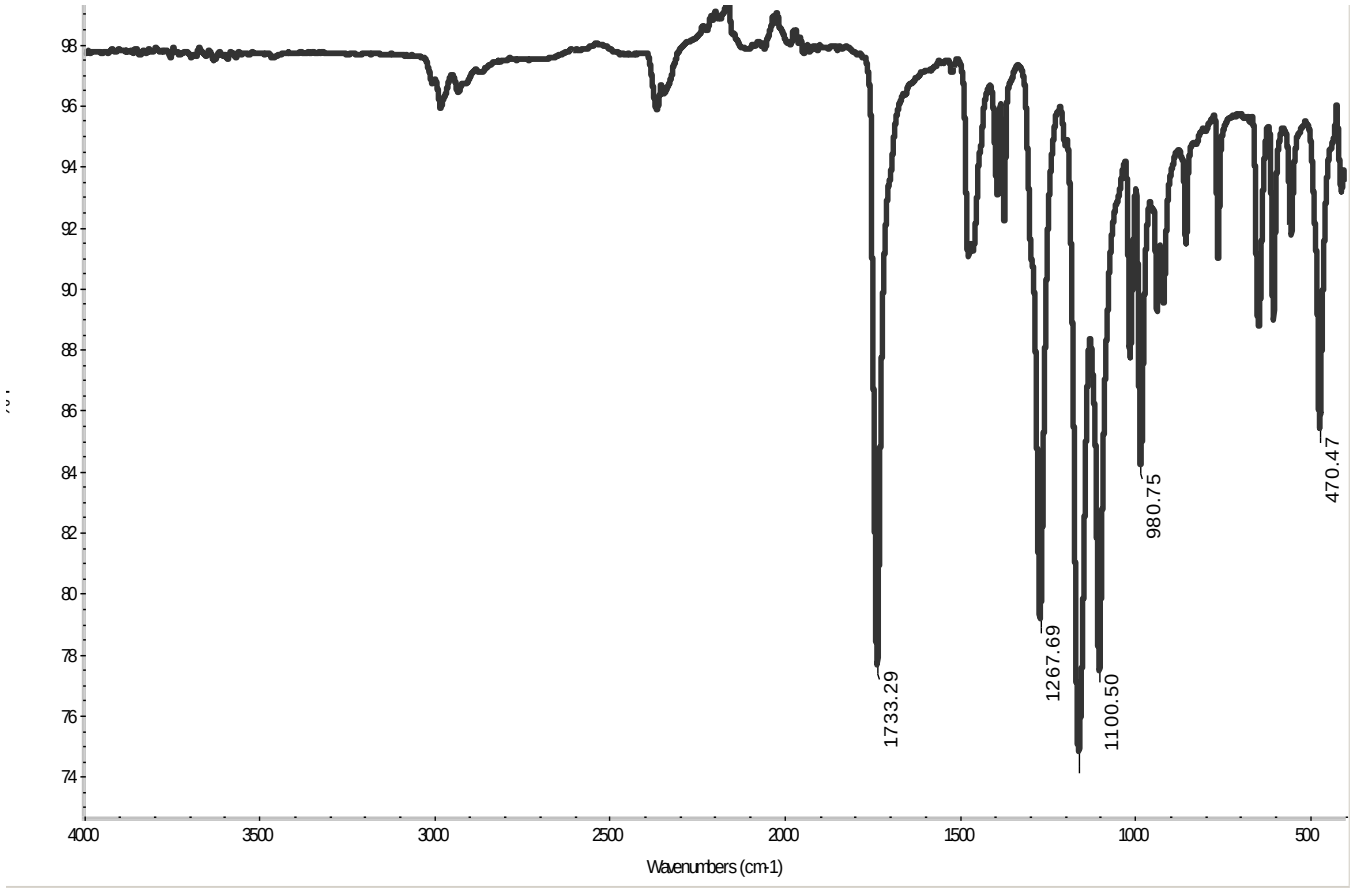

Figure A.2. FT-IR spectrum of 1.

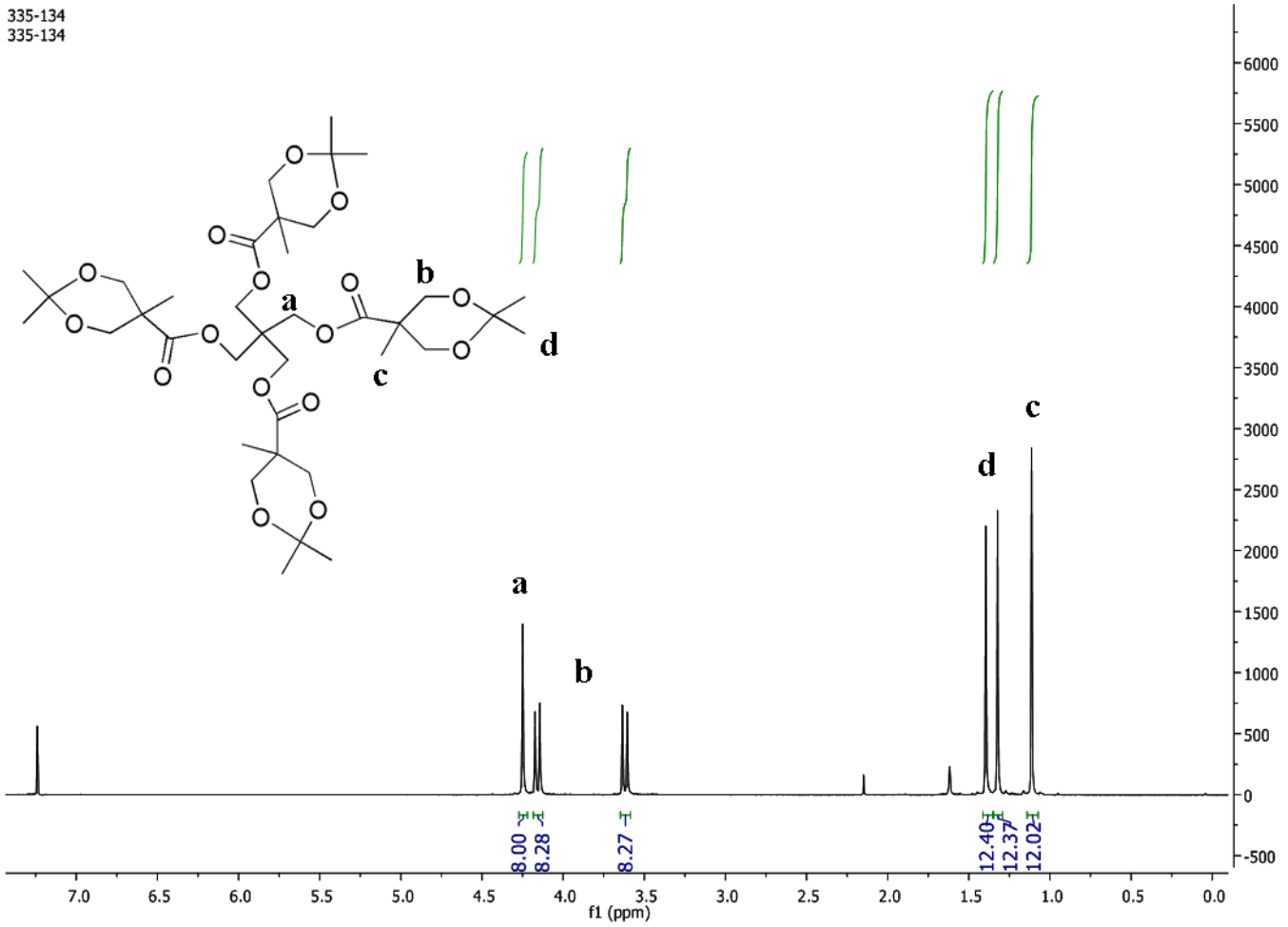

Figure A.3. ^{1}H NMR spectrum of 2.

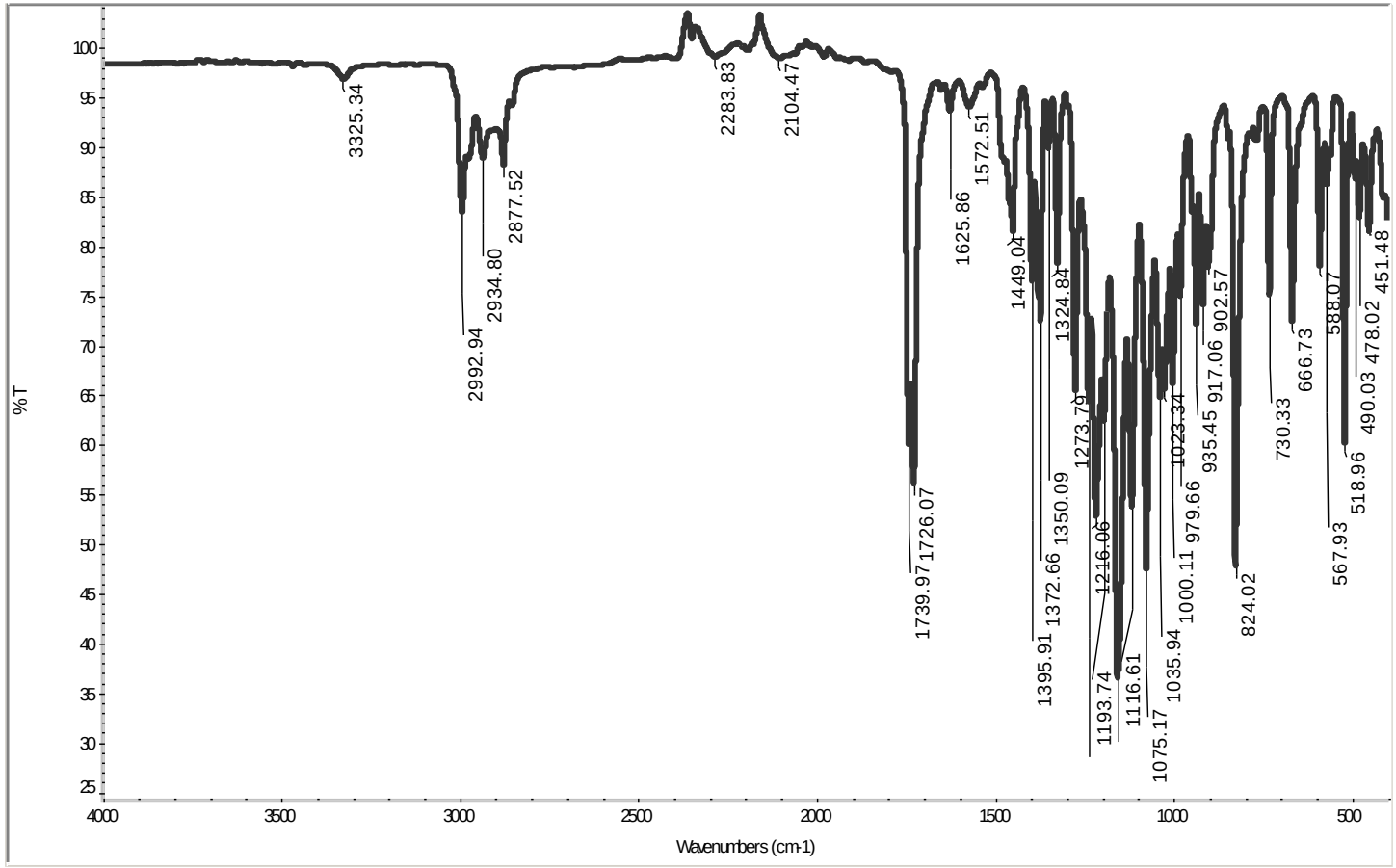

Figure A.4. FT-IR spectrum of 2.

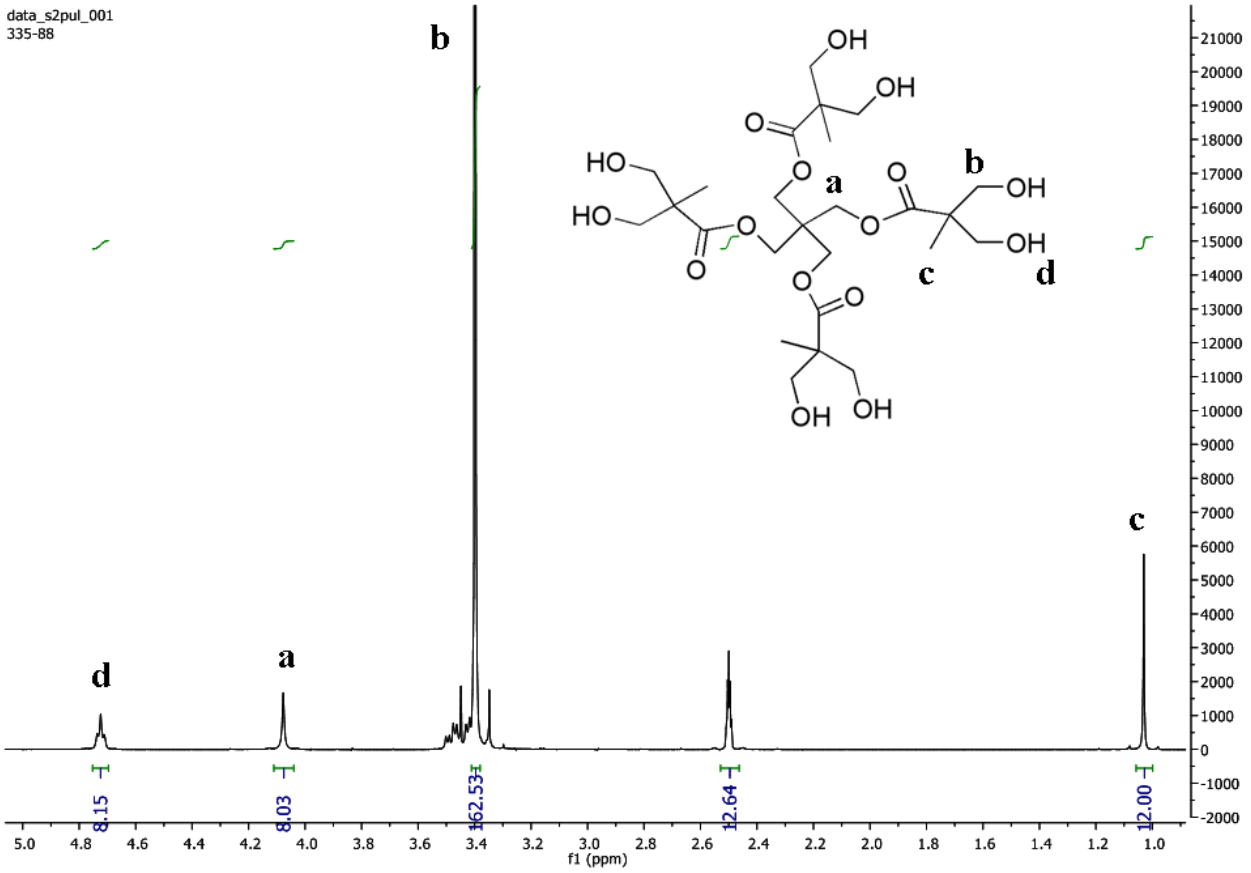

Figure A.5. ^{1}H NMR spectrum of 3.

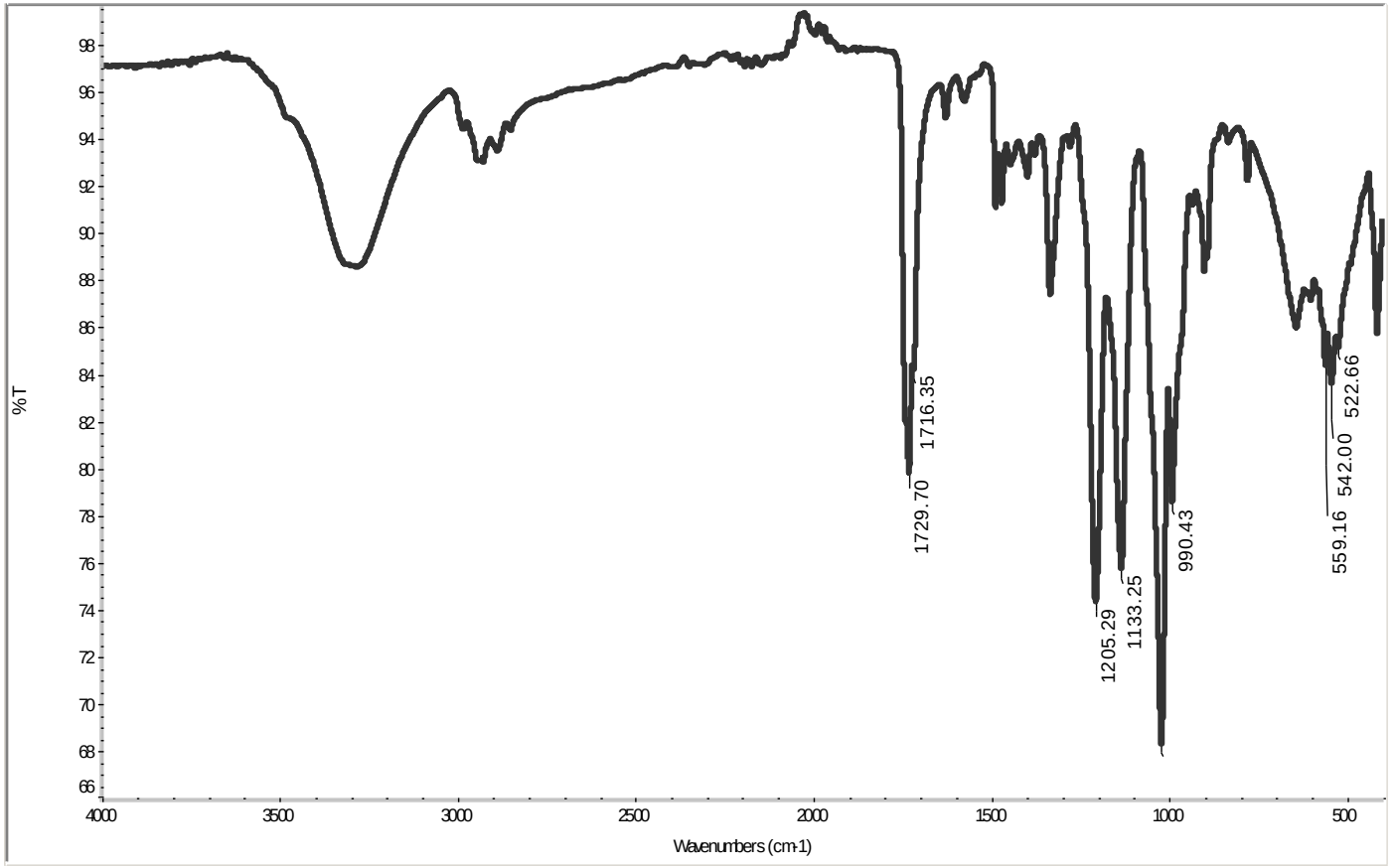

Figure A.6. FT-IR spectrum of 3.

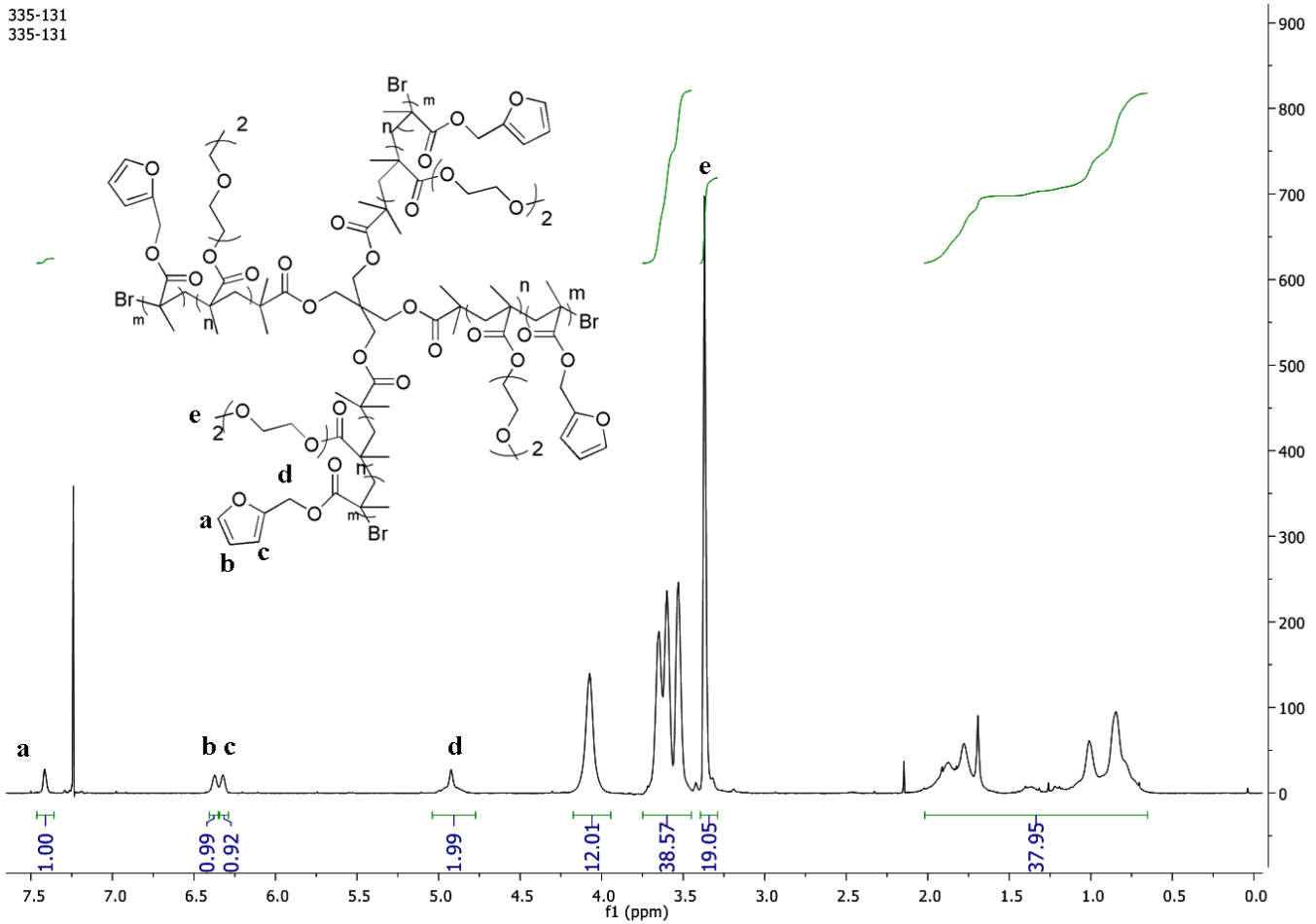

Figure A.7. ^{1}H NMR spectrum of P1.

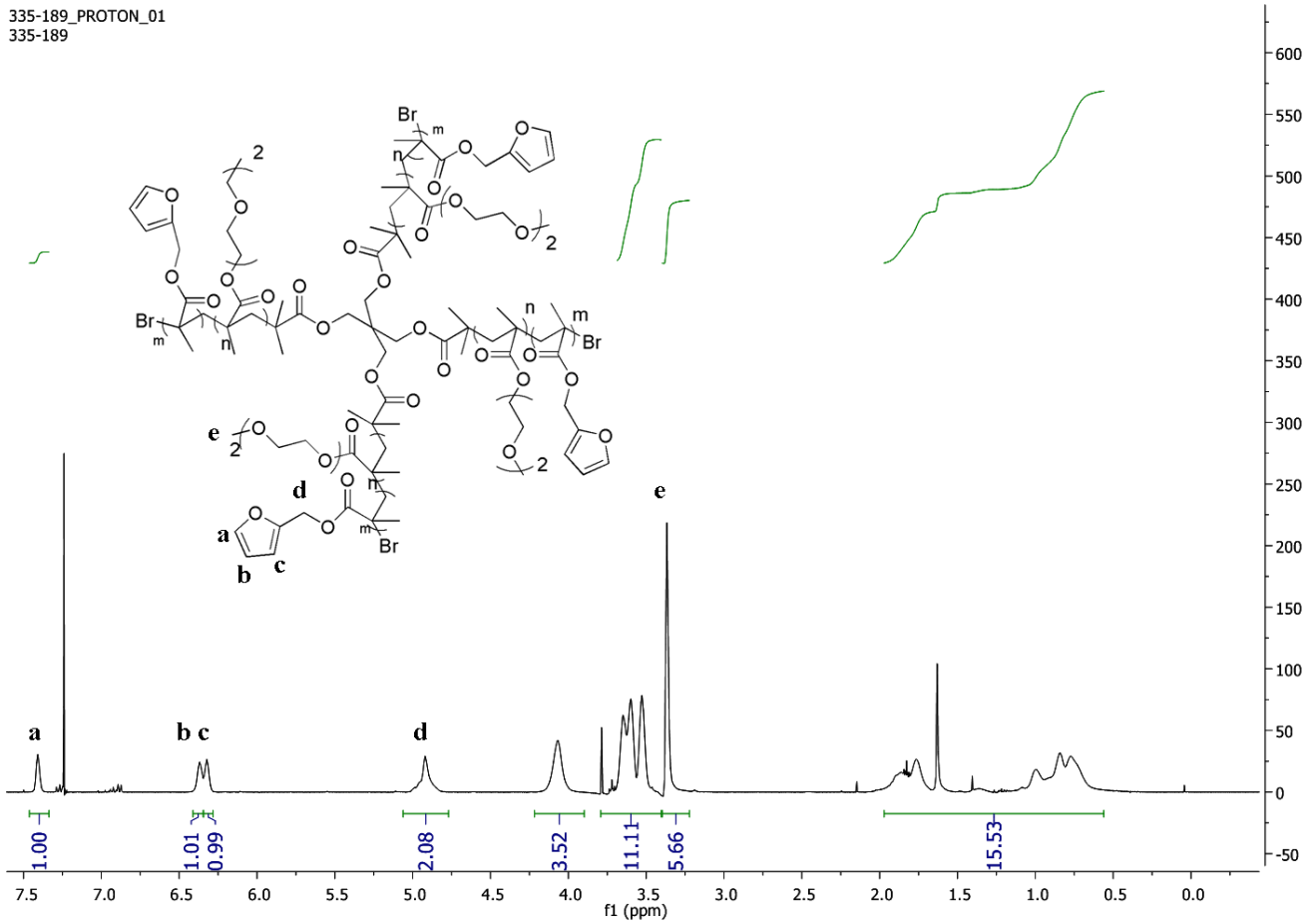

Figure A.8. ^{1}H NMR spectrum of P2.

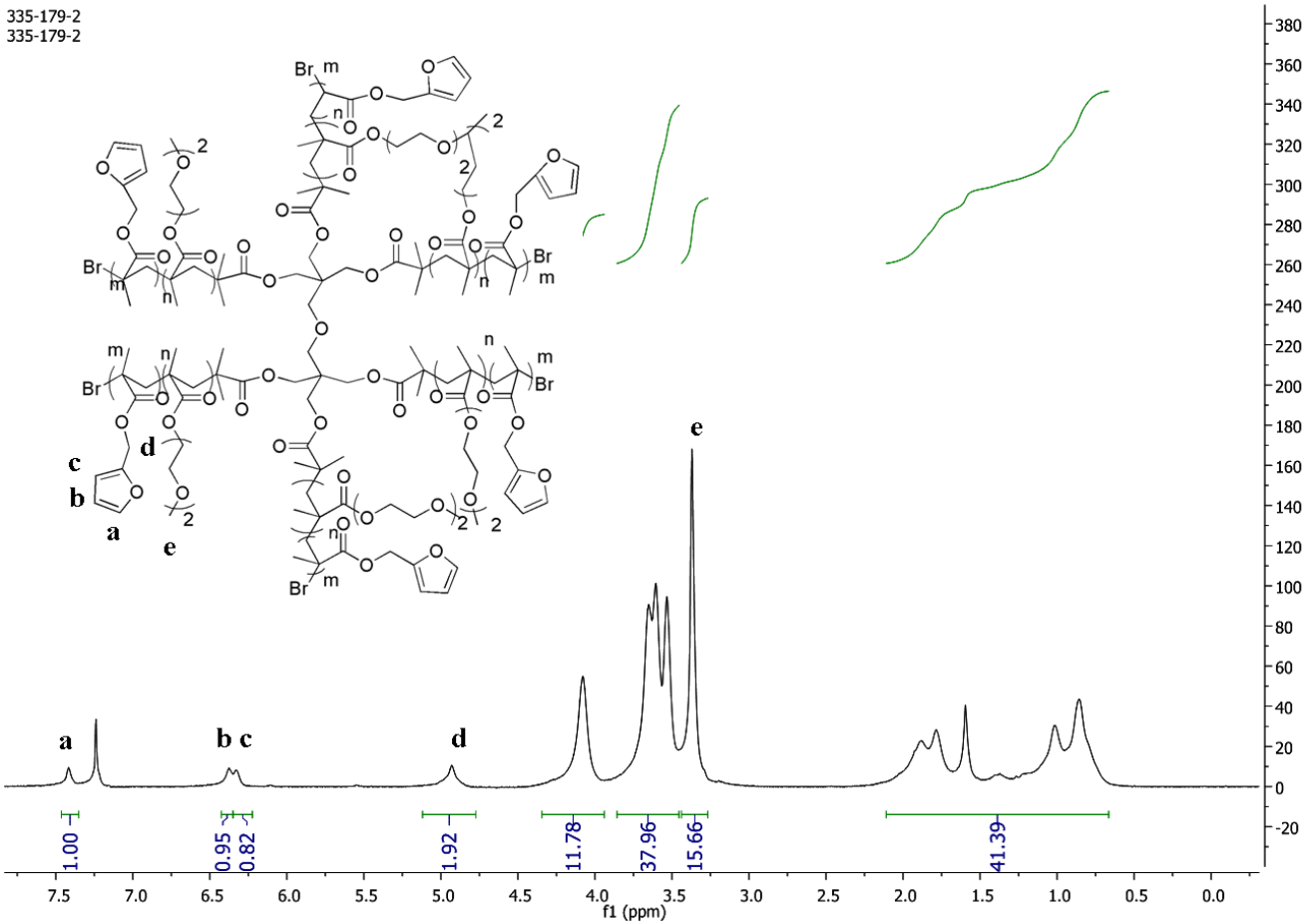

Figure A.9. ^{1}H NMR spectrum of P3.

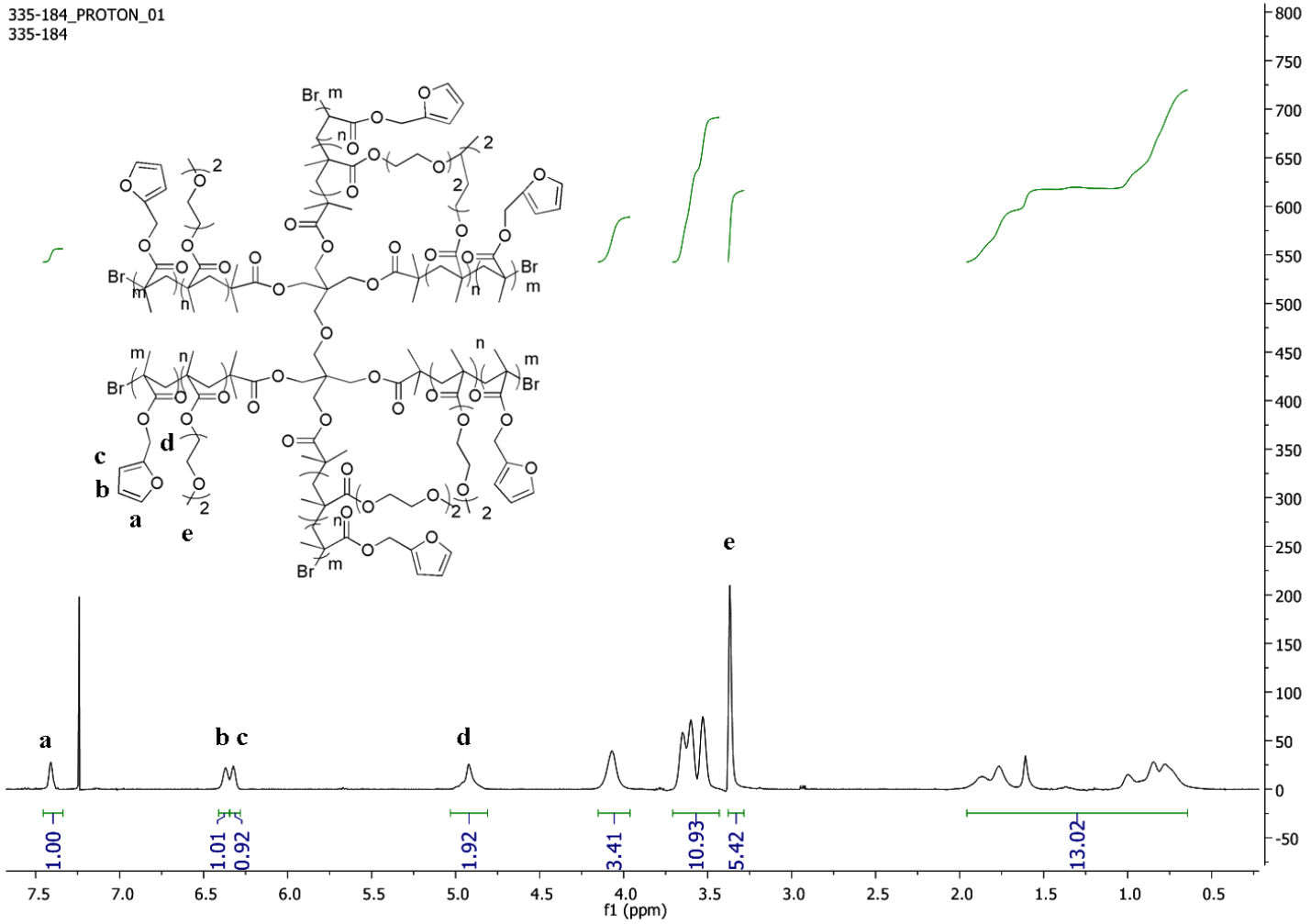

Figure A.10. ^{1}H NMR spectrum of P4.

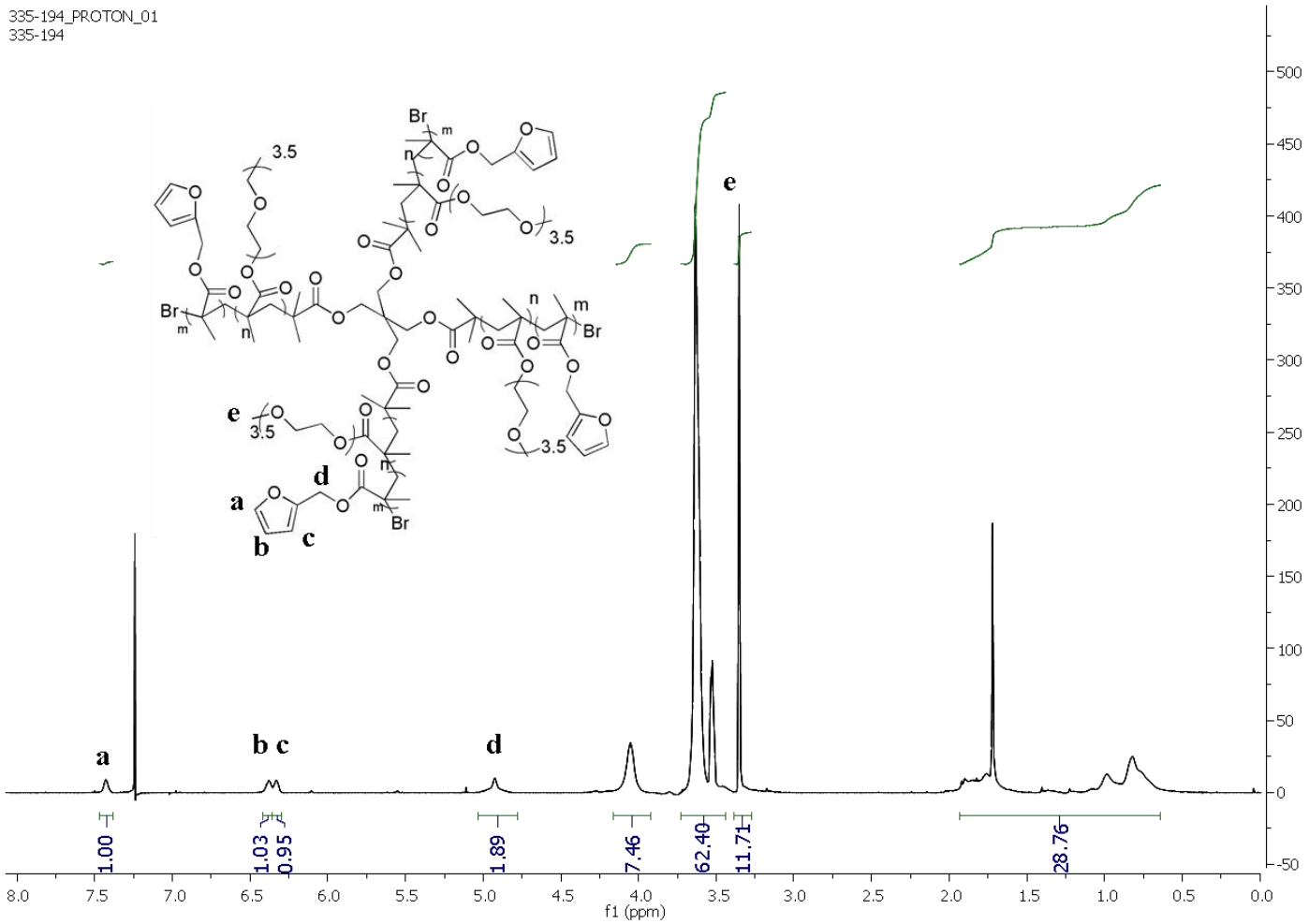

Figure A.11. ^{1}H NMR spectrum of P5.

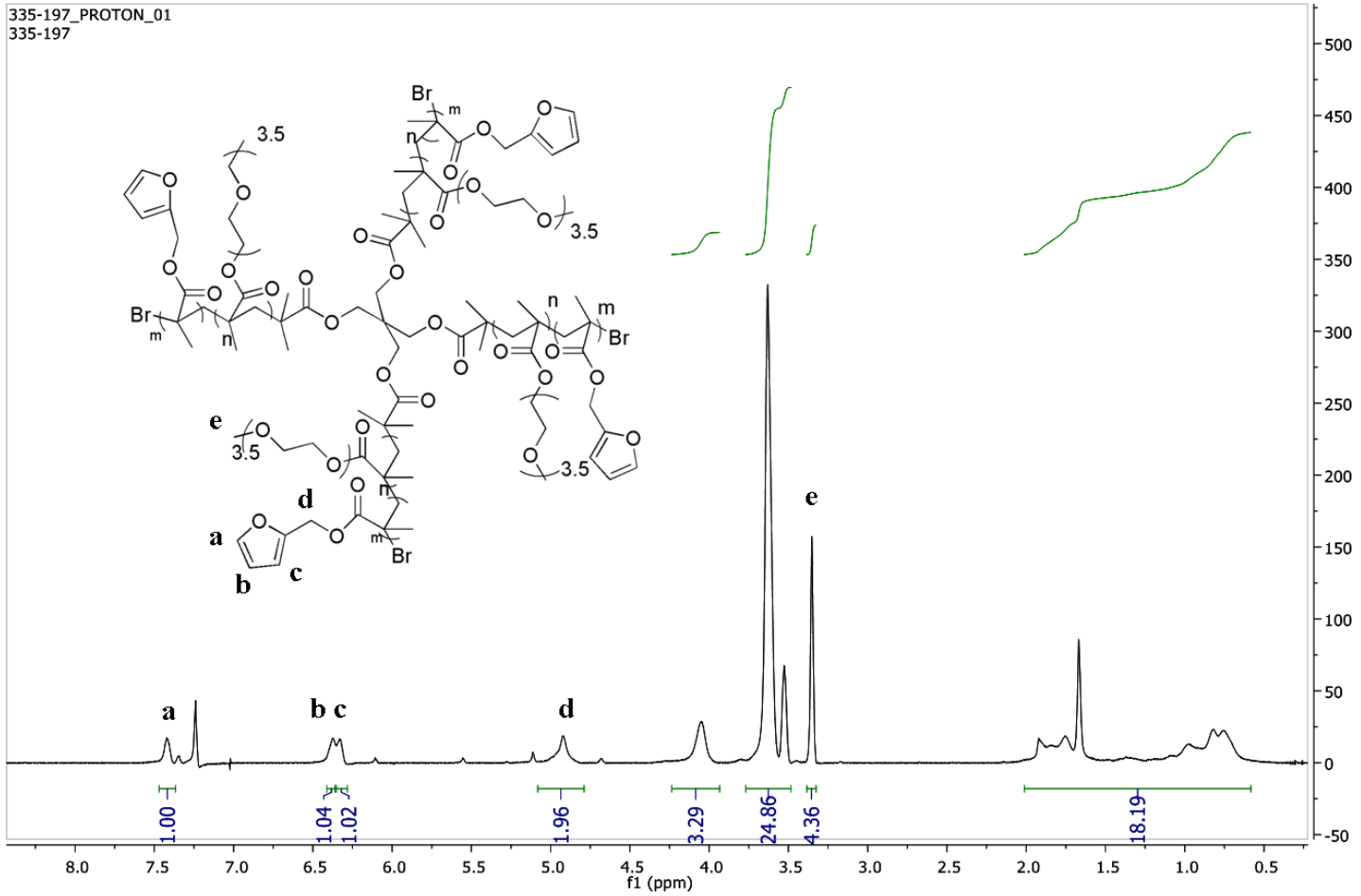

Figure A.12. ^{1}H NMR spectrum of P6.

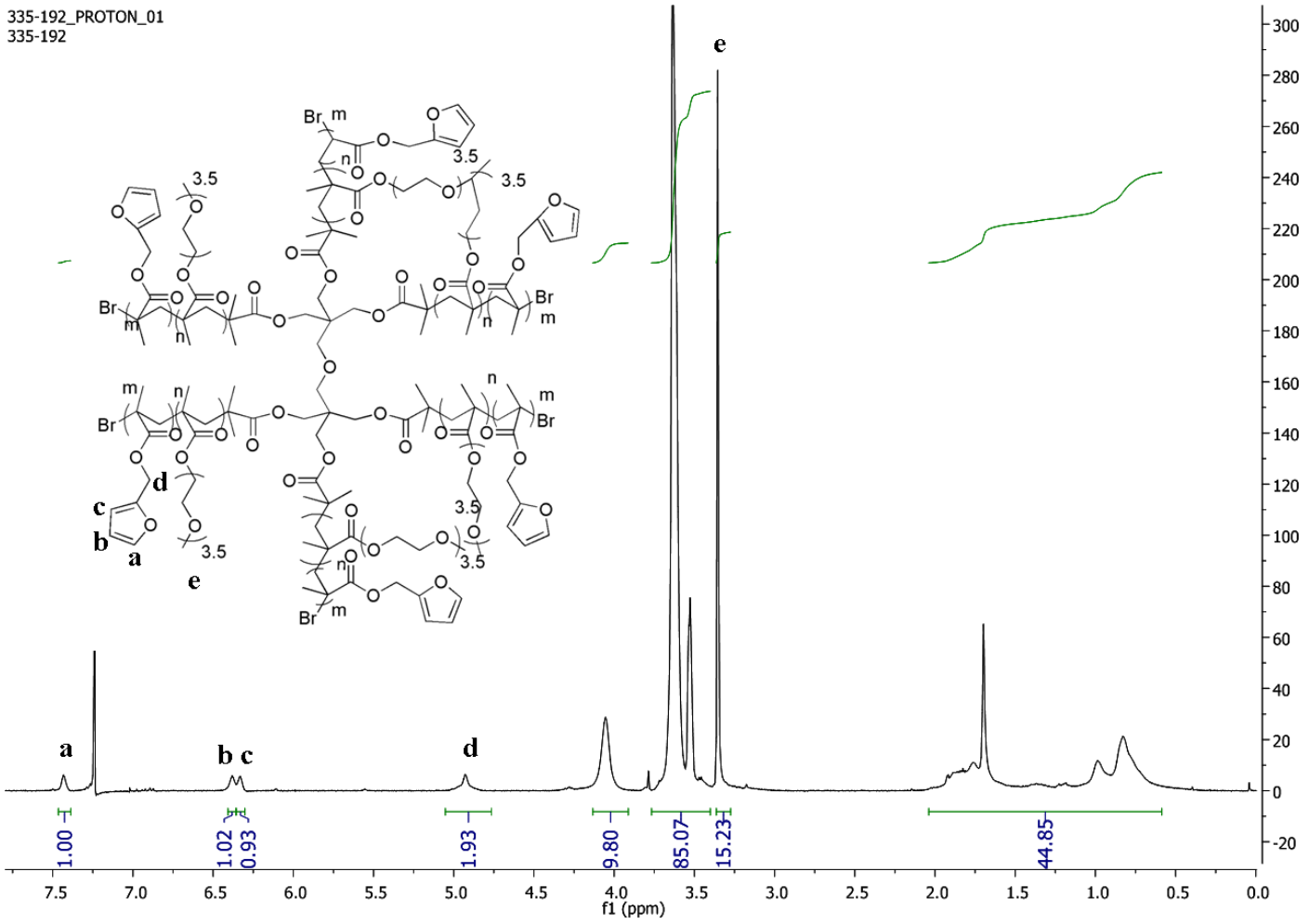

Figure A.13. ^{1}H NMR spectrum of P7.

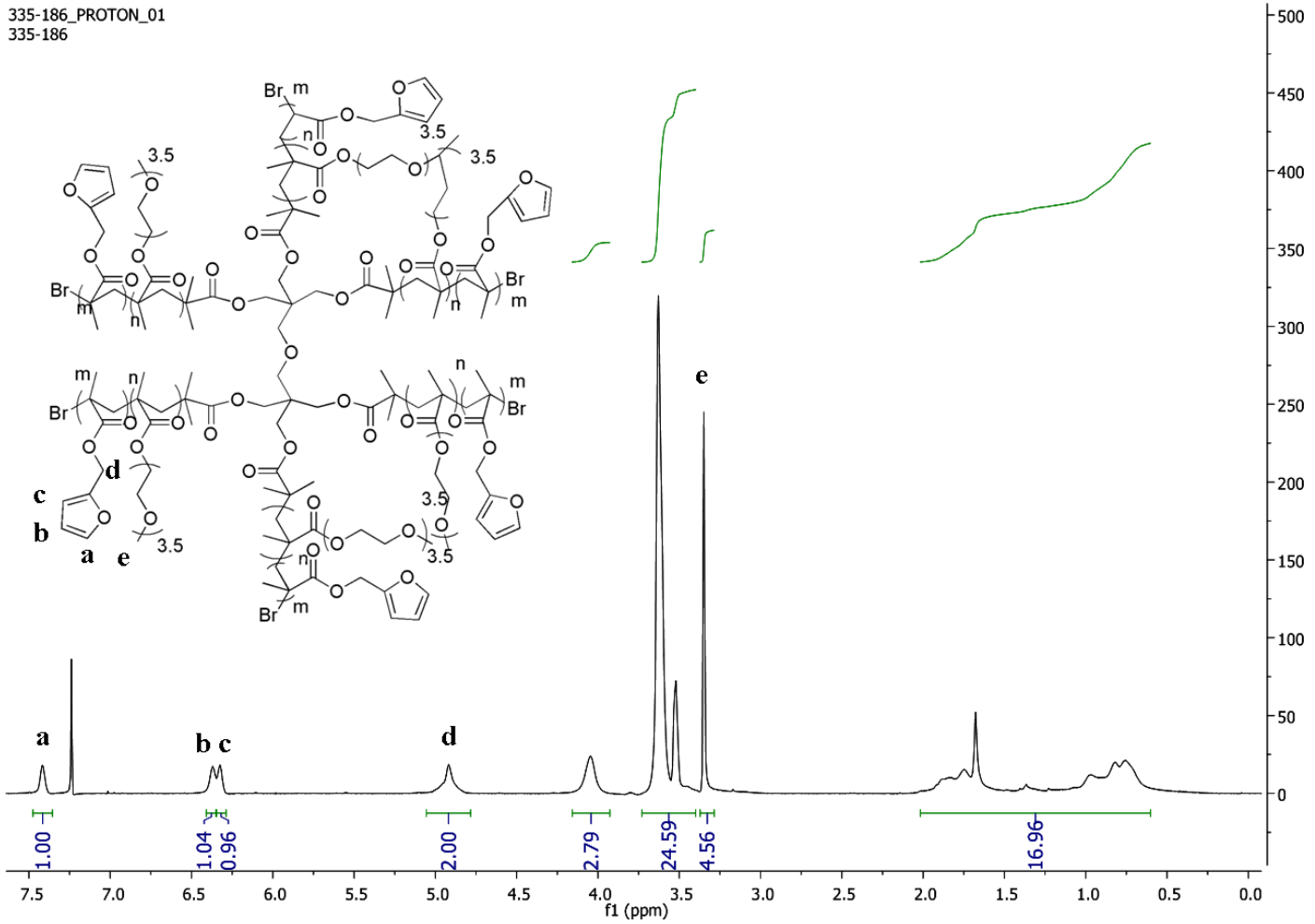

Figure A.14. ^{1}H NMR spectrum of P8.

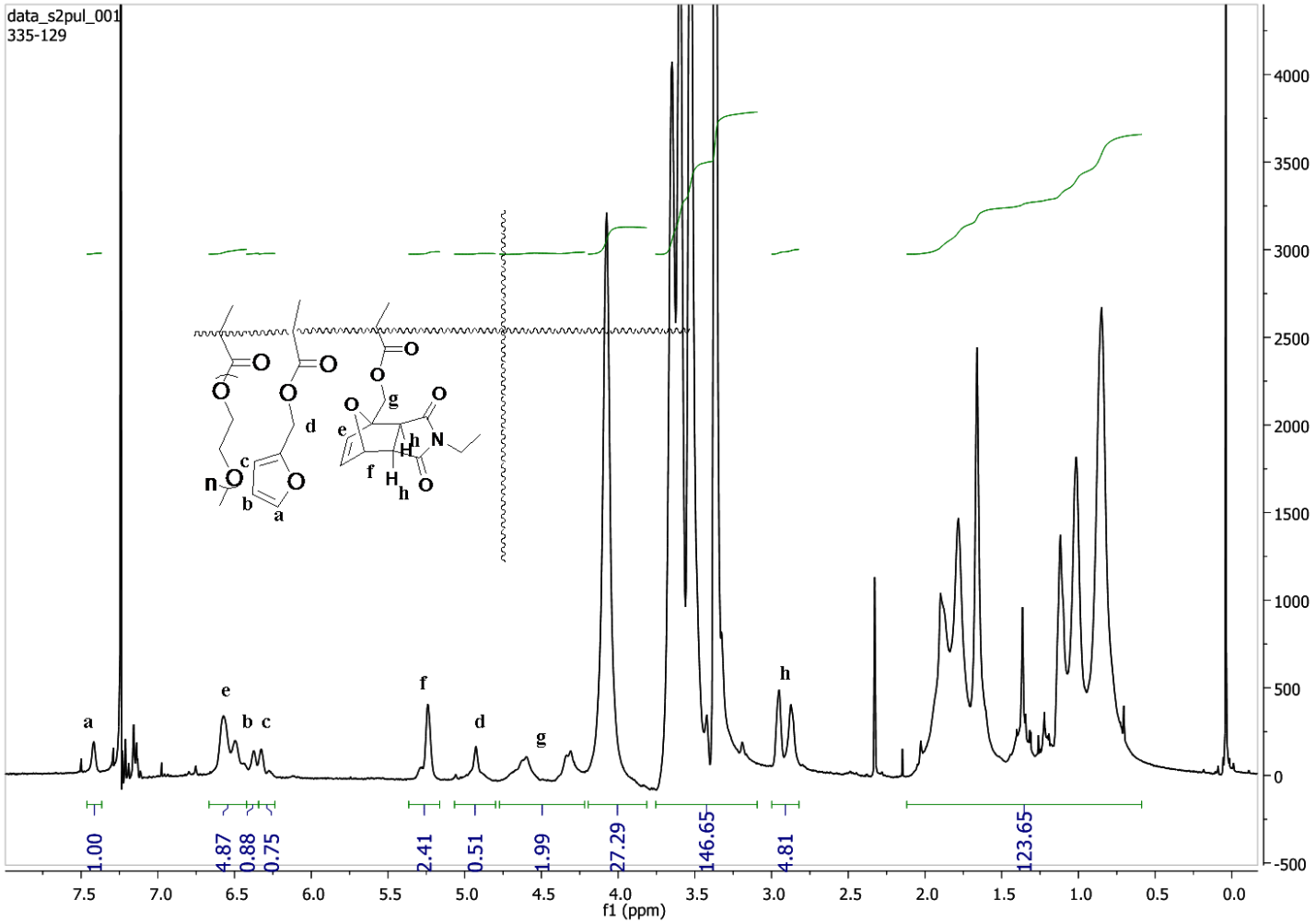

Figure A.15. ^{1}H NMR spectrum of ethyl maleimide conjugated P1 (exo).

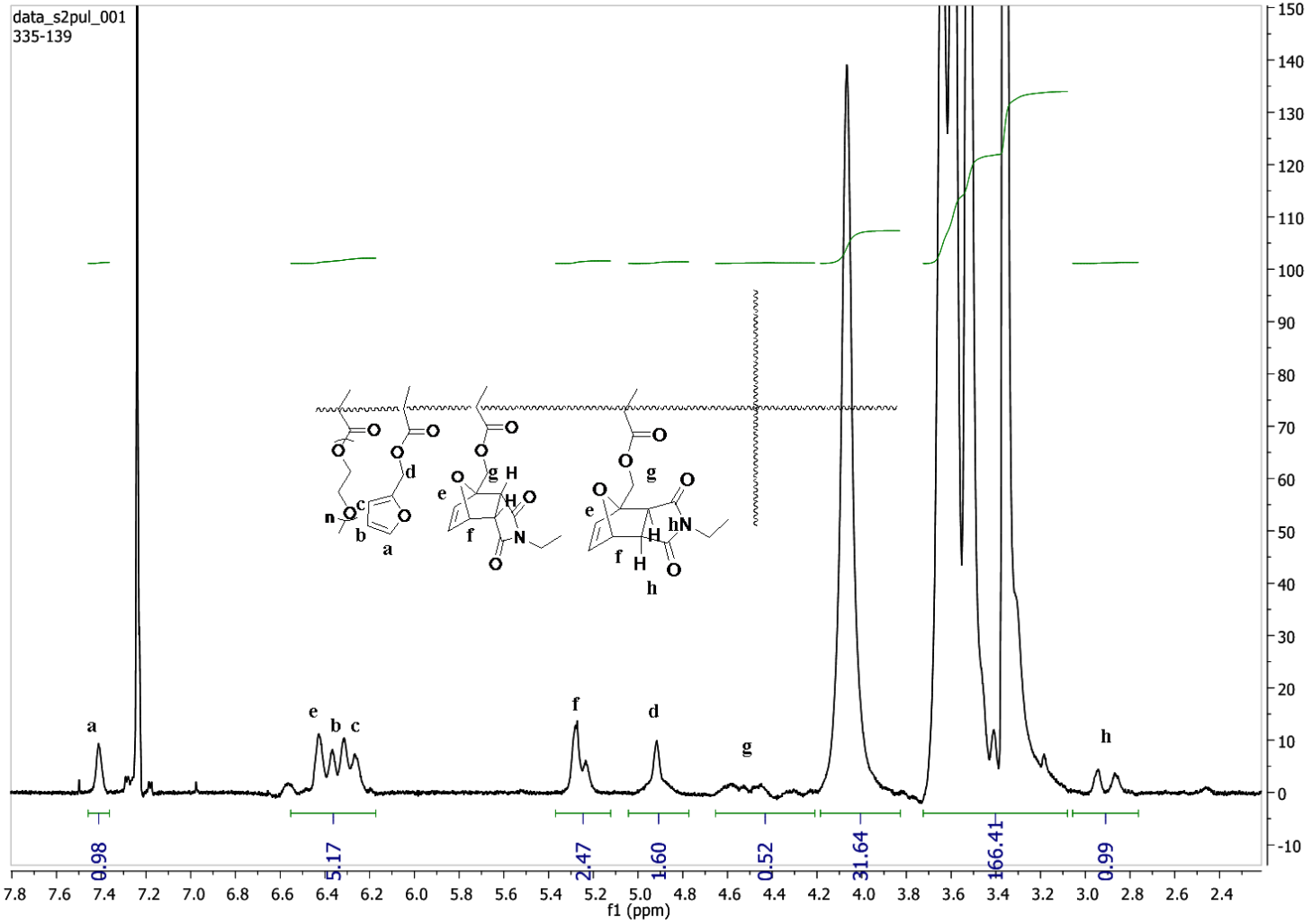

Figure A.16. ^{1}H NMR spectrum of ethyl maleimide conjugated P1 (endo/exo mixture).

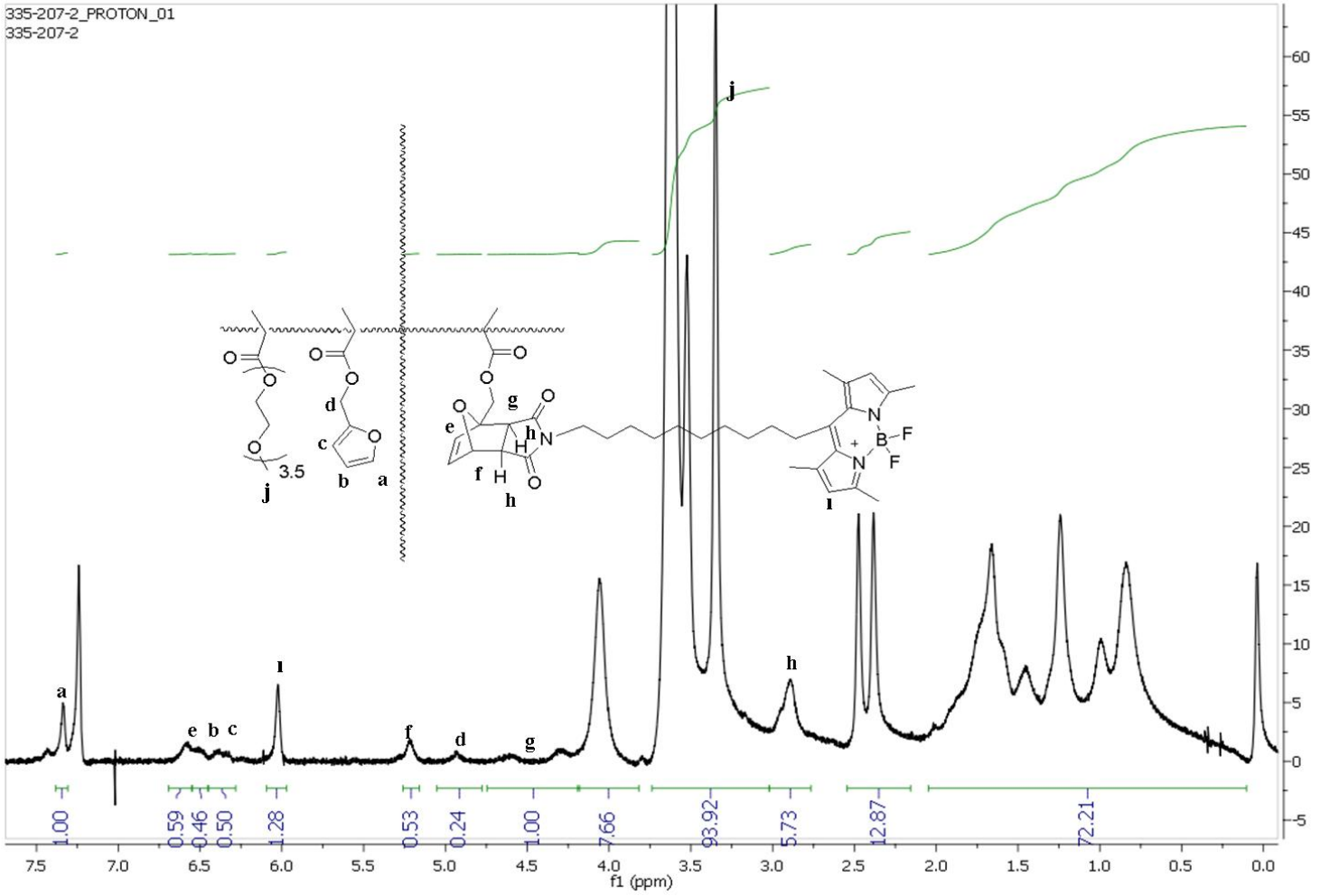

Figure A.17. ^{1}H NMR spectrum of BODIPY-maleimide cojugated P1 (exo).

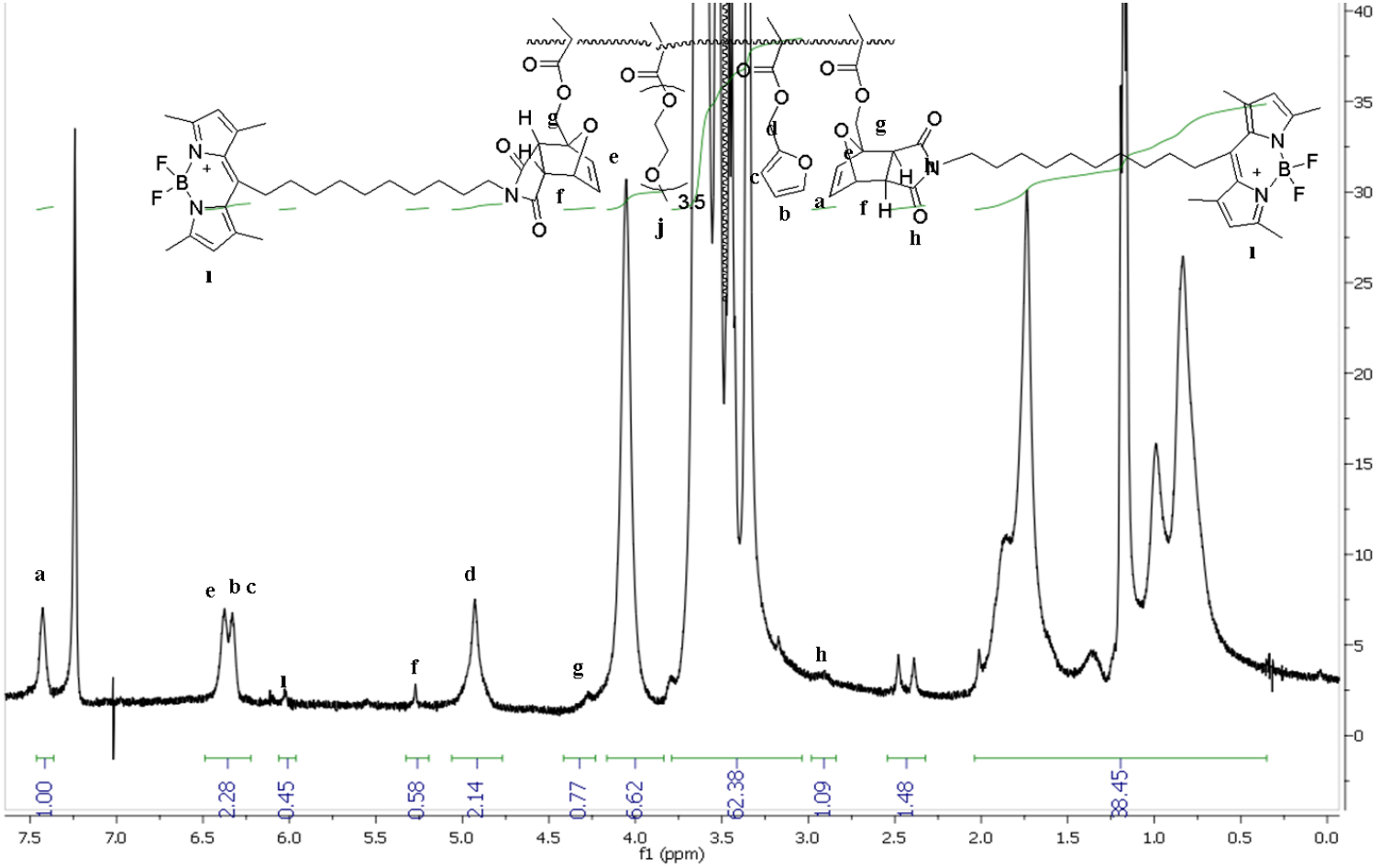

Figure A.18. ^{1}H NMR spectrum of BODIPY-maleimide conjugated P1 (exo / endo mixture).

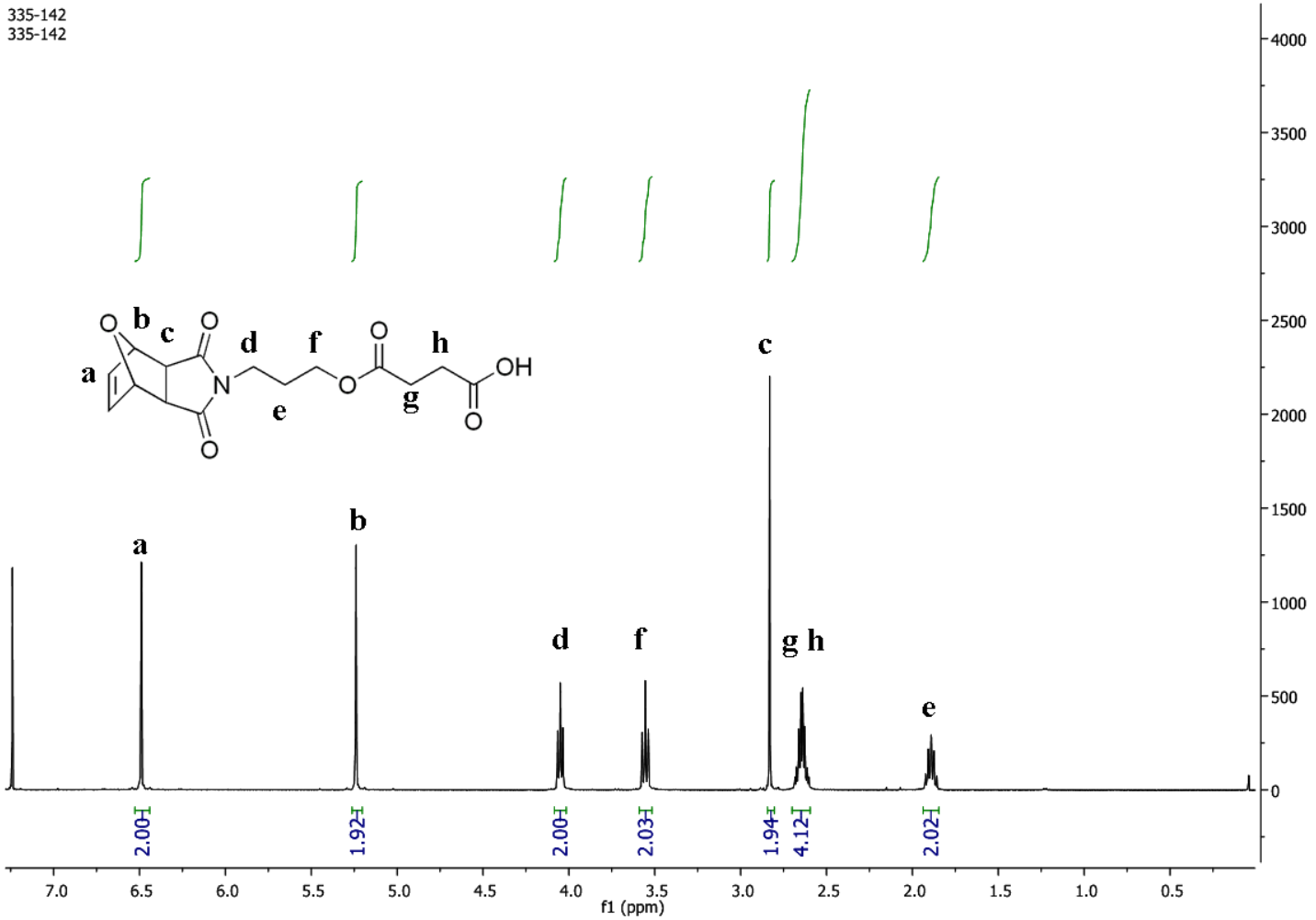

Figure A.19. ^{1}H NMR spectrum of 6.

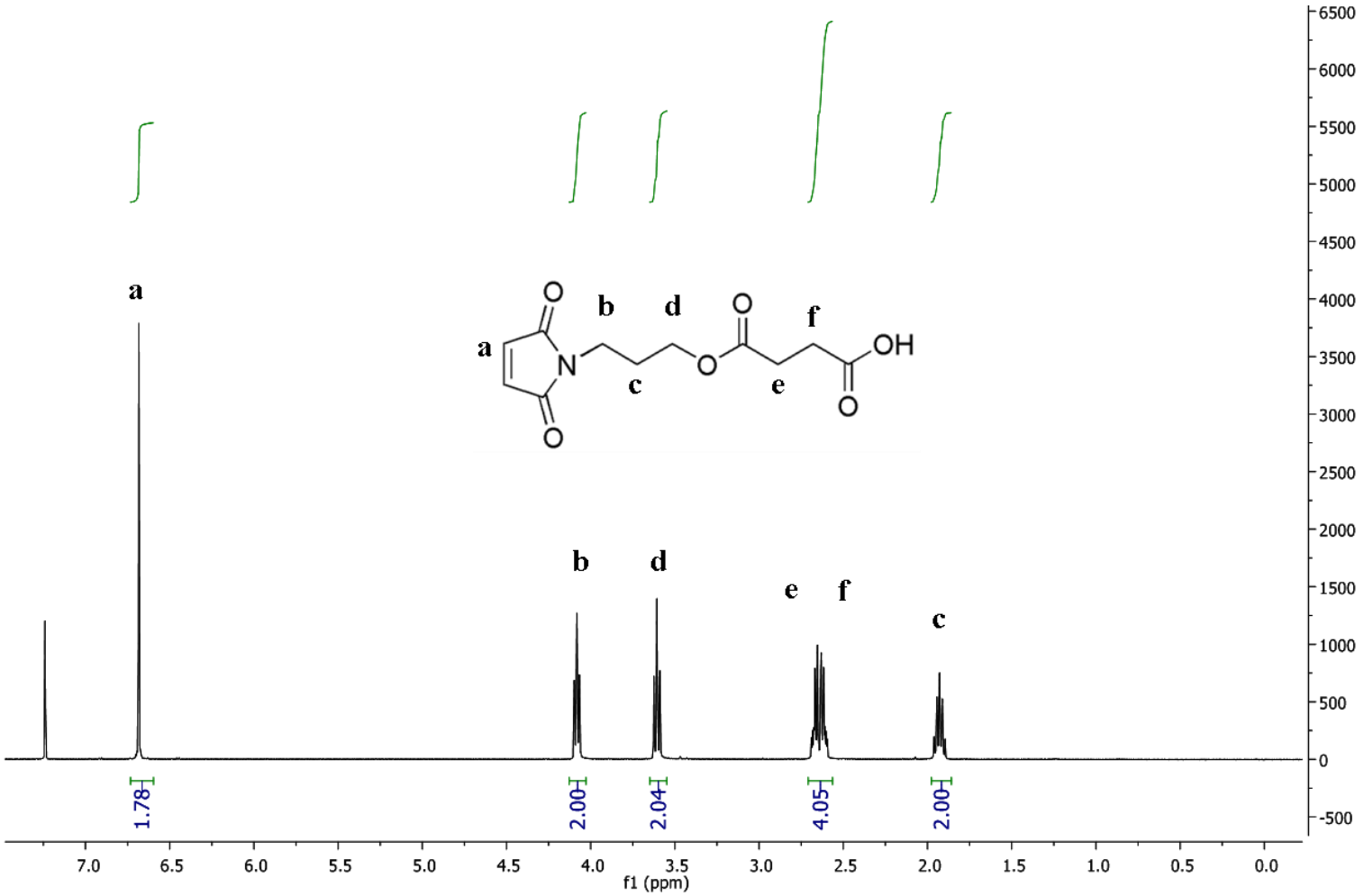

Figure A.20. ^{1}H NMR spectrum of 7.

REFERENCES

1. *Cancer,* http://www.who.int/topics/cancer/en/, May 2012.

2. *Cancer Chemotherapy,* http://www.nlm.nih.gov/medlineplus/cancerchemotherapy.html, May 2012.

3. *What Is Cancer?,* http://cancer.gov/cancertopics/cancerlibrary/what-is-cancer, May 2012.

4. Wall, M. E., M. C. Wani, C. E. Cooke, K. H. Palmer, A. T. McPhail and G. A. Sim, "Plant Antitumor Agents. I. The Isolation and Structure of Camptothecin, a Novel Alkaloidal Leukemia and Tumor Inhibitor from Camptotheca Acuminate", *Journal of American Chemical Society,* Vol. 88, pp. 3888-3890, 1966.

5. Venditto, V. J. and E. E. Simanek, "Cancer Therapies Utilizing the Camptothecins: A Review of the in Vivo Literature", *Molecular Pharmaceutics,* Vol. 7, pp. 307-349, 2010.

6. Pommier, Y. "Topoisomerase I İnhibitors: Camptothecin and Beyond", *Nature Reviews Cancer,* Vol. 6, pp. 789-802, 2006.

7. Redinbo, M.R., L. Stewart, P. Kuhn, J. J. Champoux and W. G. J. Hol, "Crystal Structure of Human Topoisomerase I in Covalent and Noncovalent Complexes with DNA", *Science,* Vol. 279, pp. 1504-1513, 1998.

8. Duncan, R., "The Dawning Era of Polymer Therapeutics", *Nature Reviews Drug Discovery,* Vol. 2, pp. 347-360, 2003.

9. Ringsdorf, H.,"Structure and Properties of Pharmacologically Active Polymers", *Journal of Polymer Science Polymer Symposia,* Vol. 51, pp. 135-153, 1975.

10. Park, J. H., S. Lee, J. Kim, K. Park, K. Kim and I. C. Kwon, "Polymeric Nanomedicine for Cancer Therapy", *Progress in Polymer Science,* Vol. 33, pp. 113-137, 2008.

11. Matsumura, Y. and H. Maeda, "A New Concept for Macromolecular Therapeutics in Cancer Chemotherapy: Mechanism of Tumoritropic Accumulation of Proteins and the Antitumor Agent Smancs", *Cancer Research,* Vol. 46, pp. 6387-6392, 1986.

12. Haag, R. and F. Kratz, "Polymer Therapeutics: Concepts and Applications", *Angewandte Chemie International Edition,* Vol. 45, pp. 1198-1215, 2006.

13. Duncan, R. and R. Gaspar, "Nanomedicine(s) Under the Microscope", *Molecular Pharmaceutics,* Vol. *8*, pp. 2101-2141, 2011.

14. Vicent, M. J. and R. Duncan, "Polymer Conjugates: Nanosized Medicines for Treating Cancer", *Trends in Biotechnology,* Vol. 24, pp. 39-47, 2006.

15. Duncan, R.; L.W. Seymour, K.B. O'Hare, P.A. Flanagan, S. Wedge, I.C. Hume,K. Ulbrich, J. Strohalm, V. Subr, F. Spreafico, M. Grandi, M. Ripamonti, M. Farao and A. Suarato, "Preclinical Evaluation of Polymer-Bound Doxorubicin", *Journal of Controlled Release,* Vol. 19, pp. 331-346,1992.

16. Gianasi, E., M Wasil, E.G Evagorou, A Keddle, G Wilson and R. Duncan, "HPMA Copolymer Platinates as Novel Antitumour Agents: In Vitro Properties, Pharmacokinetics and Antitumour Activity In Vivo", *European Journal of Cancer,* Vol.35, pp. 994-1002, 1999.

17. Li, C.; D. Yu, R. A. Newman, F. Cabral, L. C. Stephens, N. Hunter, L. Milas and S. Wallace, "Complete Regression of Well-established Tumors Using a Novel Water-soluble Poly(L-Glutamic Acid)-Paclitaxel Conjugate", *Cancer Research,* Vol. 58; 2404-2409, 1998.

18. Ochoa, L., A. Tolcher, J. Rizzo, G. Schwartz, A. Patnaik, L. Hammond, H. McCreery, L. Denis, M. Hidalgo, J. Kwiatek, J. McGuire and E. Rowinsky, "A Phase I Study of PEG-Camptothecin (PEG-CPT) in Patients with Advanced Solid

Tumors: A Novel Formulation for an Insoluble But Active Agent." *American Society of Clinical Oncology*, Vol. 19, pp. 770, 2000.

19. Fox, M. E.; F. C. Szoka and J. M. Frechet, "Soluble Polymer Carriers for the Treatment of Cancer: The Importance of Molecular Architecture", *Accounts of Chemical Research*, Vol. 42, pp. 1141-1151, 2009.

20. *Star Copolymers*, http://www.cmu.edu/maty/materials/Polymers_with_Specific _Architecture/star-copolymers.html, June 2012.

21. Gok, O.; H. Durmaz, E. S. Ozdes, G: Hizal, U. Tunca, A. Sanyal, "Maleimide-Based Thiol Reactive Multiarm Star Polymers via Diels-Alder/retro Diels-Alder Strategy" *Journal of Polymer Science Part A: Polymer Chemistry*, Vol. 48, pp. 2546-2556, 2010.

22. Schramm, O. G.; G. M. Pavlov, H. P. van Erp, M. A. R. Meier, R. Hoogenboom and U. S. Schubert, "A Versatile Approach to Unimolecular Water-Soluble Carriers: ATRP of PEGMA with Hydrophobic Star Shaped Polymeric Core Molecules as an Alternative for PEGylation", *Macromolecules,* Vol. 42, 1808-1816, 2009.

23. Cho, H. Y., H. Gao, A. Srinivasan, J. Hong, S. A. Bencherif, D. J. Siegwart, H. Paik, J. O. Hollinger and K. Matyjaszewski, "Rapid Cellular Internalization of Multifunctional Star Polymers Prepared by Atom Transfer Radical Polymerization", *Biomacromolecules*, Vol. 11, 2199-2203, 2010.

24. Matyjaszewski, K. and J. Xia, "Atom Transfer Radical Polymerization", *Chemical Rev*iews, Vol. 101, 2921-2990, 2001.

25. *Diels-Alder Reaction*, http://www.organic-chemistry.org/namedreactions/diels-alder-reaction.shtm, June 2012.

26. Sanyal, A., "Diels–Alder Cycloaddition-Cycloreversion: A Powerful Combo in Materials Design", *Macromolecular Chemistry and Physics,* Vol. 211, pp. 1417-1425, 2010.

27. Kose, M. M., G. Yesilbag and A. Sanyal, "Segment Block Dendrimers via Diels-Alder Cycloaddition", *Organic Letters*, Vol. 10, pp. 2353-2356, 2008.

28. Shi, M., J. H. Wosnick, K. Ho, A. Keating, and M. S. Shoichet, "Immuno-Polymeric Nanoparticles by Diels–Alder Chemistry", *Angewandte Chemie International Edition,* Vol. 46, pp. 6126-6131, 2007.

29. Castonguay, A., E. Wilson, N. Al-Hajaj, L. Petitjean, J. Paoletti, D. Maysinger and A. Kakar, "Thermosensitive Dendrimer Formulation for Drug Delivery at Physiologically Relevant Temperatures", *Chemical Communications,* Vol. 47, pp. 12146-12148, 2011.

30. Gevrek, T. N., R. N. Ozdeslik, G. S. Sahin, G. Yesilbag, S. Mutlu and A. Sanyal, "Functionalization of Reactive Polymeric Coatings via Diels–Alder Reaction Using Microcontact Printing", *Macromolecular Chemistry and Phys*ics, Vol. 213, pp. 166-172, 2012.

31. Durmaz, H., F. Karatas, U. Tunca and G. Hızal, "Heteroarm H-Shaped Terpolymers Through the Combination of the Diels–Alder Reaction and Controlled/Living Radical Polymerization Techniques", *Journal of Polymer Science: Part A: Polymer Chemistry,* Vol. 44, pp. 3947-3957, 2006.